JAERI-M
8723

EXPERIMENTAL DATA OF ROSA-III INTEGRAL TEST RUN 705
(ISOTHERMAL BLOWDOWN TEST WITHOUT ECCS ACTUATION)

March 1980

Motoaki OKAZAKI, Kanji TASAKA,
Hiromichi ADACHI, Yoshinari ANODA,
Kunihisa SODA, Mitsuhiro SUZUKI,
Yasuo KOIZUMI, Makoto SOBAJIMA,
Hideo MURATA, Masayoshi SHIBA

日 本 原 子 力 研 究 所
Japan Atomic Energy Research Institute

Experimental Data of ROSA-III Integral Test RUN 705
(Isothermal blowdown test without ECCS actuation)

Motoaki OKAZAKI, Kanji TASAKA, Hiromichi ADACHI, Yoshinari ANODA,
Kunihisa SODA, Mitsuhiro SUZUKI, Yasuo KOIZUMI, Makoto SOBAJIMA,
Hideo MURATA, Masayoshi SHIBA
Division of Reactor Safety, Tokai Research Establishment, JAERI

(Received January 30, 1980)

Run 705 of the ROSA-III experimental program is an isothermal blowdown test without ECCS actuation in the BWR LOCA test series simulating a double-ended break on the inlet side of a recirculation pump. Purpose of the ROSA-III test program is to provide comprehensive experimental data of thermal hydraulic behavior in BWR LOCA to assess the system computer code. ROSA-III facility is a volume-scaled (1/424) system of a large (~1000MWe) BWR for an integral test on a BWR LOCA such as a 200% double-ended offset shear break on the inlet side of the pump in a recirculation loop. Power supply to main recirculation pumps and to core heater pins were stopped about 7 and 4 seconds respectively before initiation of the blowdown for an isothermal blowdown test. The primary initial conditions are steam dome presuure 7.11MPa, steam dome temperature 559K, lower plenum subcooling 9K, and core inlet flow 0.0 kg/s. The experiment in RUN 705 was successful; graphical data are presented in this report.

Keywords : BWR, LOCA, ECCS, Integral Test, ROSA-III Facility, Blowdown, Isothermal Test.

ROSA－Ⅲ実験データレポート：Run 705
（ECCSなしの等温ブローダウン実験）

日本原子力研究所東海研究所安全工学部
岡崎元昭・田坂完二・安達公道・安濃田良成
早田邦久・鈴木光弘・小泉安郎・傍島　真
村田秀男・斯波正誼

（1980年1月30日受理）

ROSA－Ⅲ実験 Run 705は，BWR　LOCA実験シリーズの中の等温ブローダウン実験であり，再循環ポンプ入口における200％両端破断を模擬している。
ROSA－Ⅲ実験の目的は，LOCA時に一次系内に起こる熱・水力挙動を理解するための総合実験データを提供し，解析コードの評価に役立てることである。
そのため，ROSA-Ⅲ装置は1000 MWe規模の大型BWRを体積比1／424で模擬しており，再循環ポンプ入口配管における200％両端破断をはじめとするBWRのLOCAの総合実験を行なえるようになっている。ブローダウン開始の7秒前に再循環ポンプへの電力供給は停止され，同じく4秒前に炉心への電力供給が停止された。主要な初期条件は，蒸気ドーム圧力7.11 MPa，同温度559 K，下部プレナム未飽和度6 K，炉心への流量は零である。Run 705の実験は所期の目的を達成した。本報告にはその実験データをグラフで示してある。

CONTENTS

目　　次

List of Tables

List of Figures

ABBREVIATIONS

Systemes

ROSA	Rig of Safety Assessment
BWR	Boiling Water Reactor
LBWR	Large Boiling Water Reactor
ECCS	Emergency Core Cooling System
HPCS	High Pressure Core Spray
LPCS	Low Pressure Core Spray
LPCI	Low Pressure Coolant Injection
ADS	Automatic Depressurization System

Vessels

PV	Pressure Vessel
PWT	Pure Water Tank
FWT	Feed Water Tank
AT	Air Tank
CWT	Cooling Water Tank
HPCST	High Pressure Core Spray Tank
LPCST	Low Pressure Core Spray Tank
LPCIT	Low Pressure Coolant Injection Tank
POOL	Pool

Pumps

JP	Jet Pump
MRP	Main Recirculation Pump
HPWP	High Pressure Water Pump
WSP	Water Supply Pump
FWP	Feed Water Pump
HPCSP	High Pressure Core Spray Pump
LPCSP	Low Pressure Core Spray Pump
LPCIP	Low Pressure Core Injection Pump

Piping

V	Valve
AV	Air actuation Valve
CV	Control Valve
CHV	Check Valve
QSV	Quick Shut-off Valve
OR	Orifice
RD	Rupture Disk
RCN	Rapid Condencer
(2)B	(2) inchs pipe of Schedule 80
DL(+100)	Elevation (+100 mm) from the bottom of PV

Measurements

P	Pressure
D	Differential Pressure
F	Flow Rate
T	Temperature
TS	Temperature of Solid
TF	Temperature of Fuel
L	Liquid Level
LB	Liquid Level in Channel Box
LL	Liquid Level in the Lower Plenum
S	Signal
W	Power
N	Rotation Speed
DF	Density of Fluid
M	Momentum Flux

Units

K	Kelvin
kg	Kilogram
ℓ	Liter
m	Meter
mm	Milimeter
MPa	Megapascal
rpm	Revolution per Minute
s	Second
W	Watt

Miscellaneous

ESF	Engineered Safety Features
LOCA	Loss-of-Coolant Accident
LOCE	Loss-of-Coolant Experiment
MLHR	Maximum Linear Heat Rate

1. INTRODUCTION

The ROSA (Rig of Safety Assessment)-III Program is one of several water reactor research test programs conducted by JAERI (Japan Atomic Energy Research Institute).

The ROSA-III facility is a volumetrically scaled (1/424) boiling water reactor (BWR) system with electrically heated core designed to study the response of the engineered safety features (ESF) in commercial BWR systems during the postulated loss-of-coolant accident (LOCA). With recognition of the differences in commercial BWR designs and inherent distortions in reduced scale systems, the design objective for the ROSA-III facility was to produce the significant thermal-hydraulic phenomena that would occur in commercial BWR systems in the same sequence and with approximately the same time frames and magnitudes. The objectives of the ROSA-III experimental program are:

(1) To provide data required to evaluate the adequacy and improve the analytical methods currently used to predict the LOCA response of large BWRs. The performance of the ESFs, with particular emphasis on emergency core cooling systems (ECCS), and the quantitative magins of safety inherent in performance of the ESF are of primary interest.

(2) To identify and investigate any unexpected event(s) or threshold(s) in the response of either the plant or the ESF and develop analytical techniques that adequately describe and account for such unexpected behavior.

The information acquired from loss-of-coolant experiments (LOCE) is thus used for evaluation and development of LOCA analytical methods and assessment for the quantitative margins of safety of ESFs in response to a LOCA.

Run 705, conducted on March 8, is an isothermal blowdown test without ECCS actuation, simulating a double-ended break on the inlet side of a recirculation pomp. The primary objectives of the test were to:

(1) Provide data to evaluate ROSA-III emergency core cooling system (ECCS) scaling techniques in the blowdown of a system.

(2) Provide integral system code verification data on a isothermal double-ended break at the recirculation pump inlet side.

Power supplies for recirculation pump motors and core heaters were shut off before blowdown in Run 705. The initial conditions are 7.11 MPa and 559 K in the steam dome of the pressure vessel. The subcooling in the lower plenum was 6 K.

The purpose of this report is to present the data from Run 705 in an uninterpreted but readily usable form for use by the nuclear community in advance of detailed analysis and interpretation. Section II briefly describes the ROSA-III configuration, section III discusses the ROSA-III instrumentation and the methods of obtaining certain measurements, section IV summarizes Run 705 initial conditions and test procedures, and section V presents the data with supporting information for data interpretation. Section VI describes concluding remarks.

2. ROSA-III TEST FACILITY

The ROSA-III facility is a volumetrically scaled (1/424) boiling water reactor (BWR) system with electrically heated core designed to study the response of the engineered safety features (ESF) in commercial BWR systems during the postulated loss-of-coolant accident (LOCA).

The test assembly consists of four major subsystems which have been instrumented such that desirable system parameters can be measured and recorded during a LOCE. The subsystems include: (a) the pressure vessel, (b) the steam line and the feedwater line, (c) the coolant recirculation system, and (d) the ECCS. System instrumentation is discussed in Section III. The ROSA-III major components and the pressure vessel internal structure are shown schematically in Figure 2.1 and 2.2, respectively. The ROSA-III piping system is shown in Figure 2.3, and the major characteristics of the ROSA-III facility are compared with those of a LBWR in Table 2.1.

The pressure vessel simulates the pressure vessel of a BWR. It has a simulated core, a lower plenum, an upper plenum, an annular downcomer, a steam separator, a simulated steam dryer plate, and a steam dome. The core is composed of four half-length simulated fuel assemblies and a control rod simulator. Each fuel assembly contains 63 fuel rods which are spaced and supported in a square (8 × 8) array by lower and upper tie plates. The simulated fuel rod is heated electrically with chopped-cosine axial power distribution. The effective heated length is 1880 mm, one half of the active length of a BWR fuel rod. The orifice plate assembly at core inlet simulates the flow resistance of the nuclear core.

The steam line and the feedwater line simulate those of a BWR. Steam is discharged into the atmosphere through the steam line connected to the steam dome. The steam line has three branches. The first branch has a control valve to control the steady-state steam dome pressure before blowdown. The second branch simulates the automatic depressurization system (ADS). The third branch has an orifice to simulate the flow resistance of a steam turbine-generator. Immediately after the blowdown initiation, the steam line is changed from the first branch to the third one. The feedwater line is connected to the feedwater sparger located above the downcomer region. The ambient-temperature feedwater is supplied from the pure water tank (PWT) at steady state, and the feedwater tank (FWT) supplies preheated feedwater during the first two seconds in the blowdown.

The coolant recirculation system simulates the BWR recirculation loop. The system consists of two loops provided with a recirculation pump and two jet pumps in each loop. One is the intact loop which simulates the unbroken loop of a BWR and the other is the broken loop which simulates the broken loop of a BWR. The broken loop has two break simulators and a quick shutoff valve to simulate a double-ended shear break or a split break. Each break simulator is composed of an orifice which determines the break area, a rupture disk, and a spear to break the rupture disk. The break type, position, and area are experimental variables. The standard break condition is a 200 % double-ended shear break at the recirculation pump inlet side with the orifice diameter of 26.2 mm.

The ECCS of ROSA-III simulate those of a BWR. The ECC systems include HPCS, LPCS, LPCI and ADS. The spray systems, the HPCS and the LPCS, spray the emergency cooling water on the top surface of the core. The LPCI system supplies the emergency cooling water into the core-shroud directly. Each ECCS is provided with a tank, a pump, a valve, and a control system to control the valve trip delay, valve opening speed, and the pump flow rate.

3. INSTRUMENTATION

The instrumentation system of the ROSA-III was designed to obtain thermo-hydraulic data in a BWR LOCA to contribute to assess the analytical code. The channel configuration of the instrumentation differs following the renewal of the simulated fuel assembly or remodeling of the loop system. The measurement list for the present run is shown in Table 3.1. Most of the measurements are recorded on the main data acquisition system (DATAC-2000B) with a half-inch width magnetic tape and the rest are recorded on the supplemental recording system with a casset tape of 100 channel capacity (cf. Table 3.2). The list number corresponds to the fuel assembly number. In the case of list with two figures the first digit indicates the fuel assembly number and the second digit indicates the revised version number of the instrumentation system for the same assembly.

Pressure measurements are done with semi-conductor transducers measuring the piezoelectric resistance. The detector is cooled by water for the protection from high temperature environment.

Differential pressure transducers with two direct current cables convert displacement of a diaphragm to electric charge and then to proportional voltage. The pressure lead pipes are dual circular pipes for circulating cooling water to eliminate flashing of the fluid.

Flow rate is measured by orifice, venturi, turbine or electro-magnetic flow meters depending on the fluid condition and the measurement location.

Electric power for simulated fuel rods is controlled by the predetermined function of time for the after power simulation and it is measured by fast response electric power meter.

Pump revolution speed is measured by counting the number of gear blades on the axis of a pump.

On-off signals such as valve position, pump revolution direction, rupture disk break and pump power supply are converted to voltage or current and recorded in respective channels in order to specify the exact time of the signal.

Temperatures of fluid, structure materials and fuel rods are measured with thermocouples of 1.6 mmϕ or 1.0 mmϕ.

Liquid levels are measured by means of needle type electrical conductivity probes developed in the ROSA-III program. The probes are attached on the walls of core barrel and channel boxes at several elevations and detect the existence of liquid water or steam at each level.

The void fraction of fluid is measured by a needle type electrical resistance probe or a correlation type electrical capacitance probe. The former detects passing bubble and the void fraction is obtained by integrating the void signal. The latter detects the average void distribution around the probe with the capacitance. The correlation between two sensors gives the velocity of the bubble.

Fluid density in the pipe is measured by means of a gamma ray densitometer. Each gamma ray densitometer has two or three beams to estimate the flow regime. The gamma source is Cs-137 and the detector is NaI scintillator which is cooled by water.

Flow direction in the core is measured from the canti-lever contact signal. The canti-lever is moved to the direction of the fluid flow and generates a contact signal.

Two-phase flow rate measurement is done by means of the combination of two signals from drag disk, turbine and gamma ray densitometer in a pipe.

Some of measurement methods described above are still under development and further improvements are expected in accuracy and reliability.

The measurement location of each instrumentation in the measurement list are shown in the figures of flow diagram, loop instrumentation, in-vessel instrumentation, or in-core instrumentation (Figs. 3.1 - 3.14).

Simulated fuel rods are named by one alphabet and two numerals. Alphabet shows the fuel channel, the first and the second numerals show column and row in 8×8 fuel rod array, respectively, for the fuel channel C. Fuel rods in other channels are named after rotating about the center of control rod simulator to the channel C. For example, C27 shows fuel rod in the second column and seventh row of fuel rod array in the fuel channel C. A17 shows fuel rod in the eighth column and second row of fuel rod array in the fuel channel A.

The data acquisition system utilizes two recording systems of major and minor importance. The data recorded on the magnetic tape of the main acquisition system are processed by the FACOM 230-75 computer at JAERI by off-line. After the evaluation of each data by comparing the initial and the final values with the standard values of the pressure for example, the data tape is re-processed using the correct conversion factors determined from consistency examination. Data processing program developed for the ROSA-III test can compare the measured data in a figure not only with other channels of the same test but also with the data of other runs or with calculated results by LOCA analysis code such as RELAP or ALARM.

4. TEST CONDITIONS

The test conditions of Run 705 are summarized in Table 4.1. Run 705 is an isothermal blowdown test without ECCS actuation, simulating a 200 % double-ended break at the recirculation pump suction side. Before blowdown initiation, main recirculation pumps were stopped and the power supply to core heaters were shut off. During blowdown none of emergency core coolant systems was actuated.

Simulated fuel rods are named by one alphabet and two numerals. Alphabet shows the fuel channel, the first and the second numerals show column and row in 8×8 fuel rod array, respectively, for the fuel channel C. Fuel rods in other channels are named after rotating about the center of control rod simulator to the channel C. For example, C27 shows fuel rod in the second column and seventh row of fuel rod array in the fuel channel C. A17 shows fuel rod in the eighth column and second row of fuel rod array in the fuel channel A.

The data acquisition system utilizes two recording systems of major and minor importance. The data recorded on the magnetic tape of the main acquisition system are processed by the FACOM 230-75 computer at JAERI by off-line. After the evaluation of each data by comparing the initial and the final values with the standard values of the pressure for example, the data tape is re-processed using the correct conversion factors determined from consistency examination. Data processing program developed for the ROSA-III test can compare the measured data in a figure not only with other channels of the same test but also with the data of other runs or with calculated results by LOCA analysis code such as RELAP or ALARM.

4. TEST CONDITIONS

The test conditions of Run 705 are summarized in Table 4.1. Run 705 is an isothermal blowdown test without ECCS actuation, simulating a 200 % double-ended break at the recirculation pump suction side. Before blowdown initiation, main recirculation pumps were stopped and the power supply to core heaters were shut off. During blowdown none of emergency core coolant systems was actuated.

5. DATA PRESENTATION

The experiment Run 705 proceeded as planned, starting with a 200 % double-ended break simulated by breaking two rapture disks and closing the quick shut-off valve between two breaks. The sequence of major events is shown in Table 5.1. Steam line and feed water line were completely closed before initiation of blowdown following the shut off of the power supply to core heaters. The system pressure decreased monotonously from the initiation of blowdown as Run 705 is a simple isothermal blowdown at the recirculation line break without power generation in the core. The mixture levels in the core and downcomer decrease after break. The uncover time of the recirculation suction in the downcomer is about 20 seconds after break. The system pressure decreases faster after 20 seconds because of steam discharge from the break. The lower plenum flashing phenomena is unclear because the pressure decreasing rate at the initiation of boiling in the lower plenum is rather slow , as recirculation suction line was not yet uncovered. The mixture level in the lower plenum is established at approximately 40 seconds after break and decreases monotonously, as shown in Figs. 5.75, 5.76 and 5.77.

The test data are presented in Fig. 5.1 through 5.76. They are divided into five groups, system data, flow data, signal data, temperature data and water level data.
Fig. 5.1 through 5.9 and 5.13 give system data, of which Fig. 5.1 through 5.4 show pressure transients in the vessel and loops, Fig. 5.5 through 5.9 show differential pressures in the vessel and loops, and Fig. 5.13 shows rotating speeds of recirculation pumps. Fig. 5.10 through 5.12 give flow data, of which Fig. 5.10 show flow rate of main steam line and Figs. 5.11 and 5.12 show flow rates concerned with discharge flow.

Fig. 5.14 gives break signal data. Fig. 5.15 through 5.68 give temperature data, of which Fig. 5.15 through 5.22 show fluid temperatures in the system, Fig. 5.23 through 5.26 show surface temperatures of structure materials, Fig. 5.27 through 5.54 show surface temperatures of simulated fuel rods, Fig. 5.55 through 5.58 show fluid temperatures around the tie rods, Fig. 5.59 through 5.60 show fluid temperatures at channel box inlet and outlet, Fig. 5.61 through 5.63 show inner surface temperatures of channel boxed and lower plenum, Fig. 5.64 shows fluid

temperatures in the lower plenum and Fig. 5.65 through 5.68 show fluid temperatures around the upper tieplate.

Partial gas phase signal appears at 11 seconds after break in the conduction-type liquid level detector at the top part (Position 1) of the core as shown in Fig. 5.69 through 5.74 and 5.77. The simulated fuel rod dries out at 39 seconds at position 1, and fuel surface temperature deviates from the saturation temperature and becomes fairly constant after 39 seconds because of no heat generation in the heater rod and little heat removal from the rod (cf. Fig. 5.41). The fuel rod dries out from the top to the bottom following the decrease in the mixture level in the core as shown in Fig. 5.77. The bottom part (Position 7) of the core dries out at 86 seconds after break.

6. CONCLUDING REMARKS

The conduct of ROSA-III experiment Run 705 and the experimental data acquired concerning integral system phenomena associated with a loss of coolant are considered to have met the objectives as described in section I.

The ROSA-III facility and its instrumentation worked well, and the obtained experimental data are udeful for assessing computer codes for BWR LOCA/ECCS analyses in the isothermal blowdown with a 200 % double-ended break at the recirculation pump suction without ECCS actuation and without core heating.

ACKNOWLEDGMENTS

The authors are grateful to H. Itoh, H. Osaki, and T. Chiba of Safety Facility Engineering Services Section, and H. Asahi, T. Odaira, S. Sekiguchi, M. Tokoi, H. Yamada, and J. Tamura of Nuclear Engineering Corporation who conducted the experiment.

temperatures in the lower plenum and Fig. 5.65 through 5.68 show fluid temperatures around the upper tieplate.

Partial gas phase signal appears at 11 seconds after break in the conduction-type liquid level detector at the top part (Position 1) of the core as shown in Fig. 5.69 through 5.74 and 5.77. The simulated fuel rod dries out at 39 seconds at position 1, and fuel surface temperature deviates from the saturation temperature and becomes fairly constant after 39 seconds because of no heat generation in the heater rod and little heat removal from the rod (cf. Fig. 5.41). The fuel rod dries out from the top to the bottom following the decrease in the mixture level in the core as shown in Fig. 5.77. The bottom part (Position 7) of the core dries out at 86 seconds after break.

6. CONCLUDING REMARKS

The conduct of ROSA-III experiment Run 705 and the experimental data acquired concerning integral system phenomena associated with a loss of coolant are considered to have met the objectives as described in section I.

The ROSA-III facility and its instrumentation worked well, and the obtained experimental data are udeful for assessing computer codes for BWR LOCA/ECCS analyses in the isothermal blowdown with a 200 % double-ended break at the recirculation pump suction without ECCS actuation and without core heating.

ACKNOWLEDGMENTS

The authors are grateful to H. Itoh, H. Osaki, and T. Chiba of Safety Facility Engineering Services Section, and H. Asahi, T. Odaira, S. Sekiguchi, M. Tokoi, H. Yamada, and J. Tamura of Nuclear Engineering Corporation who conducted the experiment.

temperatures in the lower plenum and Fig. 5.65 through 5.68 show fluid temperatures around the upper tieplate.

Partial gas phase signal appears at 11 seconds after break in the conduction-type liquid level detector at the top part (Position 1) of the core as shown in Fig. 5.69 through 5.74 and 5.77. The simulated fuel rod dries out at 39 seconds at position 1, and fuel surface temperature deviates from the saturation temperature and becomes fairly constant after 39 seconds because of no heat generation in the heater rod and little heat removal from the rod (cf. Fig. 5.41). The fuel rod dries out from the top to the bottom following the decrease in the mixture level in the core as shown in Fig. 5.77. The bottom part (Position 7) of the core dries out at 86 seconds after break.

6. CONCLUDING REMARKS

The conduct of ROSA-III experiment Run 705 and the experimental data acquired concerning integral system phenomena associated with a loss of coolant are considered to have met the objectives as described in section I.

The ROSA-III facility and its instrumentation worked well, and the obtained experimental data are udeful for assessing computer codes for BWR LOCA/ECCS analyses in the isothermal blowdown with a 200 % double-ended break at the recirculation pump suction without ECCS actuation and without core heating.

ACKNOWLEDGMENTS

The authors are grateful to H. Itoh, H. Osaki, and T. Chiba of Safety Facility Engineering Services Section, and H. Asahi, T. Odaira, S. Sekiguchi, M. Tokoi, H. Yamada, and J. Tamura of Nuclear Engineering Corporation who conducted the experiment.

Table 2.1 Primary characteristics of BWR-6 and ROSA-Ⅲ.

	BWR-6	ROSA-III	BWR/ROSA
No. of Recirc. Loops	2	2	1
No. of Jet Pumps	24	4	6
No. of Separators	251	1	251
No. of Fuel Assemblies	848	4	212
Active Fuel Length (m)	3.76	1.88	2
Total Coolant Volume (m^3)	623	1.37	455
Power (MW)	3800	4.24	896
Pressure (MPa)	7.23	7.23	1
Core Flow (kg/sec)	1.39×10^4	36.4	382
Recirculation Flow (l/sec)	2970	7.01	424
Feedwater Flow (kg/sec)	2060	4.86	424
Feedwater Temp (°K)	489	489	1

Table 3.1 POSA-III measurement List 2

CH No.	Item	Symb.	Location	Descriptions	LOC. Fig. No.	Ronge 8_1 Output	Accu racy	Data Fig. No.	Measurement comments
1	Press.	P - 1	Lower Plenum		3.2	0∿100kg/cm^2 0∿10 V	±1.08 % F.S.	5.1	Initial values are
2	"	P - 2	Mixing Plenum		"	"	"	"	adjusted to precise
3	"	P - 3	Steam Dome		"	"	"	"	pressure gauge data.
4	"	P - 4	Downcomer Bottom		"	"	"	"	
5	"	P - 5	JP - 3 Drive	broken loop	3.3	"	"	5.2	
6	"	P - 6	JP - 4 Drive	"	"	"	"	"	
7	"	P - 7	JP - 3 Suction	"	"	"	"	"	
8	"	P - 8	JP - 4 Suction	"	"	"	"	"	
9	"	P - 9	MRP - 1 Suction	intact loop	3.4	"	"	5.3	
10	"	P -10	MRP - 2 Suction	broken loop	3.3	"	"	"	
11	"	P -11	MRP - 2 Discharge	"	"	"	"	"	
12	"	P -12	Above Break A	pump side	"	"	"	5.4	
13	"	P -13	Below Break A	"	"	"	"	"	
14	"	P -14	Above Break B	vessel side	"	"	"	"	
15	"	P -15	Below Break B	"	"	"	"	"	
16	"	P -16	Steam Line	"	"	"	"	5.1	

CH. No.	Item	Symb.	Location	Description	LOC. Fig. No.	Range 8_1 Output	Accuracy	Data Fig. No.	Measurement comments
17	Diff. P	D - 1	Lower PL.-Mixing PL.		3.2	-0.5∿3.5kg/cm^2 2∿10 V	±0.63 % F.S.	5.5	
18	"	D - 2	Mixing PL.-Steam Dome		"	-0.1∿0.9kg/cm^2 2∿10 V	"	"	
19	"	D - 3	Lower Plenum Head		"	0∿1.5kg/cm^2 2∿10 V	"		not measured
20	"	D - 4	Downcomer Head		"	0∿1.0kg/cm^2 2∿10 V	"	5.6	
21	"	D - 5	PV. Bottom-Top		"	-1.0∿9.0kg/cm^2 2∿10 V	"	5.5	
22	"	D - 6	JP - 1 Discharge-Suction	intact loop	3.4	-1.0∿3.0kg/cm^2 2∿10 V	"	5.7	
23	"	D - 7	JP - 1 Drive-Suction	"	"	0∿25 kg/cm^2 2∿10 V	"	"	
24	"	D - 8	JP - 2 Discharge-Suction	"	"	-1.0∿3.0kg/cm^2 2∿10 V	"	"	
25	"	D - 9	JP - 2 Drive-Suction	"	"	0∿25 kg/cm^2 2∿10 V	"	"	
26	"	D -10	JP - 3 Discharge-Suction	broken loop	3.3	-1.0∿3.0kg/cm^2 2∿10 V	"	5.8	
27	"	D -11	JP - 3 Drive-Suction	"	"	-5.0∿25 kg/cm^2 2∿10 V	"	"	
28	"	D -12	JP - 4 Discharge-Suction	"	"	-1.0∿3.0kg/cm^2 2∿10 V	"	"	
29	"	D -13	JP - 4 Drive-Suction	"	"	-5.0∿25 kg/cm^2 2∿10 V	"	"	
30	"	D -14	MRP - 1 Discharge-Suction	intact loop	3.4	-1.0∿25 kg/cm^2 2∿10 V	"	5.9	
31	"	D -15	MRP - 2 Discharge-Suction	broken loop	3.3	-1.0∿25 kg/cm^2 2∿10 V	"	"	
32	Flow	F - 1	Main Steam Line		3.6	0∿15 kg/sec 2∿10 V	±0.92 % F.S.		not measured
33	"	F - 2	ADS. Steam Line		"	0∿3.0kg/sec 2∿10 V	"	5.10	

CH. No.	Item	Symb.	Location	Descriptions	LOC. Fig. No.	Renge & Output	Accu racy	Data Fig. No.	Measurement comments
34	Flow	F - 3	Condensed Water A		3.5	0∿250kg/sec 2∿10 V	±1.4% F.S.	5.11	
35	"	F - 4	Cooling Water A		"	"	"	"	
36	"	F - 5	Condensed Water B		"	"	"	5.12	
37	"	F - 6	Cooling Water B		"	"	"	"	
38	"	F - 7	HPCS (Mixing Plenum)	not used	3.1	0∿150 ℓ/min 2∿10 V	±0.79 % F.S.		
39	"	F - 8	HPCS (Lower Plenum)	"	"	"	"		
40	"	F - 9	LPCS (Mixing Plenum)	"	"	"	"		
41	"	F -10	LPCS (Lower Plenum)	"	"	"	"		
42	"	F -11	LPCI (Mixing Plenum)	"	"	0∿500 ℓ/min 2∿10 V	"		
43	"	F -12	LPCI (Lower Plenum)	"	"	"	"		
44	"	F -13	LPCI MRP - 2 Suction	"	"	0∿250 ℓ/min 2∿10 V	"		
45	"	F -14	LPCI MRP - 1 Suction	"	"	"	"		
46	"	F -15	Transient Feed Water	"	3.7	0∿600 ℓ/min 2∿10 V	"		
47	"	F -16	Steady Feed Water	"	"	0∿250 ℓ/min 2∿10 V	"		
48	"	F -17	JP - 1 Discharge	intact loop	3.4	0∿1000ℓ/min 2∿10 V	±0.88 % F.S.		not measured
49	"	F -18	JP - 2 Discharge	"		"	"		"
50	"	F -19	JP - 3 Discharge +	broken loop	3.3	"	±0.92 % F.S.		"

CH. No.	Item	Symb.	Location	Descriptions	Fig. No.	Range & Output	Accuracy	Data Fig. No.	Measurement comments
51	Flow	F -20	JP - 3 Discharge -	reverse flow	3.3	0∿300 ℓ/min 2∿10 V	±0.92 % F.S.		not measured
52	"	F -21	JP - 4 Discharge +		"	0∿1000ℓ/min 2∿10 V	"		"
53	"	F -22	JP - 4 Discharge -	reverse flow	"	0∿300 ℓ/min 2∿10 V	"		"
54	Power	W - 1	550 KVA Power	not used		0∿550 KVA 0∿10 V	±1.0% F.S.		
55	"	W - 2	1800 KVA Power	"		0∿1700 KVA 0∿10 V	"		
56	"	W - 3	2100 KVA Power	"		0∿2100 KVA 0∿10 V	"		
57	Rev. No	N - 1	MRP - 1	intact loop	3.4	0∿5000 rpm 0∿10 V	±1.08 % F.S.	5.13	
58	"	N - 2	MRP - 2	broken loop	3.3	"	"	"	
59	Signal	S - 1	Break Signal A		3.5	0 ∿ 5 V	-	5.14	cf. sequence of events
60	"	S - 2	Break Signal B		"	"	-	"	(Table 5.1)
61	"	S - 3	QSV Signal		"	close open 0 ∿ 5 V	-	"	
62	"	S - 9	Transient Feed Water	not used	3.7	"	-		
63	"	S -10	Main Steam Isolation Valve	"	3.6	"	-		
64	"	S -11	Steam Line Valve	"	"	"	-		
65	Temp.	T - 1	Lower Plenum	recirculation inlet fluid temp.	3.8	0 ∿ 400 °C 0 ∿ 10 V	±0.64 % F.S.	5.15	
66	"	T - 2	Mixing Plenum	fluid temp.	3.2	"	"	"	
67	"	T - 3	Steam Dome	"	"	"	"	"	

CH. No.	Item	Symb.	Location	Descriptions	Fig. No.	Range & Output	Accuracy	Data Fig. No.	Measurement comments
68	Temp.	T - 4	Upper Downcomer	fluid temp.	3.2	0 ∼ 400 °C 0 ∼ 10 V	±0.64 % F.S.	5.15	
69	"	T - 5	Lower Downcomer	"	3.8	"	"	"	
70	"	T - 6	JP - 1 Driving Water	"	3.4	"	"	5.16	
71	"	T - 7	JP - 2 Driving Water	"	"	"	"	"	
72	"	T - 8	JP - 3 Driving Water	"	3.3	"	"	5.17	
73	"	T - 9	JP - 4 Driving Water	"	"	"	"	"	
74	"	T -10	JP - 1 Discharge	"	3.4	"	"	5.16	
75	"	T -11	JP - 2 Discharge	"	"	"	"	"	
76	"	T -12	JP - 3 Discharge	"	3.3	"	"	5.17	
77	"	T -13	JP - 4 Discharge	"	"	"	"	"	
78	"	T -14	MRP - 1 Suction	"	3.4	"	"	5.18	
79	"	T -15	MRP - 1 Discharge	"	"	"	"	"	
80	"	T -16	MRP - 2 Suction	"	3.3	"	"	5.19	
81	"	T -17	MRP - 2 Discharge	"	"	"	"	"	
82	"	T -18	Above Break A	"	3.5	"	"	"	
83	"	T -19	Above Break B	"	"	"	"	"	
84	"	T -20	Condensed Water A	"	"	"	"	5.20	

CH. No.	Item	Symb.	Location	Descriptions	Fig. No.	Range & Output	Accuracy	Data Fig. No.	Measurement comments
85	Temp.	T -21	Condensed Water B	fluid temp.	3.5	0 ∿ 400 °C 0 ∿ 10 V	±0.64 % F.S.	5.21	
86	"	T -22	Discharged Steam Above V.	"	3.6	"	"	5.22	
87	"	T -23	Discharged Steam Below V.	"	"	"	"		not measured
88	"	TS-15	Dummy Block B Side 3	slab surface temp.	3.11	"	"	5.23	
89	"	TS-18	Dummy Block B Side 6	"	"	"	"	"	
90	"	TS-21	Dummy Block O Side 9	"	"	"	"	"	
91	"	TS-24	Dummy Block O Side 12	"	"	"	"	"	
92	"	TS-25	JP - 1 Diffuser Wall	slab temp.	3.4	"	"	5.24	
93	"	TS-26	JP - 2 Diffuser Wall	"	"	"	"	"	
94	"	TS-27	JP - 3 Diffuser Wall	"	3.3	"	"	"	
95	"	TS-28	JP - 4 Diffuser Wall	"	"	"	"	"	
96	"	TS-29	PV. Wall Inside 1 - 1	"	3.8	"	"	5.25	
97	"	TS-30	PV. Inner Surface 1 - 2	"	"	"	"	"	
98	"	TS-31	PV. Inner Surface 1 - 3	slab surface temp.	"	"	"	"	
99	"	TS-32	PV. Wall Inside 2	"	"	"	"	5.26	
100	"	TS-33	PV. Wall Inside 3	slab temp.	"	"	"	"	

CH. No.	Item	Symb.	Location	Descriptions	LOC. Fig. No.	Range 8_1 Output	Accu racy	Data Fig. No.	Measurement comments
101	Temp.	TS-34	PV. Wall Inside 4	slab temp.	3.8	0 ∿ 400 °C 0 ∿ 10 V	±0.64 % F.S.	5.26	
102	"	TS-35	Lower Plenum Inner Surface	surface temp.	"	"	"	5.25	
103	"	TS-36	Lower Plenum Wall Inside	slab temp.	"	"	"	"	
104	"	TF2- 1	A - 11 Fuel Rod Pos. 3	surface temp.	3.12	0 ∿ 1200 °C 0 ∿ 10 V	"	5.27	
105	"	TF2- 2	" 4	"	"	"	"	"	
106	"	TF2- 3	" 5	"	"	"	"	"	
107	"	- 4	A - 13 Fuel Rod Pos. 3	"	"	"	"	5.28	
108	"	- 5	" 4	"	"	"	"	"	
109	"	- 6	" 5	"	"	"	"	"	
110	"	- 7	A - 15 Fuel Rod Pos. 3	"	"	"	"	5.29	
111	"	- 8	" 4	"	"	"	"	"	
112	"	- 9	" 5	"	"	"	"	"	
113	"	-10	A - 17 Fuel Rod Pos. 3	"	"	"	"	5.30	
114	"	-11	" 4	"	"	"	"	"	
115	"	-12	" 5	"	"	"	"	"	
116	"	-13	A - 31 Fuel Rod Pos. 3	"	"	"	"	5.31	
117	"	-14	" 4	"	"	"	"	"	

OH. No.	Item	Symb.	Location	Descriptions	LOC. Fig. No.	Range & Output	Accuracy	Data Fig. No.	Measurement comments
118	Temp.	TF2-15	A - 31 Fuel Rod Pos. 5	surface temp.	3.12	0 ∿ 1200 °C 0 ∿ 10 V	±0.64 % F.S.	5.31	
119	"	-16	A - 33 Fuel Rod Pos. 1	"	"	"	"	5.32	
120	"	-17	" 2	"	"	"	"	"	
121	"	-18	" 3	"	"	"	"	"	
122	"	-19	" 4	"	"	"	"	"	
123	"	-20	" 5	"	"	"	"	"	
124	"	-21	" 6	"	"	"	"	"	
125	"	-22	" 7	"	"	"	"	"	
126	"	-23	A - 35 Fuel Rod Pos. 3	"	"	"	"	5.33	
127	"	-24	" 4	"	"	"	"	"	
128	"	-25	" 5	"	"	"	"	"	
129	"	-26	A - 37 Fuel Rod Pos. 3	"	"	"	"	5.34	
130	"	-27	" 4	"	"	"	"	"	
131	"	-28	" 5	"	"	"	"	"	
132	"	-29	A - 51 Fuel Rod Pos. 3	"	"	"	"	5.35	
133	"	-30	" 4	"	"	"	"	"	
134	"	-31	" 5	"	"	"	"	"	

CH. No.	Item	Symb.	Location	Descriptions	LOC. Fig. No.	Range 8_1 Output	Accy racy	Data Fig. No.	Measurement comments
135	Temp.	TF2-32	A - 53 Fuel Rod Pos. 3	surface temp.	3.12	0 ∿ 1200 °C 0 ∿ 10 V	±0.64 % F.S.	5.36	
136	"	-33	" 4	"	"	"	"	"	
137	"	-34	" 5	"	"	"	"	"	
138	"	-35	A - 57 Fuel Rod Pos. 3	"	"	"	"	5.37	
139	"	-36	" 4	"	"	0 ∿ 1220 °C 0 ∿ 10 V	"	"	
140	"	-37	" 5	"	"	"	"	"	
141	"	-38	A - 71 Fuel Rod Pos. 3	"	"	"	"	5.38	
142	"	-39	" 4	"	"	"	"	"	
143	"	-40	" 5	"	"	"	"	"	
144	"	-41	A - 73 Fuel Rod Pos. 3	"	"	"	"	5.39	
145	"	-42	" 4	"	"	"	"	"	
146	"	-43	" 5	"	"	"	"	"	
147	"	-44	A - 75 Fuel Rod Pos. 3	"	"	"	"	5.40	
148	"	-45	" 4	"	"	"	"	"	
149	"	-46	" 5	"	"	"	"	"	
150	"	TF2-47	A - 77 Fuel Rod Pos. 1	"	"	"	"	5.41	

CH. No.	Item	Symb	Locations	Descriptions	LOC. Fig. No.	Range θ_1 Output	Accu racy	Data Fig. No.	Measurement comments
151	Temp.	TF2-48	A - 77 Fuel Rod Pos. 2	surface temp.	3.12	0 ∿ 1220 °C 0 ∿ 10 V	±0.64 % F.S.	5.41	
152	"	-49	" 3	"	"	"	"	"	
153	"	-50	" 4	"	"	"	"	"	
154	"	-51	" 5	"	"	"	"	"	
155	"	-52	" 6	"	"	"	"	"	
156	"	-53	" 7	"	"	"	"	"	
157	"	-54	B - 15 Fuel Rod Pos. 1	"	"	"	"	5.42	
158	"	-55	" 2	"	"	"	"	"	
159	"	-56	" 3	"	"	"	"	"	
160	"	-57	" 4	"	"	"	"	"	
161	"	-58	" 5	"	"	"	"	"	
162	"	-59	" 6	"	"	"	"	"	
163	"	-60	" 7	"	"	"	"	"	
164	"	-61	B - 85 Fuel Rod Pos. 1	"	"	"	"	5.43	
165	"	-62	" 2	"	"	"	"	"	
166	"	-63	" 3	"	"	"	"	"	
167	"	-64	" 4	"	"	"	"	"	

CH. No.	Item	Symb.	Location	Descriptions	LOC. Fig. No.	Range 8_1 Output	Accuracy	Data Fig. No.	Measurement comments
168	Temp.	TF2-65	B - 85 Fuel Rod Pos. 5	surface temp.	3.12	0 ∿ 1220 °C 0 ∿ 10 V	±0.64 % F.S.	5.43	
169	"	-66	" 6	"	"	"	"	"	
170	"	-67	" 7	"	"	0 ∿ 976 °C 0 ∿ 10 V	"	"	
171	"	-68	C - 11 Fuel Rod Pos. 3	"	"	"	"	5.44	
172	"	-69	" 4	"	"	"	"	"	
173	"	-70	" 5	"	"	"	"	"	
174	"	-71	C - 13 Fuel Rod Pos. 3	"	"	"	"	5.45	
175	"	-72	" 4	"	"	"	"	"	
176	"	-73	" 5	"	"	"	"	"	
177	"	-74	C - 15 Fuel Rod Pos. 3	"	"	"	"	5.46	
178	"	-75	" 4	"	"	"	"	"	
179	"	-76	" 5	"	"	"	"	"	
180	"	-77	C - 31 Fuel Rod Pos. 3	"	"	"	"	5.47	
181	"	-78	" 4	"	"	"	"	"	
182	"	-79	" 5	"	"	"	"	"	
183	"	-80	C - 33 Fuel Rod Pos. 1	"	"	"	"	5.48	
184	"	-81	" 2	"	"	"	"	"	

CH. No.	Item	Symb.	Location	Descriptions	LOC. Fig. No.	Range & Output	Accuracy	Data Fig. No.	Measurement comments
185	Temp.	TF2-82	C - 33 Fuel Rod Pos. 3	surface temp.	3.12	0 ~ 976 °C 0 ~ 10 V	±0.64 % F.S.	5.48	
186	"	-83	" 4	"	"	"	"	"	
187	"	-84	" 5	"	"	"	"	"	
188	"	-85	" 6	"	"	"	"	"	
189	"	-86	" 7	"	"	"	"	"	
190	"	-87	C - 35 Fuel Rod Pos. 3	"	"	"	"	5.49	
191	"	-88	" 4	"	"	"	"	"	
192	"	-89	" 5	"	"	"	"	"	
193	"	-90	C - 51 Fuel Rod Pos. 3	"	"	"	"	5.50	
194	"	-91	" 4	"	"	"	"	"	
195	"	-92	" 5	"	"	"	"	"	
196	"	-93	C - 53 Fuel Rod Pos. 3	"	"	"	"	5.51	
197	"	-94	" 4	"	"	"	"	"	
198	"	-95	" 5	"	"	"	"	"	
199	"	-96	C - 77 Fuel Rod Pos. 1	"	"	"	"	5.52	
200	"	-97	" 2	"	"	"	"	"	

CH. No.	Item	Symb.	Location	Descriptions	LOC. Fig. No.	Range 8_1 Output	Accuracy	Data Fig. No.	Measurement comments
201	Temp.	TF2-98	C - 77 Fuel Rod Pos. 3	surface temp.	3.12	0 ∿ 976 °C 0 ∿ 10 V	±0.64 % F.S.	5.52	
202	"	- 99	" 4	"	"	"	"	"	
203	"	-100	" 5	"	"	"	"	"	
204	"	-101	" 6	"	"	"	"	"	
205	"	-102	" 7	"	"	"	"	"	
206	"	-103	D - 27 Fuel Rod Pos. 1	"	"	"	"	5.53	
207	"	-104	" 2	"	"	"	"	"	
208	"	-105	" 3	"	"	"	"	"	
209	"	-106	" 4	"	"	"	"	"	
210	"	-107	" 5	"	"	"	"	"	
211	"	-108	" 6	"	"	"	"	"	
212	"	-109	" 7	"	"	"	"	"	
213	"	-110	D - 88 Fuel Rod Pos. 1	"	"	"	"	5.54	
214	"	-111	" 2	"	"	"	"	"	
215	"	-112	" 3	"	"	"	"	"	
216	"	-113	" 4	"	"	"	"	"	
217	"	-114	" 5	"	"	"	"	"	

CH. No.	Item	Symb.	Location	Descriptions	LOC. Fig. No.	Range 8_1 Output	Accu racy	Data Fig. No.	Measurement comments
218	Temp.	TF2-115	D - 88 Fuel Rod Pos. 6	surface temp.	3.12	0 ∿ 976 °C 0 ∿ 10 V	±0.64 % F.S.	5.54	
219	"	-116	" 7	"	"	"	"	"	
220	"	-117	A - 55 Tie Rod Pos. 1	fluid temp.	"	"	"	5.55	
221	"	-118	" 2	"	"	"	"	"	
222	"	-119	" 3	"	"	"	"	"	
223	"	-120	" 4	"	"	"	"	"	
224	"	-121	" 5	"	"	"	"	"	
225	"	-122	" 6	"	"	"	"	"	
226	"	-123	" 7	"	"	"	"	"	
227	"	-124	B - 55 Tie Rod Pos. 1	"	"	"	"	5.56	
228	"	-125	" 2	"	"	"	"	"	
229	"	-126	" 3	"	"	"	"	"	
230	"	-127	" 4	"	"	"	"	"	
231	"	-128	" 5	"	"	"	"	"	
232	"	-129	" 6	"	"	"	"	"	
233	"	-130	" 7	"	"	"	"	"	
234	"	-131	C - 55 Tie Rod Pos. 1	"	"	"	"	5.57	

CH. No.	Item	Symb.	Location	Descriptions	LOC. Fig. No.	Range 8_1 Output	Accuracy	Data Fig. No.	Measurement comments
235	Temp.	TF2-132	C - 55 Tie Rod Pos. 2	fluid temp.	3.12	0 ∿ 976 °C 0 ∿ 10 V	±0.64 % F.S.	5.57	
236	"	-133	" 3	"	"	"	"	"	
237	"	-134	" 4	"	"	"	"	"	
238	"	-135	" 5	"	"	"	"	"	
239	"	-136	" 6	"	"	"	"	"	
240	"	-137	" 7	"	"	"	"	"	
241	"	-138	D - 55 Tie Rod Pos. 1	"	"	"	"	5.58	
242	"	-139	" 2	"	"	"	"	"	
243	"	-140	" 3	"	"	"	"	"	
244	"	-144	" 4	"	"	"	"	"	
245	"	-141	" 5	"	"	"	"	"	
246	"	-143	" 6	"	"	"	"	"	
247	"	-144	" 7	"	"	"	"	"	
248	"	TC- 1	Channel Box A Outlet	"	"	"	"	5.59	
249	"	- 2	" A Inlet	"	"	"	"	5.60	
250	"	- 3	" B Outlet	"	"	"	"	5.59	

CH. No.	Item	Symb.	Location	Descriptions	LOC. Fig. No.	Range & Output	Accuracy	Data Fig. No.	Measurement comments
251	Temp.	TC- 4	Channel Box B Inlet	fluid temp.	3.12	0 ∿ 976 °C 0 ∿ 10 V	±0.64 % F.S.	5.60	
252	"	- 5	" C Outlet	"	"	"	"	5.59	
253	"	- 6	" C Inlet	"	"	"	"	5.60	
254	"	- 7	" D Outlet	"	"	"	"	5.59	
255	"	- 8	" D Inlet	"	"	"	"	5.60	
256	"	TB- 1	C.B. Inner Surface Pos. A-1	surface temp.	3.12 3.13	"	"	5.61	
257	"	- 2	" A-2	"	"	"	"	"	
258	"	- 3	" A-3	"	"	"	"	"	
259	"	- 4	" A-4	"	"	"	"	"	
260	"	- 5	" A-5	"	"	"	"	"	
261	"	- 6	" A-6	"	"	"	"	"	
262	"	- 7	" A-7	"	"	"	"	"	
263	"	- 8	C.B. Inner Surface Pos. A-8	"	"	"	"	5.62	
264	"	- 9	" A-9	"	"	"	"	"	
265	"	-10	" A-10	"	"	"	"	"	
266	"	-11	" A-11	"	"	"	"	"	
267	"	-12	" A-12	"	"	"	"	"	

CH. No.	Item	Symb.	Location	Descriptions	LOC. Fig. No.	Range 8₁ Output	Accu racy	Data Fig. No.	Measurement comments
268	Temp.	TB-13	C.B. Inner Surface pos.A-13	surface temp.	3.12 3.13	0 ∿ 976 °C 0 ∿ 10 V	±0.64 % F.S.	5.62	
269	"	-14	" A-14	"	"	"	"	"	
270	"	TP- 1	Lower PL. 0° High	"	3.10	"	"	5.63	
271	"	- 2	" Middle	"	"	"	"	"	
272	"	- 3	" Low	"	"	"	"	"	
273	"	- 4	Lower PL. 180° High	"	"	"	"	"	
274	"	- 5	" Middle	"	"	"	"	"	
275	"	- 6	" Low	"	"	"	"	"	
276	"	- 7	Low PL. Center Low	fluid temp.	"	"	"	5.64	
277	"	- 8	" Bottom	"	"	"	"	"	
278	"	- 9	Lower PL. Guide Tube	"	"	"	"	"	
279	"	-10	Lower PL. Outer Bottom	"	"	"	"	"	
280	"	TG2- 1	Upper Tieplate A Up. 1	"	3.12	"	"	5.65	
281	"	- 2	" 2	"	"	"	"	"	
282	"	- 3	" 3	"	"	"	"	"	
283	"	- 4	" 4	"	"	"	"	"	
284	"	- 5	" 5	"	"	"		"	

CH. No.	Item	Symb.	Location	Descriptions	LOC. Fig. No.	Range & Output	Accu racy	Data Fig. No.	Measurement comments
285	Temp.	TG2- 6	Upper Tieplate A Up. 6	fluid temp.	3.12	0 ∿ 976 °C 0 ∿ 10 V	±0.64 % F.S.	5.66	
286	"	- 7	" 7	"	"	"	"	"	
287	"	- 8	" 8	"	"	"	"	"	
288	"	- 9	" 9	"	"	"	"	"	
289	"	-10	" 10	"	"	"	"	"	
290	"	-11	Upper Tieplate A low 11	"	"	"	"	5.67	
291	"	-12	" 12	"	"	"	"	"	
292	"	-13	" 13	"	"	"	"	"	
293	"	-14	" 14	"	"	"	"	"	
294	"	-15	" 15	"	"	"	"	"	
295	"	-16	" 16	"	"	"	"	5.68	
296	"	-17	" 17	"	"	"	"	"	
297	"	-18	" 18	"	"	"	"	"	
298	"	-19	" 19	"	"	"	"	"	
299	"	-20	" 20	"	"	"	"	"	
300	Water Level	LB- 1	C.B. Water Level Pos. 1-1		"	ON ∿ OFF 0 ∿ 10 V		5.69	

CH. No.	Item	Symb.	Location	Descriptions	LOC. Fig. No.	Range 8_1 Output	Accuracy	Data Fig. No.	Measurement comments
301	Water Level	LB- 2	C.B. Water Level Pos. 1-2		3.12 3.13	ON - OFF		5.69	
302	"	- 3	" 1-3		"	"		"	
303	"	- 4	" 1-4		"	"		"	
304	"	- 5	" 1-5		"	"		5.70	
305	"	- 6	" 1-6		"	"		"	
306	"	- 7	" 1-7		"	"		"	
307	"	- 8	C.B. Water Level Pos. 2-1		"	"		5.71	
308	"	- 9	" 2-2		"	"		"	
309	"	-10	" 2-3		"	"		"	
310	"	-11	" 2-4		"	"		"	
311	"	-12	" 2-5		"	"		5.72	
312	"	-13	" 2-6		"	"		"	
313	"	-14	" 2-7		"	"		"	
314	"	-15	C.B. Water Level Pos. 3-1		"	"		5.73	
315	"	-16	" 3-2		"	"		"	
316	"	-17	" 3-3		"	"		"	
317	"	-18	" 3-4		"	"		"	

CH. No.	Item	Symb.	Location	Descriptions	LOC. Fig. No.	Range & Output	Accu racy	Data Fig. No.	Measurement comments
318	Water Level	LB-19	C.B. Water Level Pos. 3-5		3.12 3.13	On - OFF		5.74	
319	"	-20	" 3-6		"	"		"	
320	"	-21	" 3-7		"	"		"	
321	"	LL- 1	Lower PL. Center High		3.10	"		5.75	
322	"	- 2	" Middle 1		"	"		"	
323	"	- 3	" Middle 2		"	"		"	
324	"	- 4	" Low		"	"		"	
325	"	- 5	Lower PL. 0° Low		"	"		5.76	
326	"	- 6	" Bottom		"	"			sensor failed
327	"	- 7	Lower PL. 180° Low		"	"		5.76	
328	"	- 8	" Bottom		"	"			sensor failed
329	Void	VE- 1	Lower PL. Void 0°		3.12	0 ~ 1.0 0 ~ 10 V			not measured
330	"	- 2	" Center		"	"			"
331	"	- 3	" 180°		"	"			"
332	"	- 4	Outlet of Channel A		"	"			"
333	"	- 5	"		"	"			"
334	"	- 6	"		"	"			"

CH. No.	Item	Symb	Location	Descriptions	LOC. Fig. No.	Range 8_1 Output	Accu racy	Data Fig. No.	Measurement comments
335	Void	VE- 7	Outlet of Channel B		3.12	0 ∿ 1.0 0 ∿ 10 V			not measured
336	"	- 8	"		"	"			"
337	"	- 9	"		"	"			"
338	"	-10	Outlet of Channel C		"	"			"
339	"	-11	"		"	"			"
340	"	-12	"		"	"			"
341	"	-13	Outlet of Channel D		"	"			"
342	"	-14	"		"	"			"
343	"	-15	"		"	"			"
344	"	VP- 1	Lower PL. Void 1-1		"	"			"
345	"	- 2	" 1-2		"	"			"
346	"	- 3	" 2-1		"	"			"
347	"	- 4	" 2-2		"	"			"
348	Flow	FE- 1	Channel A Outlet			0∿3.0m/sec 0∿10 V			"
349	"	- 2	" B "			"			"
350	"	- 3	" C "			"			"

CH. No.	Item	Symb.	Location	Descriptions	LOC. Fig. No.	Range & Output	Accu racy	Data Fig. No.	Measurement comments
351	Direc.	FE- 4	Channel D Outlet			0∿3.0m/sec 0∿10 V			not measured
352	"	FD- 1	Channel A Outlet			Pos.-Neg. +10∿-10 V			undefined data
353	"	- 2	" B "			"			"
354	"	- 3	" C "			"			"
355	"	- 4	" D "			"			"
356	Dens.	DF- 1	J.P. - 1.2 Outlet Beam 1			0∿1000kg/m^3 0∿10 V			not measured
357	"	- 2	" 2			"			"
358	"	- 3	" 3			"			"
359	"	- 4	JP - 3.4 Outlet Beam 1			"			"
360	"	- 5	" 2			"			"
361	"	- 6	" 3			"			"
362	"	- 7	Break A Beam 1			"			"
363	"	- 8	Break A Beam 2			"			"
364	Mome. F	M - 1	JP - 1.2 Outlet			0∿1.5×10^5kg/m.s^2 0∿10 V			"
365	"	- 2	JP - 3.4 Outlet			"			"
366	"	- 3	Break A			"			"
367	Flow	F -23	JP - 1.2 Outlet			0∿30 ℓ/sec 0∿10 V			"

CH. No.	Item	Symb.	Location	Descriptions	LOC. Fig. No.	Range & Output	Accu racy	Data Fig. No.	Measurement comments
368	Flow	F -24	JP - 3.4 Outlet			0∿30 ℓ/sec 0∿10 V			not measured
369	"	-25	Break A			0∿30kg/sec 0∿10 V			"
370	Press.	P -17	JP - 1.2 Outlet			0∿100kg/cm^2 0∿10 V			"
371	"	-18	JP - 3.4 "			"			"
372	"	-19	Break A			"			"
373	Temp	T -24	JP - 1.2 Outlet			0 ∿ 400 °C 0 ∿ 10 V			"
374	"	-25	JP - 3.4 "			"			"
375	"	-26	Break A			"			"
426		LP- 1	550 KVA Power	not used	-				
427		LP- 2	1800 KVA Power	"	-				
428		LP- 3	2100 KVA Power	"					
429		MF- 1	Dis. Flow A	pump side				5.11	
430		MF- 2	Dis. Flow B	vessel side				5.12	
431		MF- 3	JP - 1,2 Outlet	not used					
432		MF- 4	JP - 3,4 Outlet	"					
433		MF- 5	Break A	"					
434		MF- 7	JP - 1,2 Outlet	"					

CH. No.	Item	Symb.	Location	Descriptions	LOC. Fig. No.	Range 8_1 Output	Accu racy	Data Fig. No.	Measurement comments
435		MF- 8	JP - 3,4 Outlet	not used					
436		MF- 9	Break A	"					
437		X - 1	Break A	pump side			5.20		
438		X - 2	Break B	vessel side			5.21		
439		X - 3	JP - 1,2 Outlet	not used					
440		X - 4	JP - 3,4 Outlet	"					
441		X - 5	Break A	"					
442		DF-10	JP - 1,2 Outlet	"					
443		DF-11	JP - 3,4 Outlet	"					
444		DF-12	Break A	"					
445		DF-14	JP - 1,2 Out Av.	"					
446		DF-15	JP - 3,4 Out Av.	"					
447		DF-16	Break A Av.	"					
448		FG- 1	JP - 1,2 Outlet	"					
449		FG- 2	JP - 3,4 Outlet	"					
450		FG- 3	Break A	"					

Table 3.2 List of instrumentation for supplemental recording system

ch. No.	Item	Symb.	Location	Descriptions	LOC. Fig. No.	Range	Data Fig. No.	Measurement comments
539	Slab temp.	TS- 1	Core barrel A 1			0∿400°C		undefined data
540	‖	TS- 2	‖ A 2			‖		"
541		TS- 3	A 3					"
542		TS- 4	A 4					"
543		TS- 5	A 5					"
544		TS- 6	A 6					"
545		TS- 7	Core barrel C 7					"
546		TS- 8	‖ C 8					"
547		TS- 9	C 9					"
548		TS-10	C10					"
549		TS-11	C11					"
550		TS-12	C12					"
551		TS-13	Dummy block. B side 1					"
552		TS-14	‖ B side 2					"
553		TS-16	B side 4					"
554		TS-17	B side 5					"
555		TS-19	O side 7					"
556		TS-20	O side 8					"
557		TS-22	O side 10					"
558		TS-23	O side 11					"

ch. No.	Item	Symb.	Location	Descriptions	LOC. Fig. No.	Range	Data Fig. No.	Measurement comments
559	Direction of rev.	RD- 1	Main recirc. pump 1			pos.∿neg.		undefined data
560	‖	RD- 2	‖ 2			‖		"
561	Signal	S - 4	Cooling water valve A			open∿close		"
562	‖	S - 5	‖ B			‖		"
563	‖	S - 6	HPCS valve			‖		"
564	‖	S - 7	LPCS valve			‖		"
565	‖	S - 8	LPCI valve			‖		"
566	‖	S -12	ADS valve			‖		"
567	‖	S -13	MRP-1 power			ON∿OFF		"
568	‖	S -14	MRP-2 power			‖		"
591	Liquid level	L - 1	Lower plenum			‖		"
592	‖	L - 2	‖			‖		"
593	‖	L - 3	‖			‖		"
594	‖	L - 4	‖			‖		"
595	‖	L - 5	‖			‖		"
596	‖	L - 6	Mixing plenum			‖		"
597	‖	L - 7	Downcomer			‖		"
598	‖	L - 8	‖			‖		"
599	‖	L - 9	‖			‖		"
600	‖	L -10	‖			‖		"

Table 4.1 Test conditions of the ROSA-III Run 705

Parameter		Specified Value	Measured Value
Break Conditions			
Location		Recirculation pump suction	
Type		Double ended	
Break Orifice Diameter	(mm)	26.2/26.2	
Initial System Conditions			
Steam Dome Pressure	(MPa)	7.16	7.11
Lower Plenum Temperature	(K)	560	551
Lower Plenum Subcooling	(K)	6	6
Core Inlet Flow Rate	(kg/s)	0	0
Broken Loop Flow Rate	(m^3/s)	0	0
Intact Loop Flow Rate	(m^3/s)	0	0
Core Outlet Quality	(−)	0	0
Power Level	(kW)	0	0
Maximum Linear Heat Rate			
of Region 1 [9 rods]	(kW/m)	0	0
Region 2 [108 rods]	(kW/m)	0	0
Region 3 [135 rods]	(kW/m)	0	0
Power Curve			
Water Level in PV	(m)	4.62	4.64
Feedwater Conditions			
Steady State Line			
Temperature	(K)	−	−
Flow Rate	(m^3/s)	0	0

Table 4.1 (Continued)

Parameter		Spesified Value	Measured Value
Feedwater Conditions (Continued)			
Transient Line			
Temperature	(K)	-	-
Flow Rate	(m^3/s)	0	0
Termination Time	(s)	-	-
Steam Discharge Conditions			
Steady State Line			
Flow Rate	(kg/s)	0	0
Transient Line			
Flow Rate	(kg/s)	0	0
Orifice Diameter	(mm)	-	-
Termination Time	(s)	-	-
ECCS Conditions			
HPCS			
Injection Location			
Initiation Time	(s)		
at Pressure in PV	(MPa)		
Water Level in PV	(m)		
Coolant Temperature	(K)		
Injection Flow Rate	(m^3/s)		

Table 4.1 (Continued)

Parameter		Specified Value	Measured Value
ECCS Conditions (Continued)			
LPCS			
Injection Location			
Initiation Time	(s)		
at Pressure in PV	(MPa)		
Water Level in PV	(m)		
Coolant Temperature	(K)		
Injection Flow Rate	(m^3/s)		
LPCI			
Injection Location			
Initiation Time	(s)		
at Pressure in PV	(MPa)		
Coolant Temperature	(K)		
Injection Flow Rate	(m^3/s)		
ADS Conditions			
Valve Opening Time	(s)		
Valve Closed Time	(s)		
Flow Rate	(m^3/s)		
Orifice Diameter	(mm)		

Table 5.1 Sequence of events in Run 705

EVENTS	Time (s)
Break	0
Partial gas phase signal at the top of core	11
Recirculation suction uncovering	20
Dry out at the top of core (pos. 1)	39
Lower Plenum mixture level formation	40
Dry out at the bottom of core (Pos. 7)	86

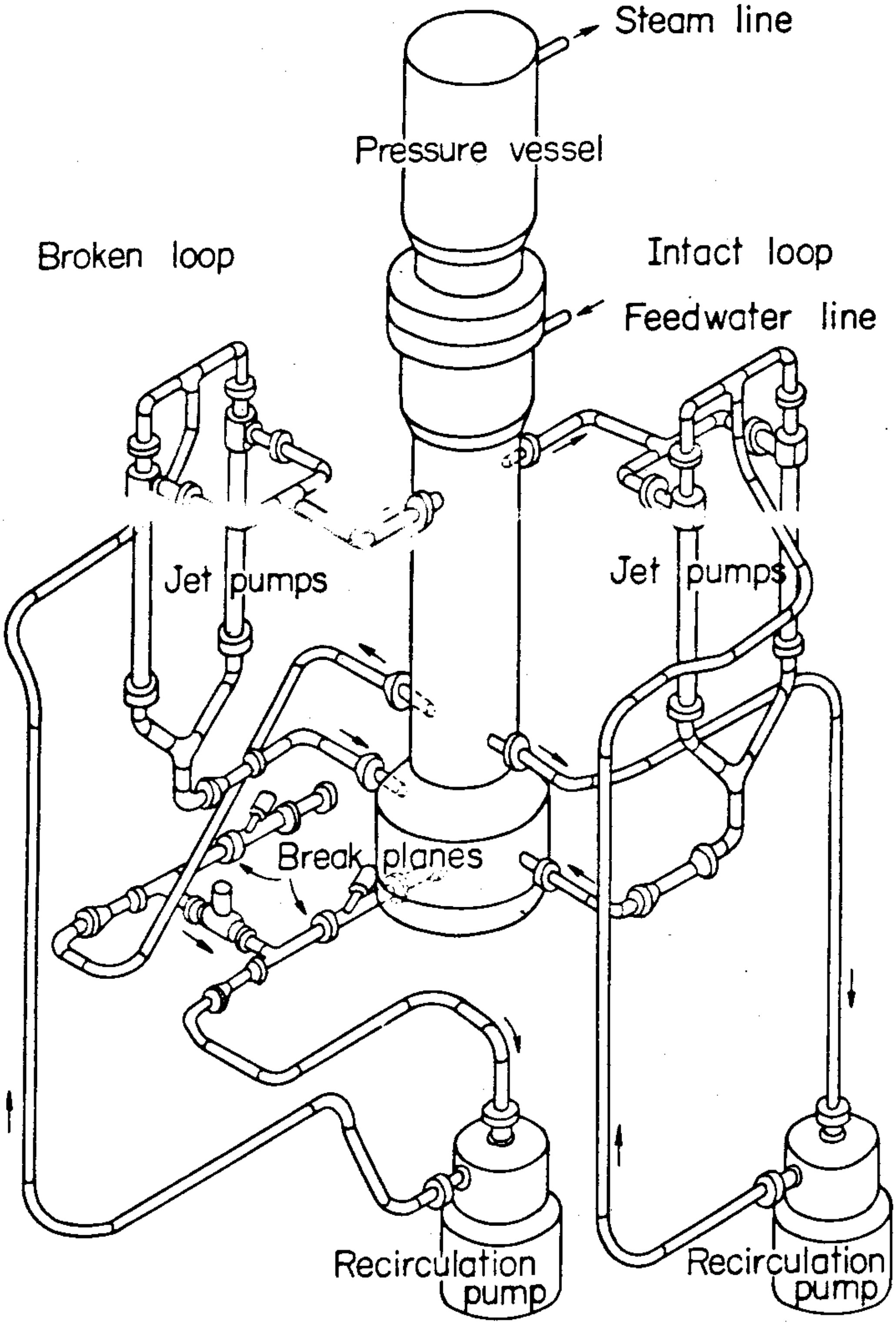

Fig. 2.1 Schematic diagram of ROSA-III test facility.

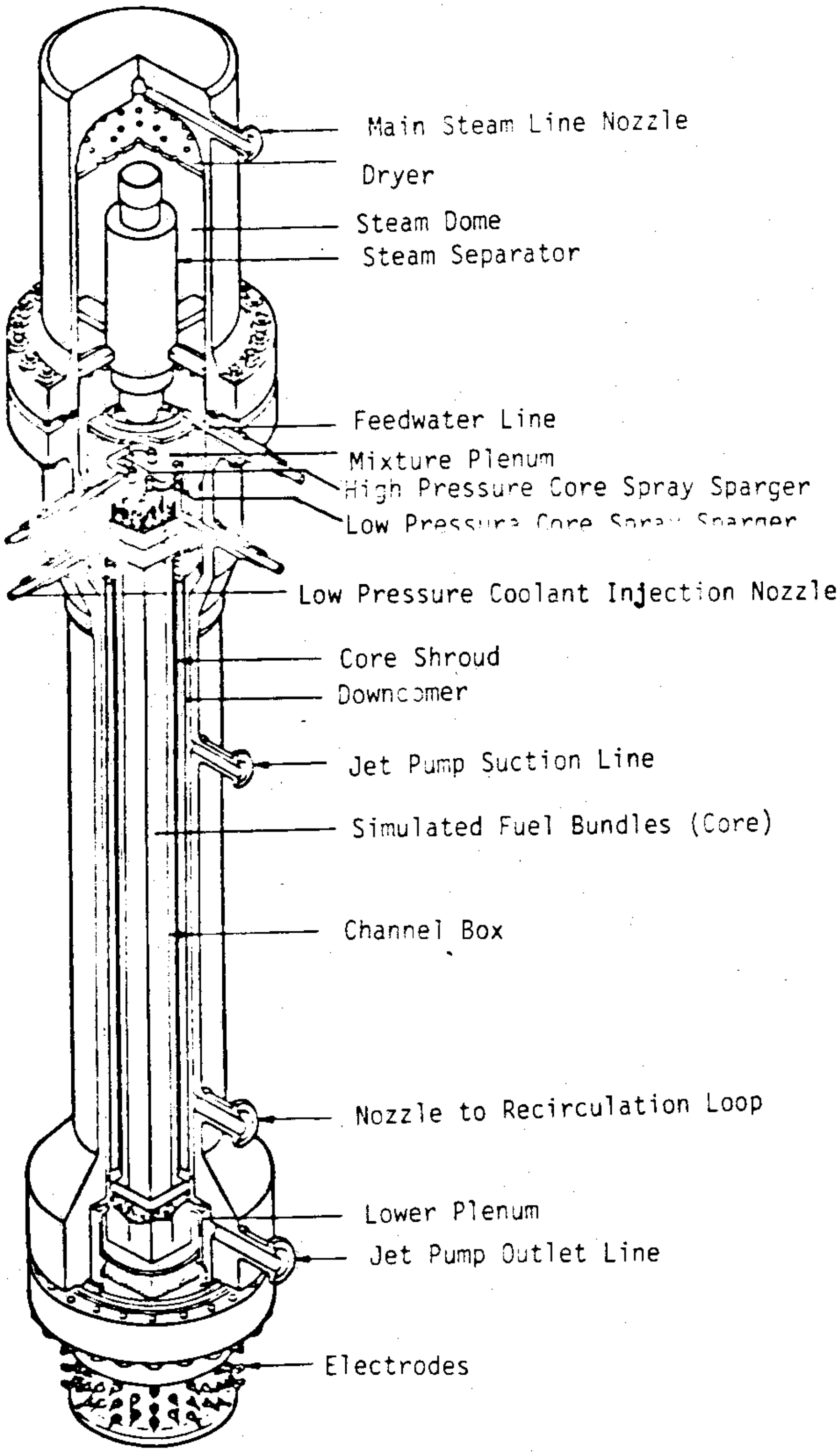

Fig. 2.2 Internal structure of pressure vessel of ROSA-III.

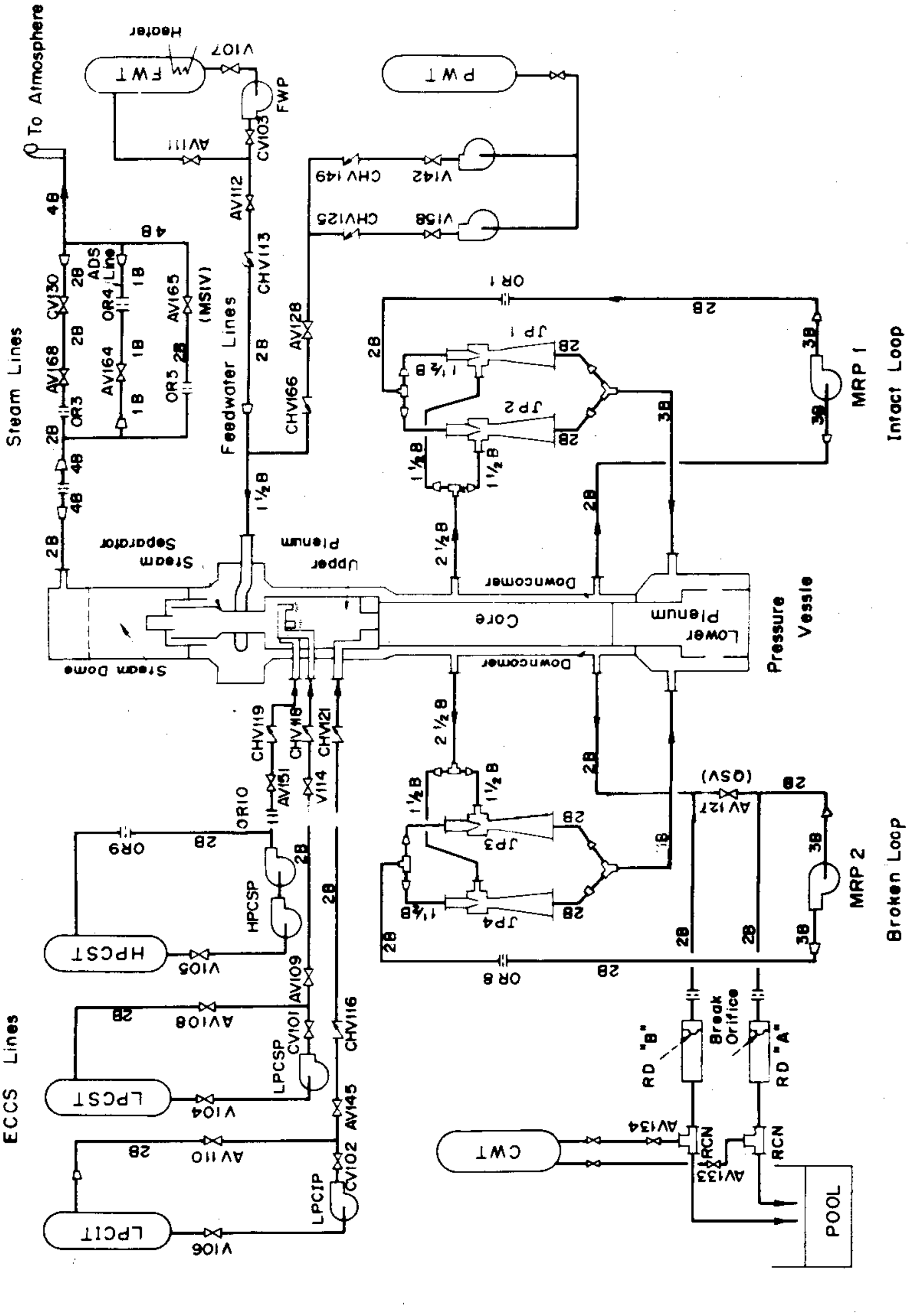

Fig. 2.3 ROSA-III piping schematic

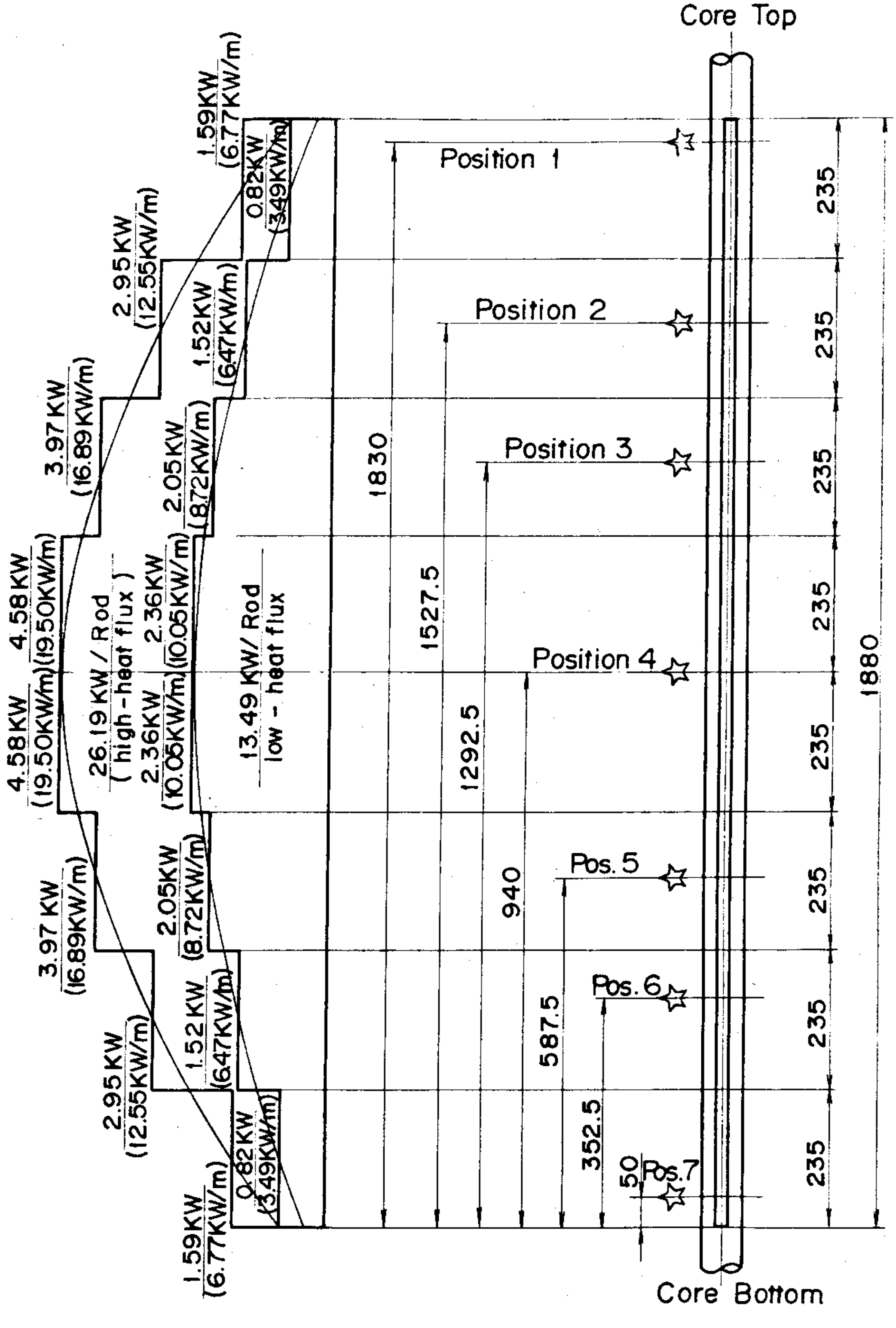

Fig. 2.4 Axial power distribution of heater rod

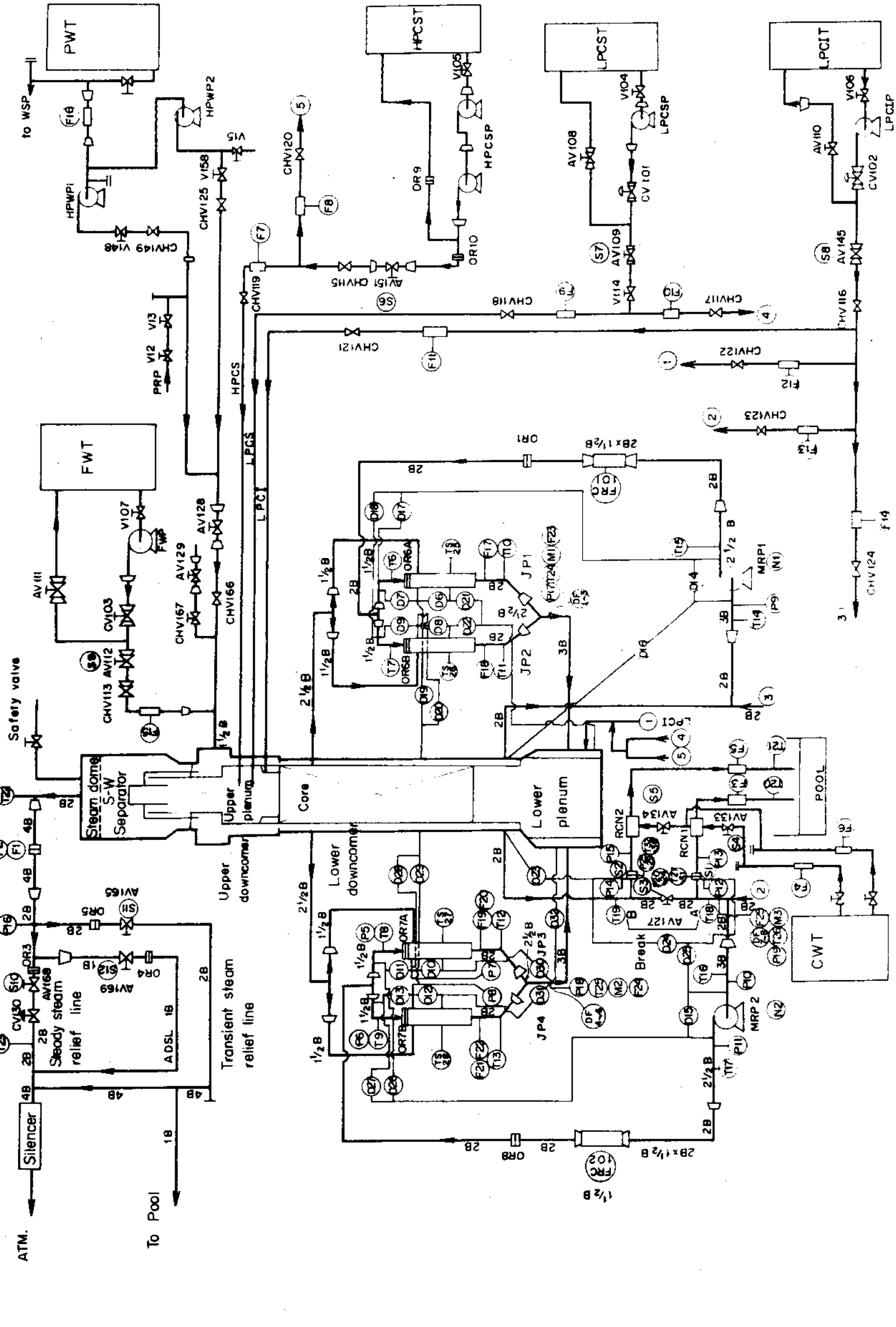

Fig. 3.1 Flow diagram and instrumentation location of ROSA-III facility.

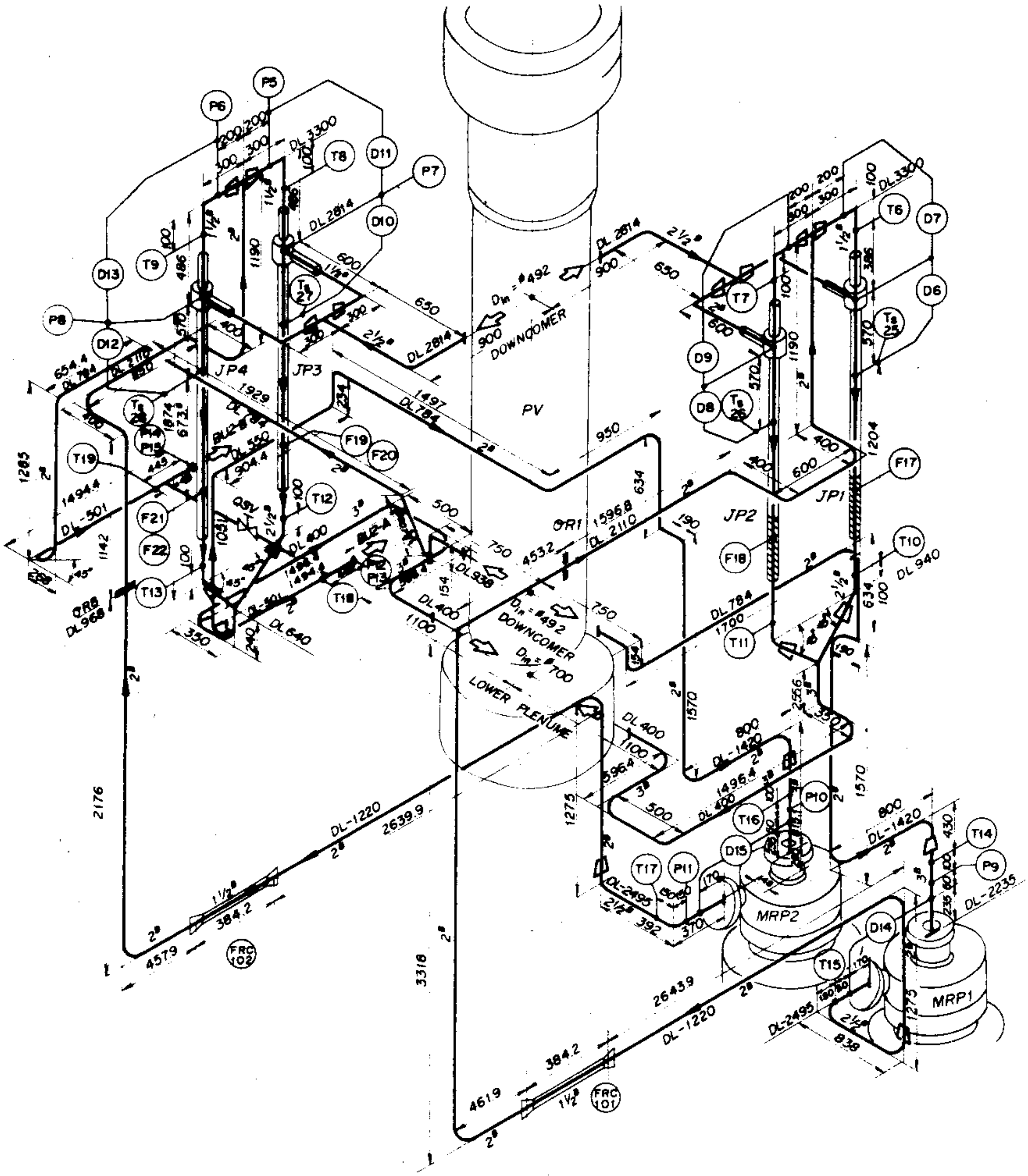

Fig. 3.2 ROSA-III recirculation loops with instrumentation.

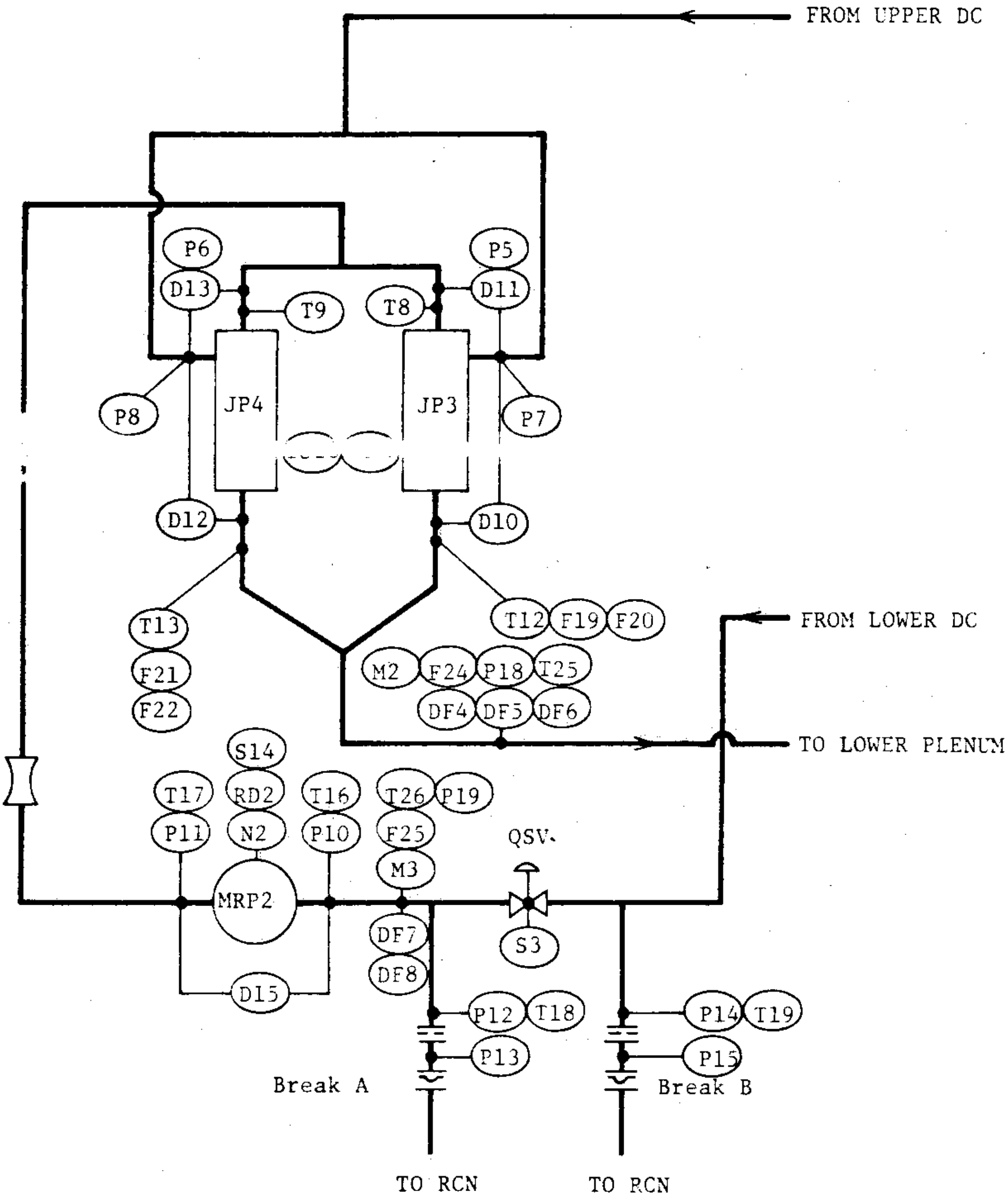

Fig. 3.3 Instrumentation in the broken loop.

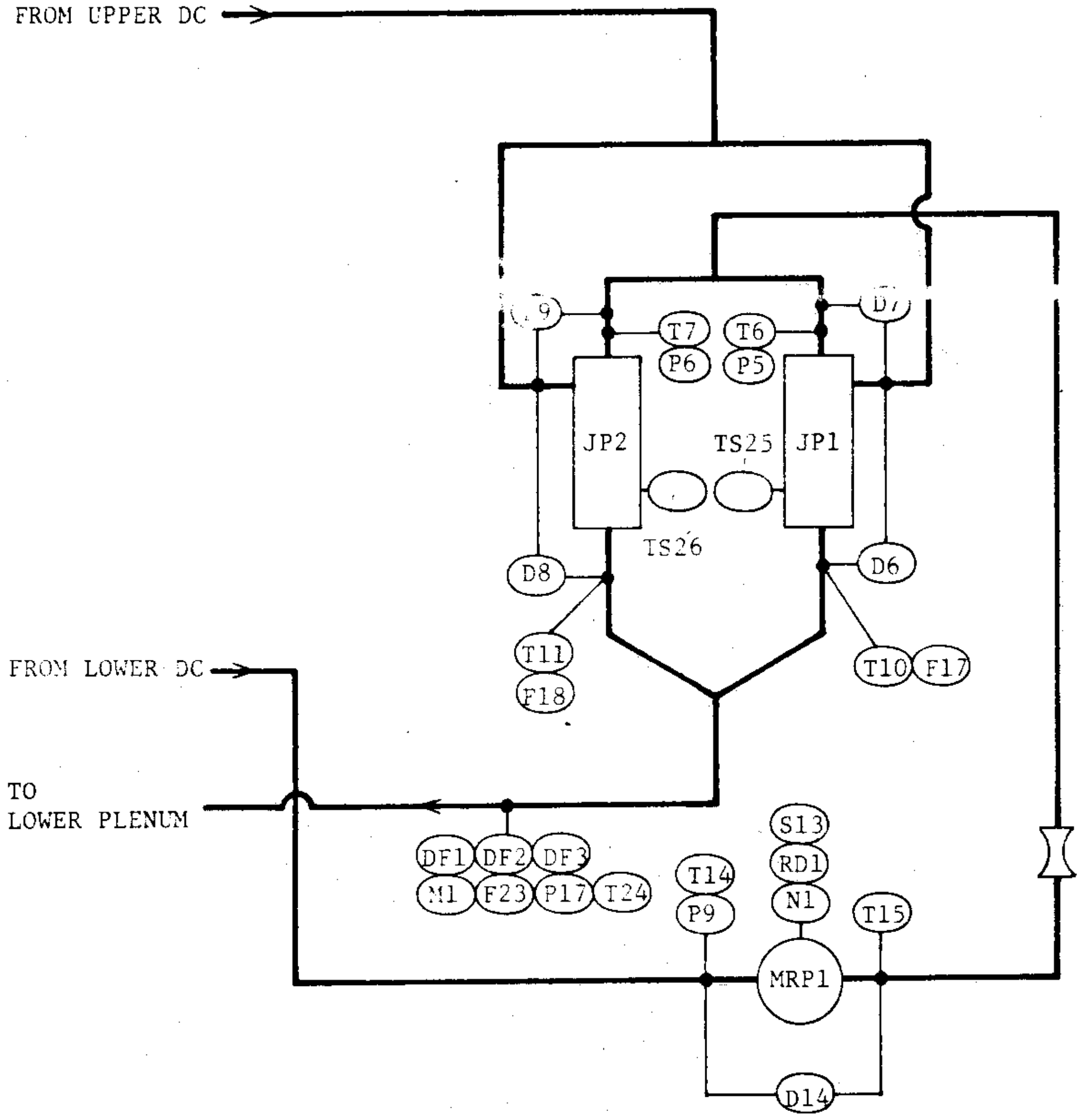

Fig. 3.4 Instrumentation in the intact loop.

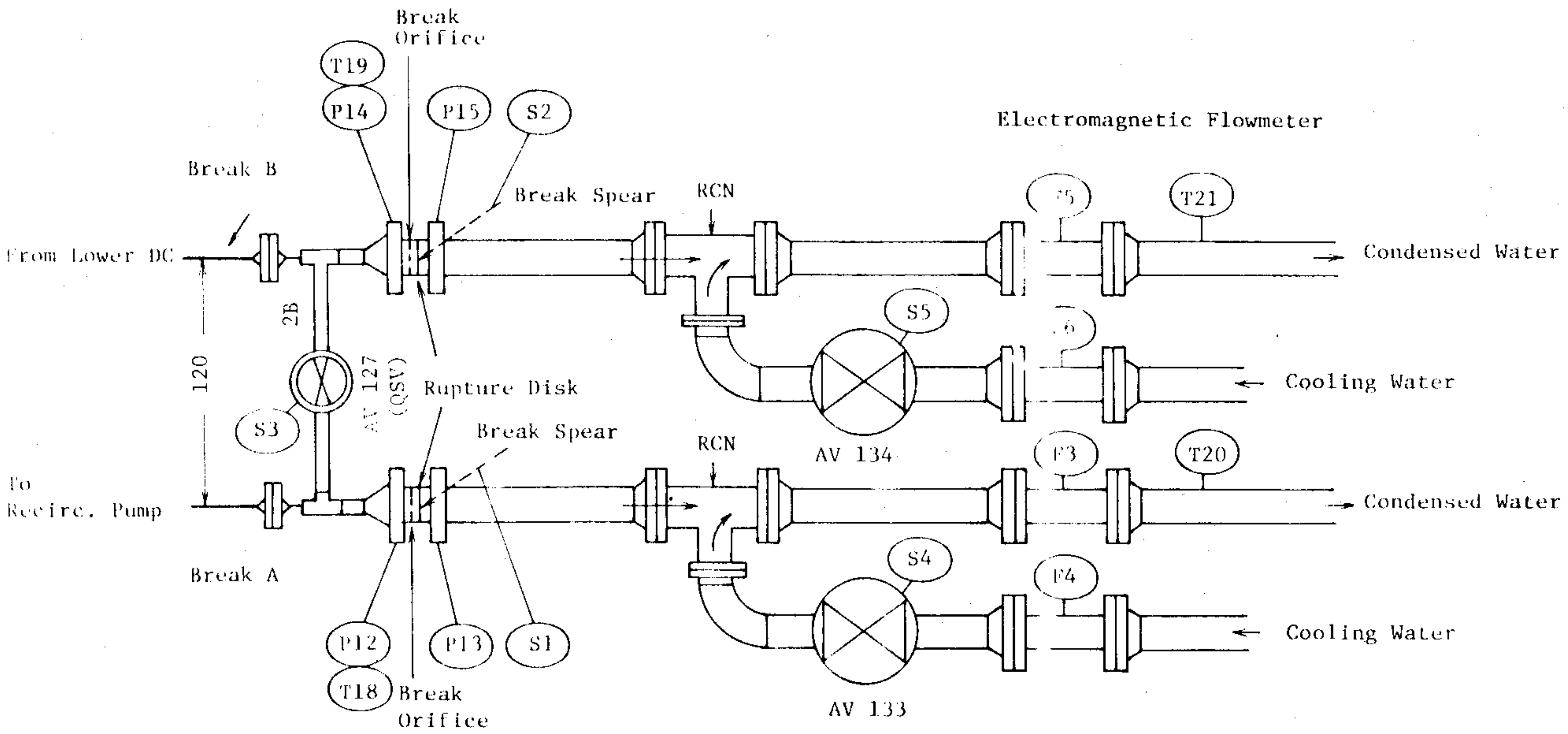

Fig. 3.5 Instrumentation in the break unit.

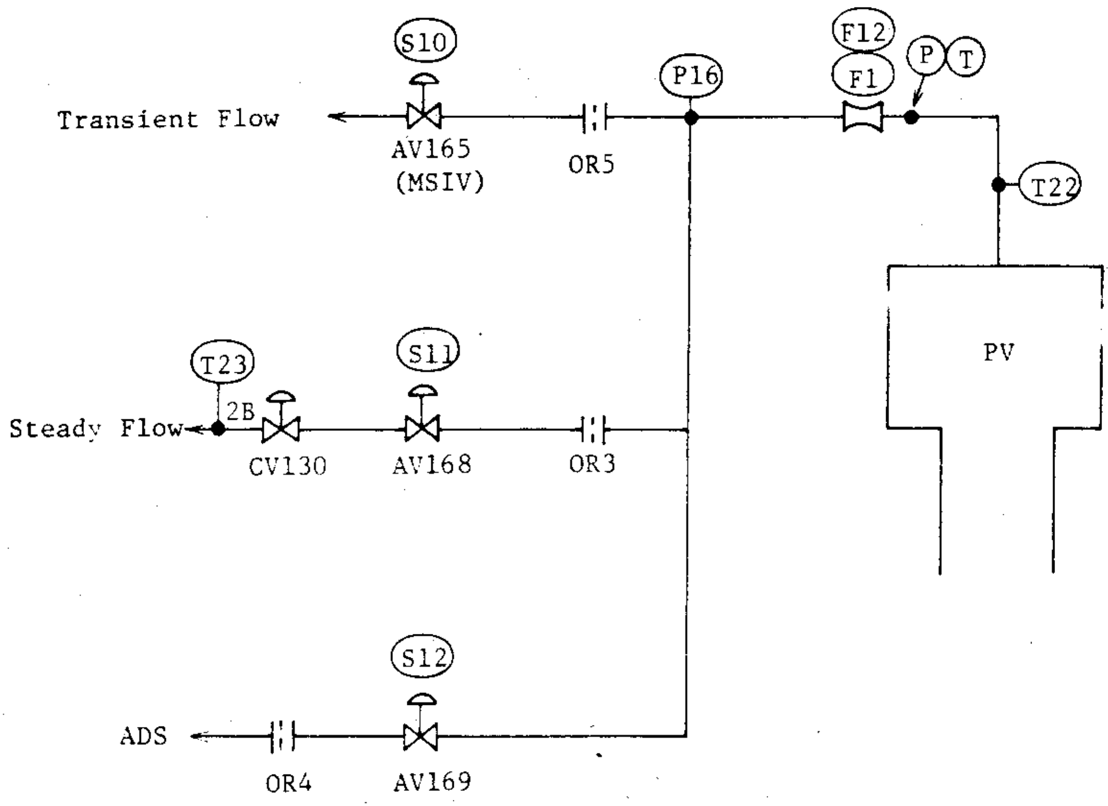

Fig. 3.6 Instrumentation in the steam line.

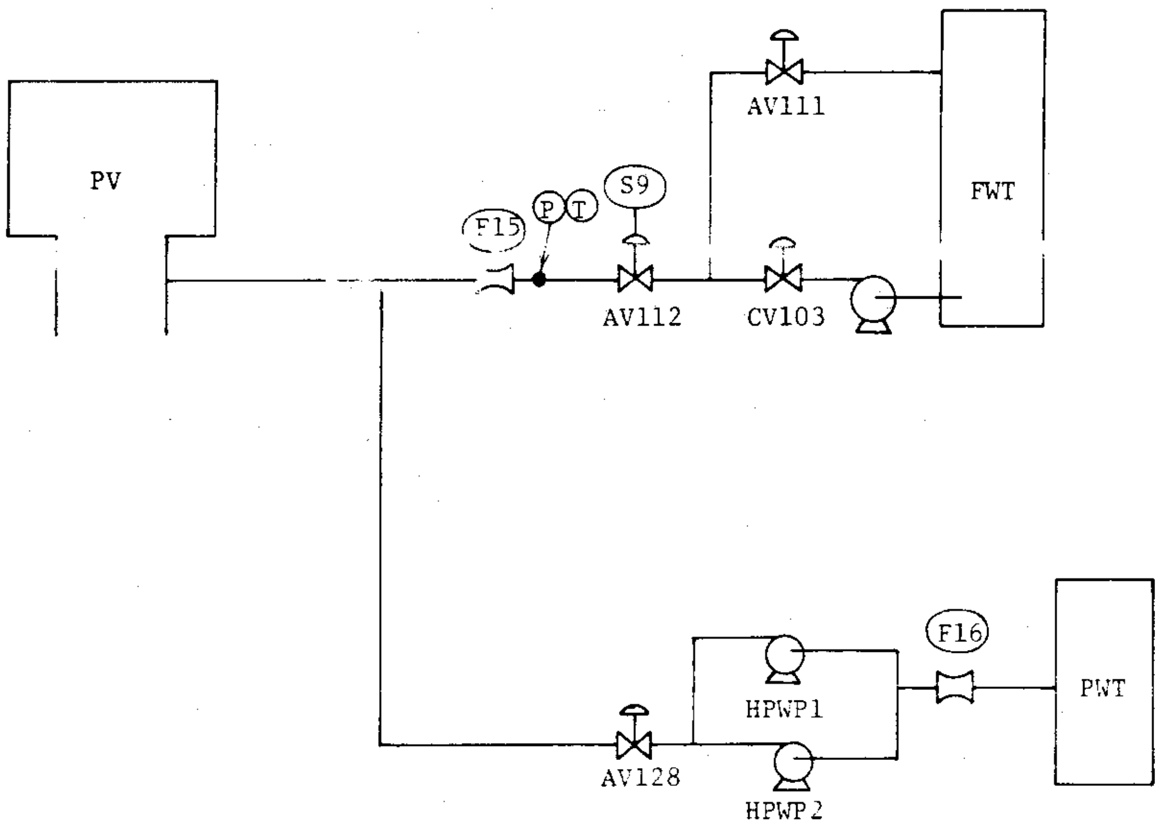

Fig. 3.7 Instrumentation in the feedwater line.

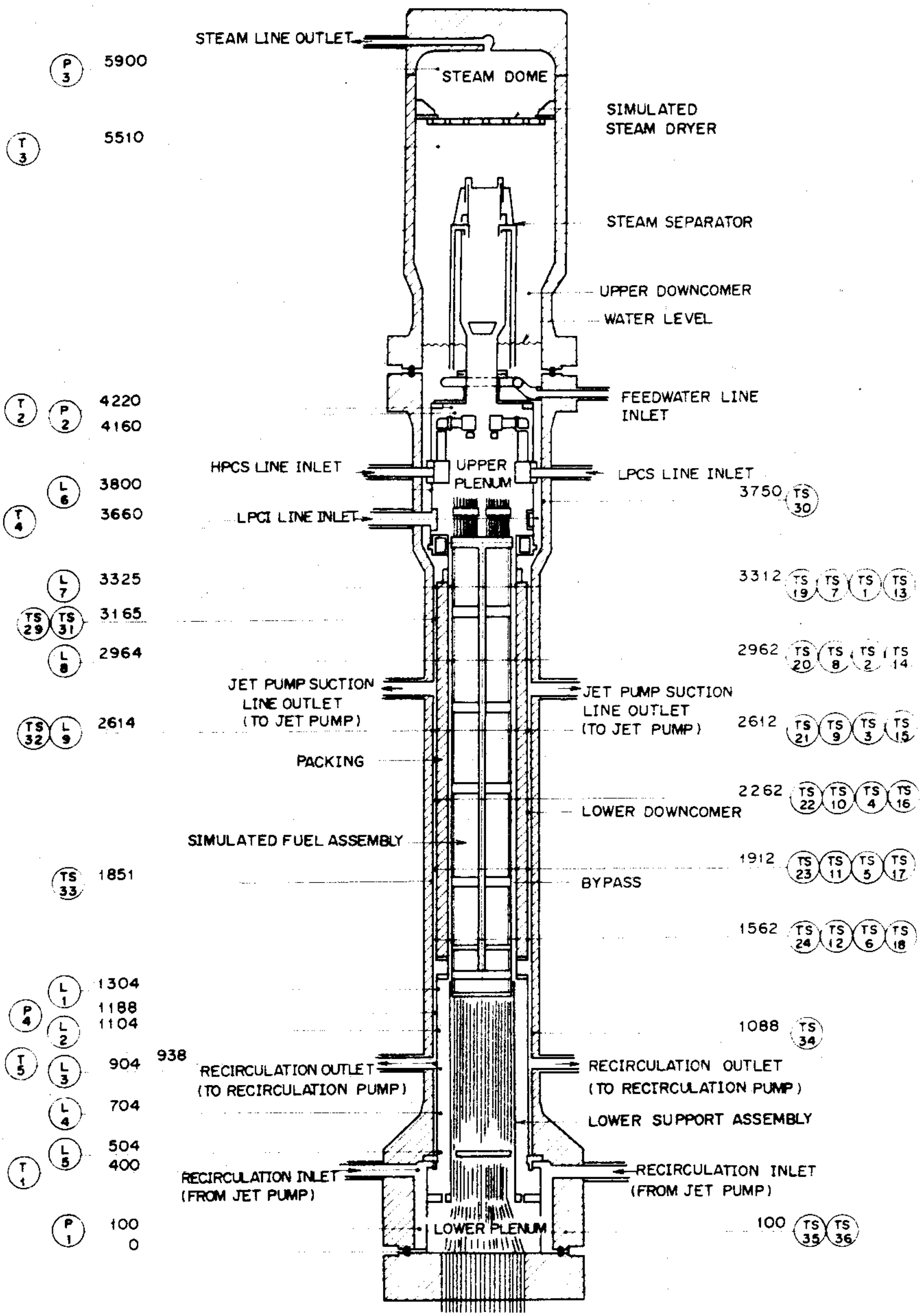

Fig. 3.8 ROSA-III pressure vessel with instrumentation.

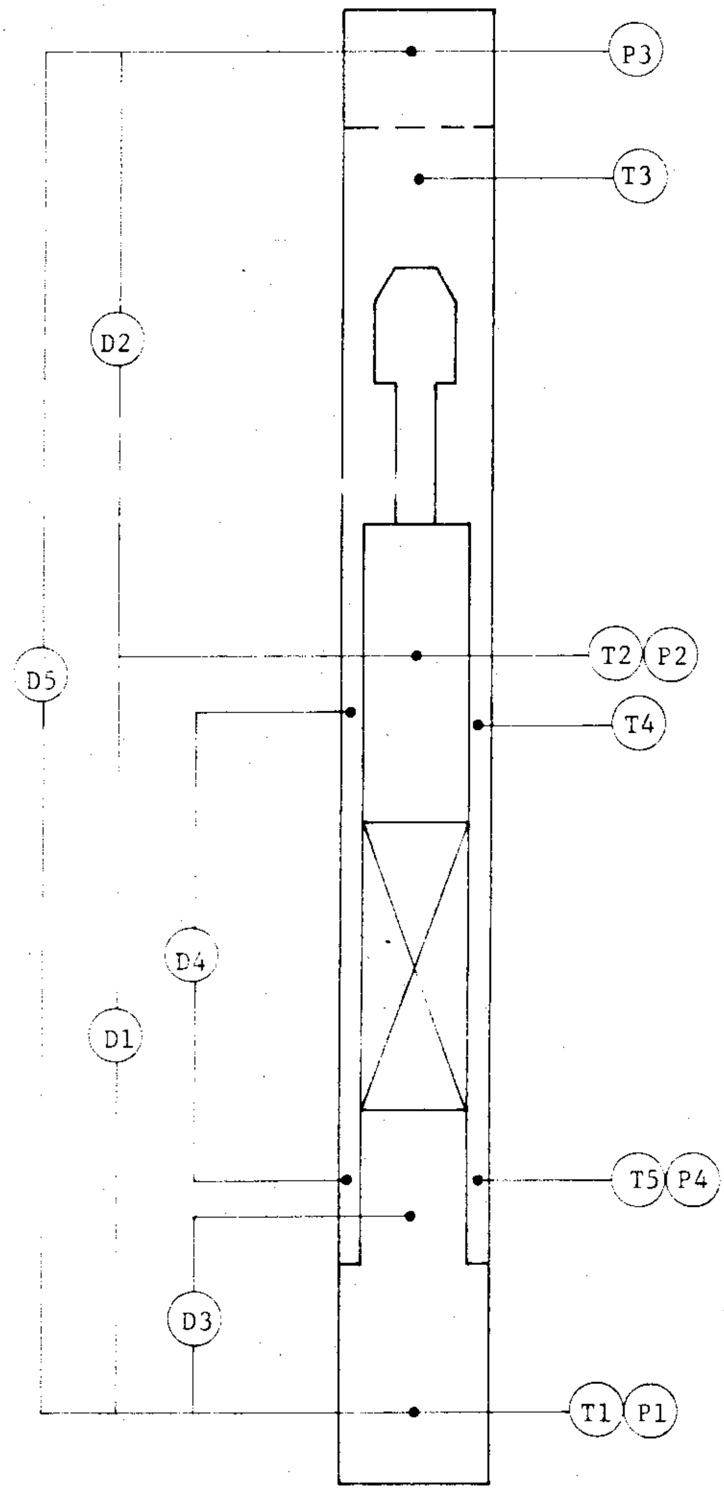

Fig. 3.9 Instrumentation in the pressure vessel.

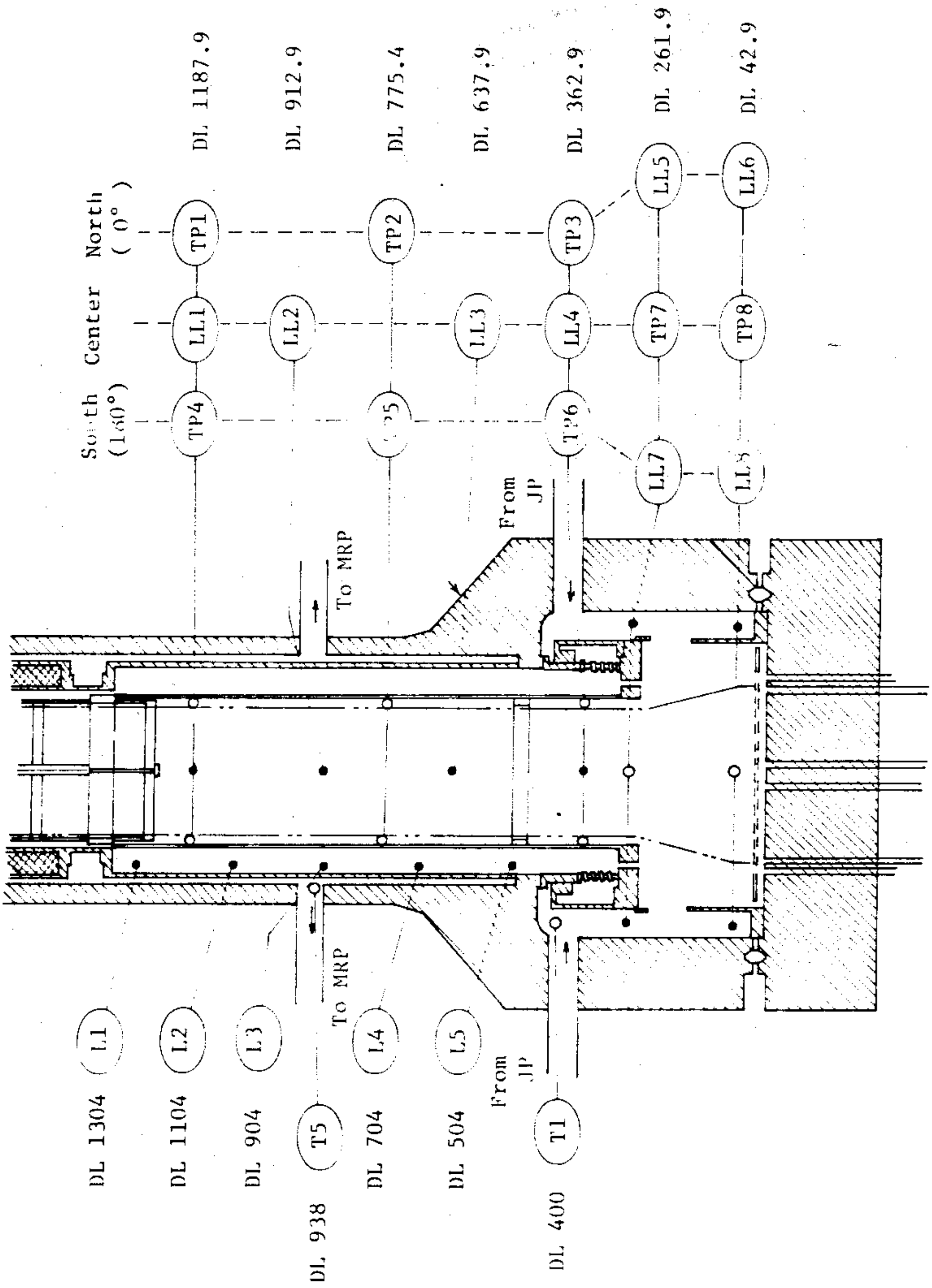

Fig. 3.10 Instrumentation location in lower plenum.

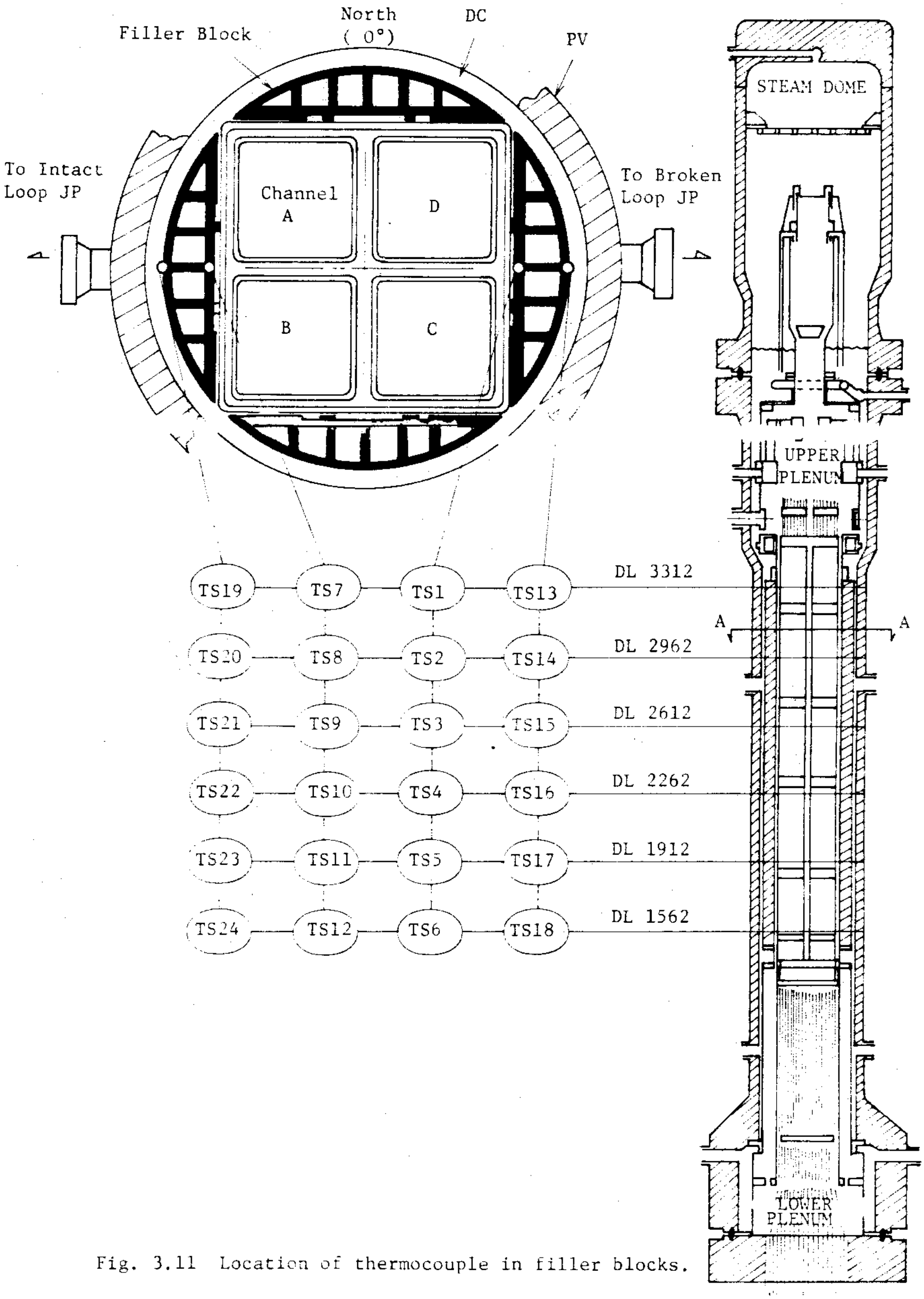

Fig. 3.11 Location of thermocouple in filler blocks.

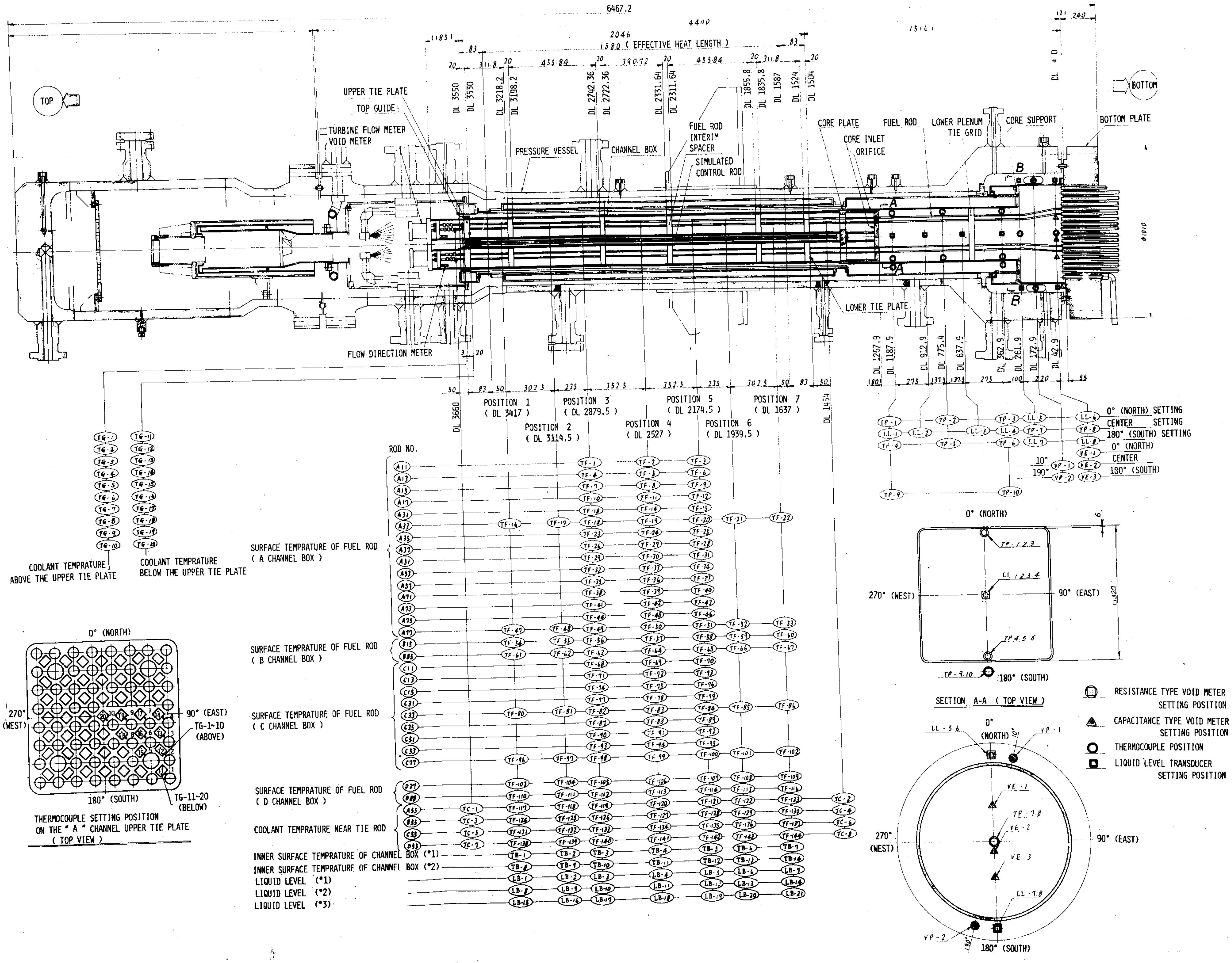

Fig. 3.12 ROSA-III core and lower plenum instrumentation (Assembly No. 2)

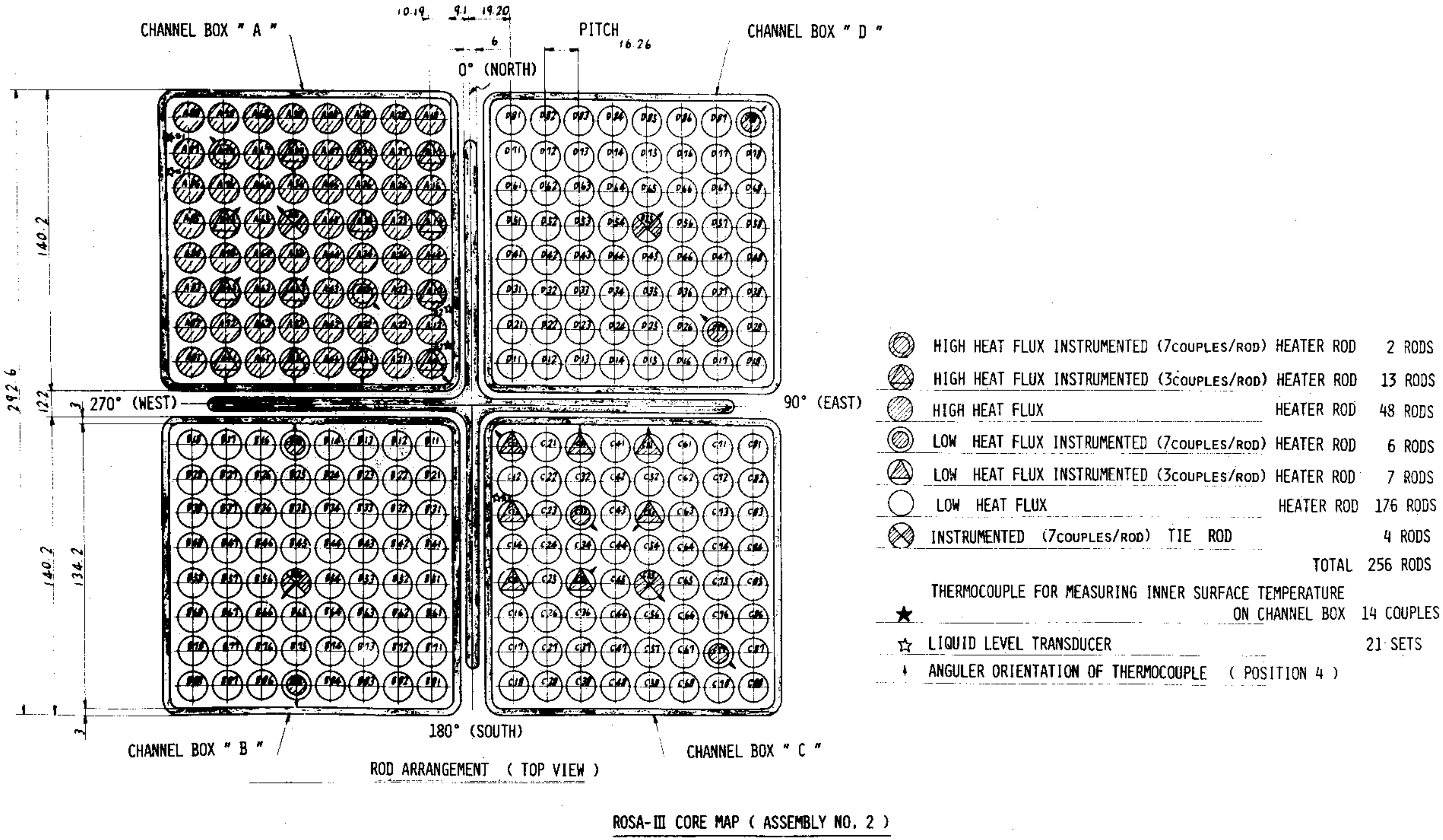

Fig. 3.13 ROSA-III core map

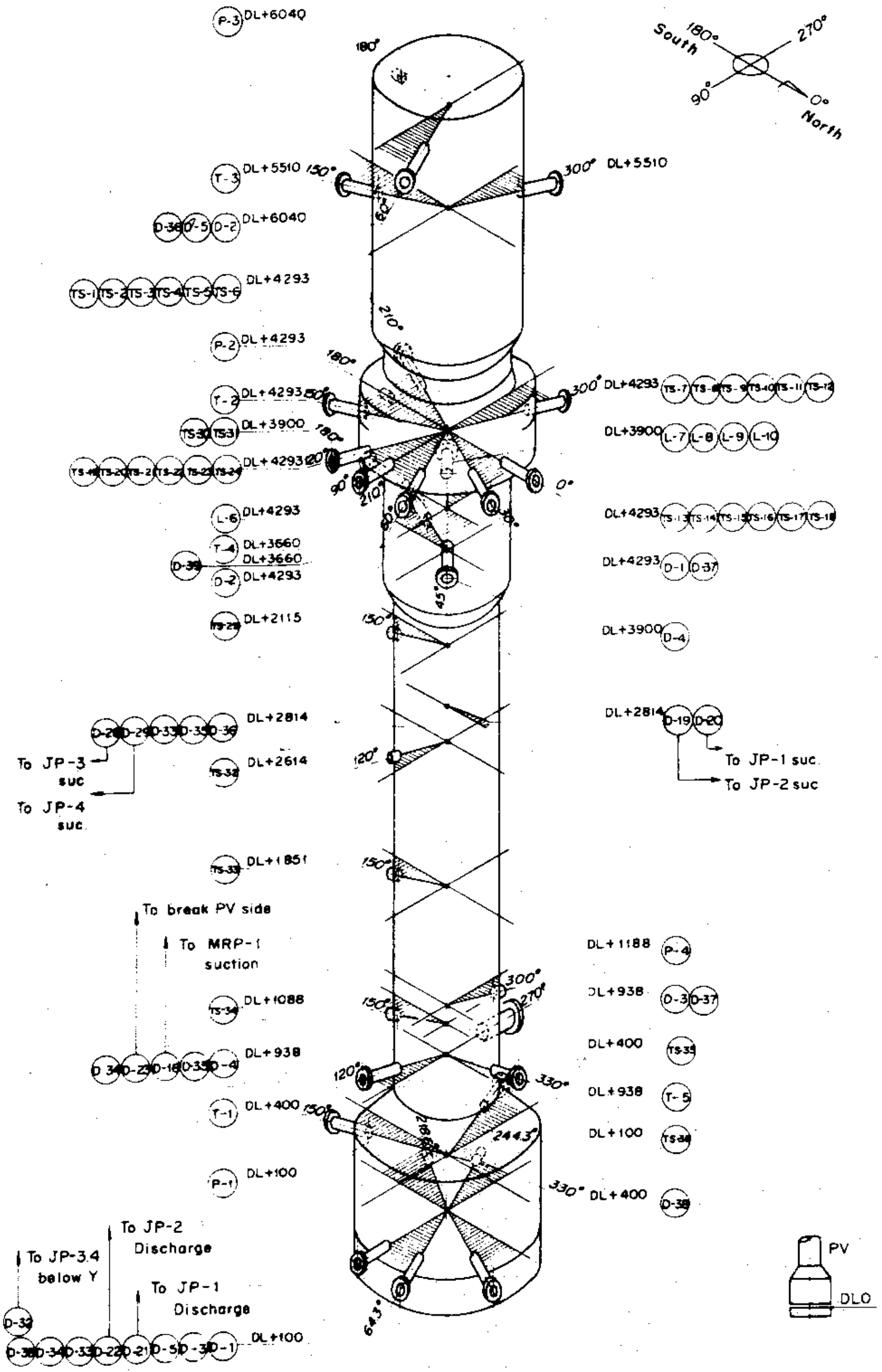

Fig. 3.14 Lead out nozzles for measurement in the pressure vessel.

1	1.01700E-01	-5.00000E+00	1.00000E+00	2	9.89000E-02	0.0	1.00000E+00
3	1.00600E-01	-4.00000E+00	1.00000E+00	4	9.93100E-02	2.50000E+01	1.00000E+00
16	1.03300E-01	1.00000E+01	1.00000E+00				

DELT-T 733 (MS) DATE 79-12-12 NO-1

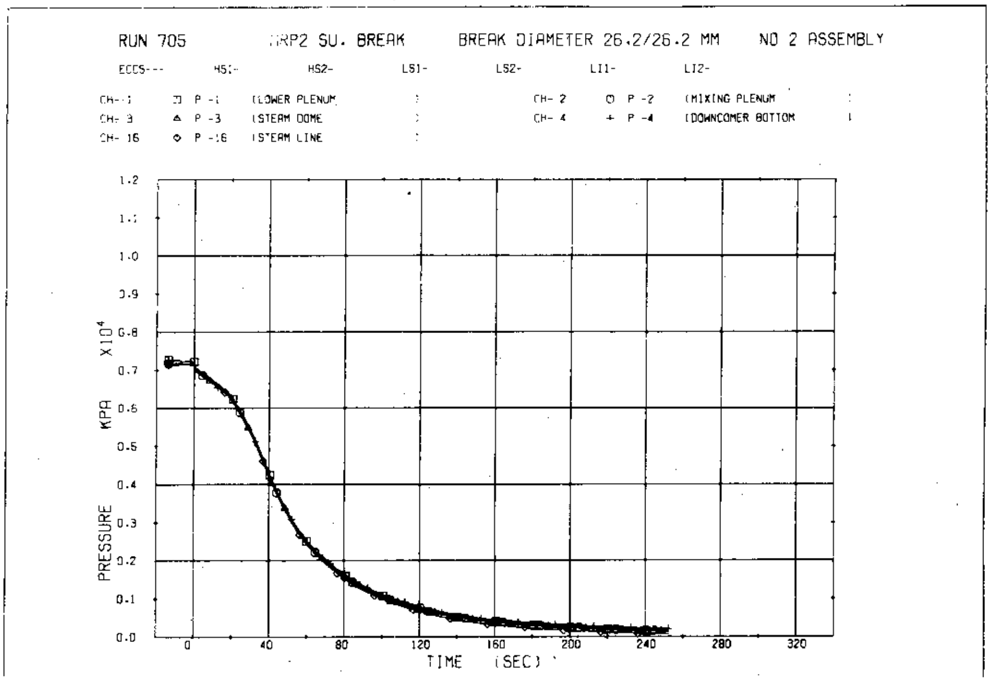

Fig. 5. 1 Pressures in pressure vessel

5	9.82500E-02	2.00000E+01	1.00000E+00	6	1.01830E-01	5.00000E+00	1.00000E+00
7	1.00100E-01	4.00000E+00	1.00000E+00	8	9.95800E-02	0.0	1.00000E+00

DELT-T 733 (MS) DATE 79-12-12 NO-2

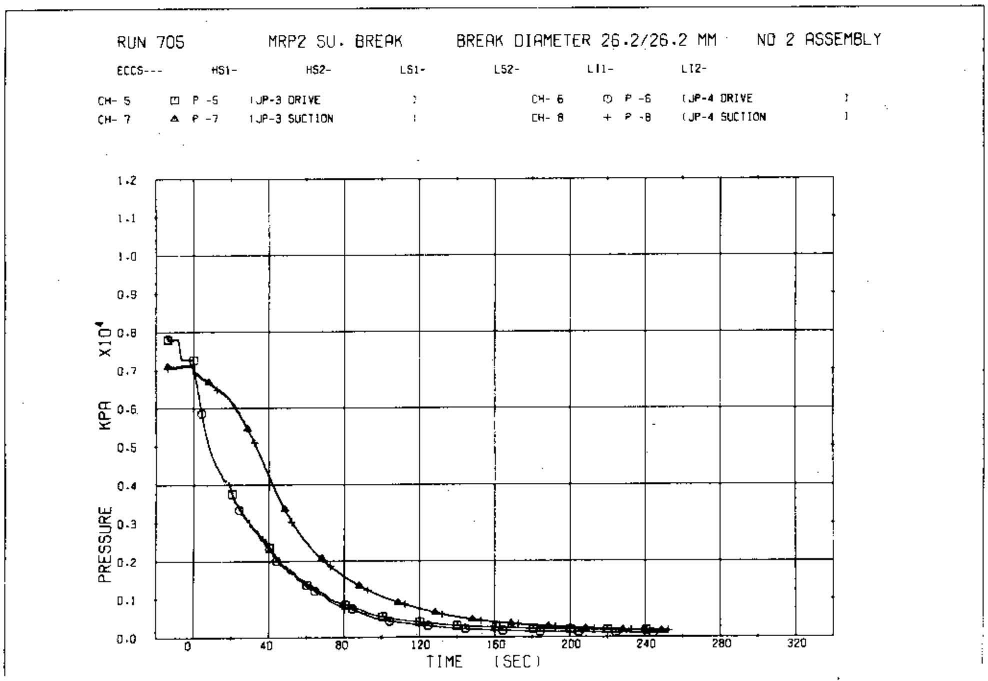

Fig. 5.2 Pressures in jet pumps

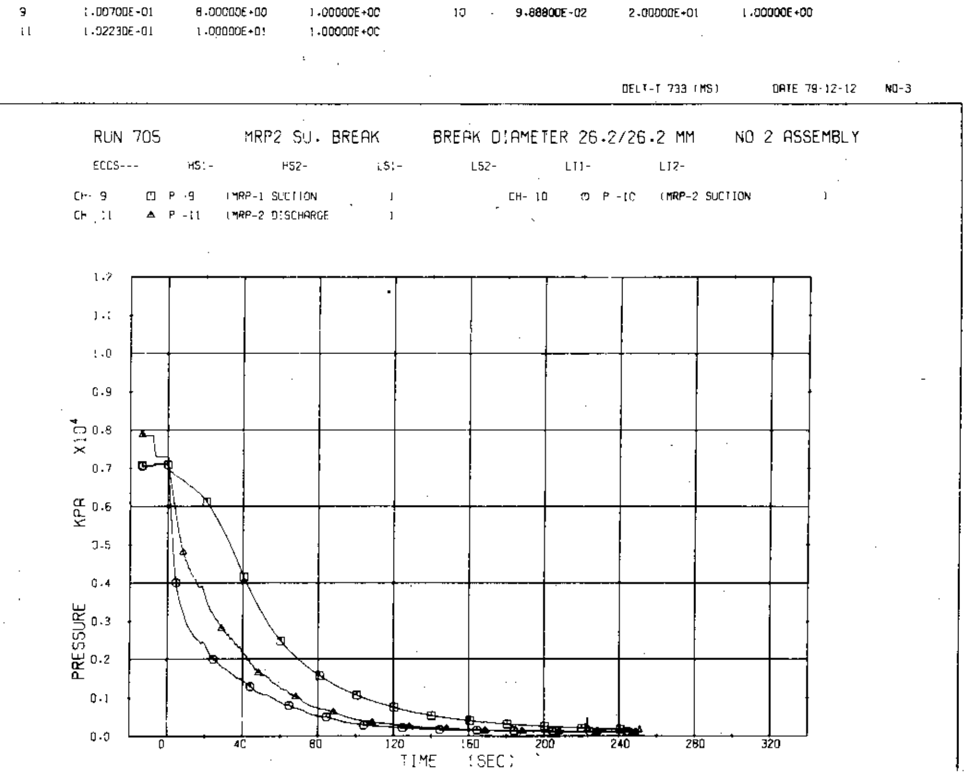

Fig. 5. 3 Pressures at recirculation pump suction

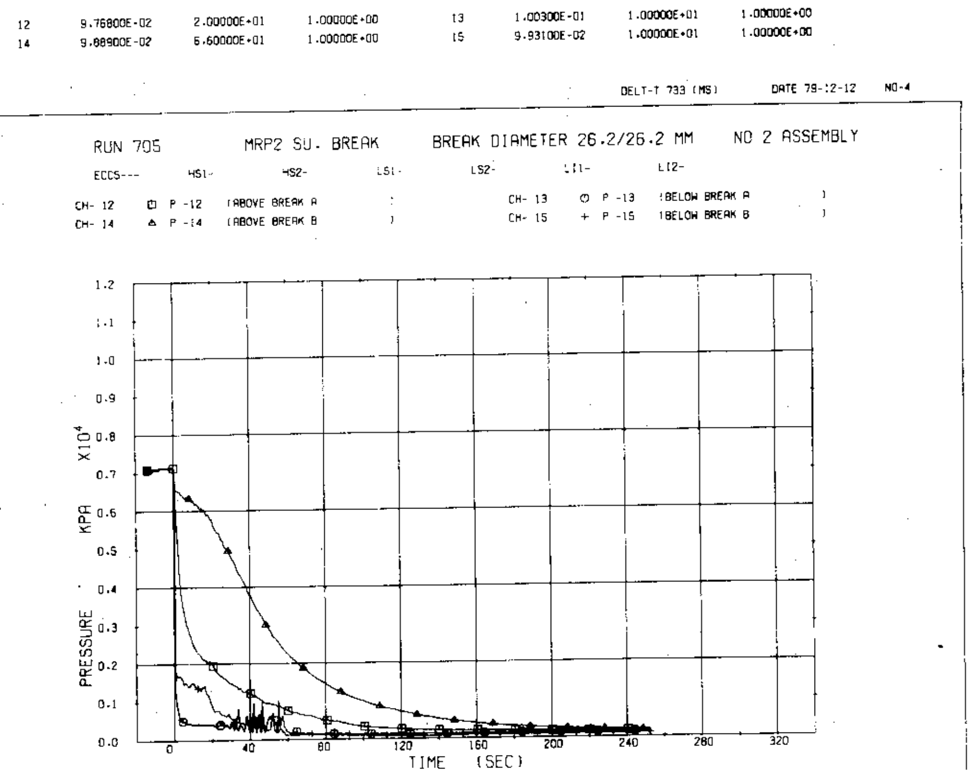

Fig. 5.4 Pressures at immediate up- and down-streams of the break

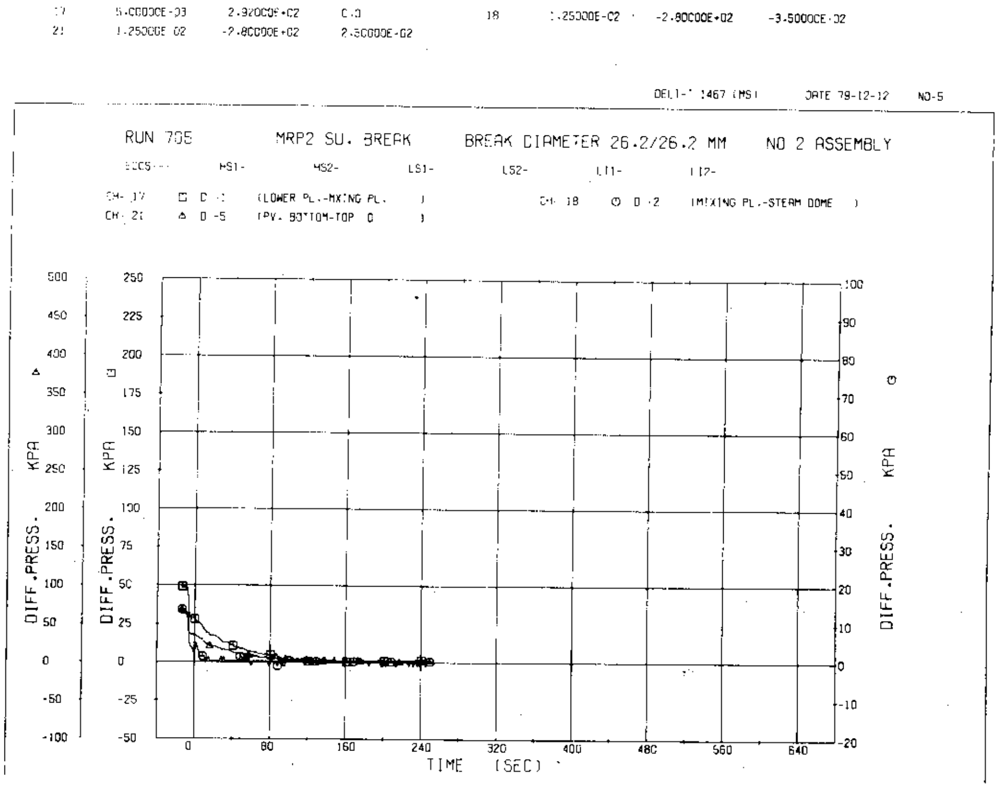

Fig. 5. 5 Differential pressures between lower plenum and upper plenum, and upper plenum and steam dome.

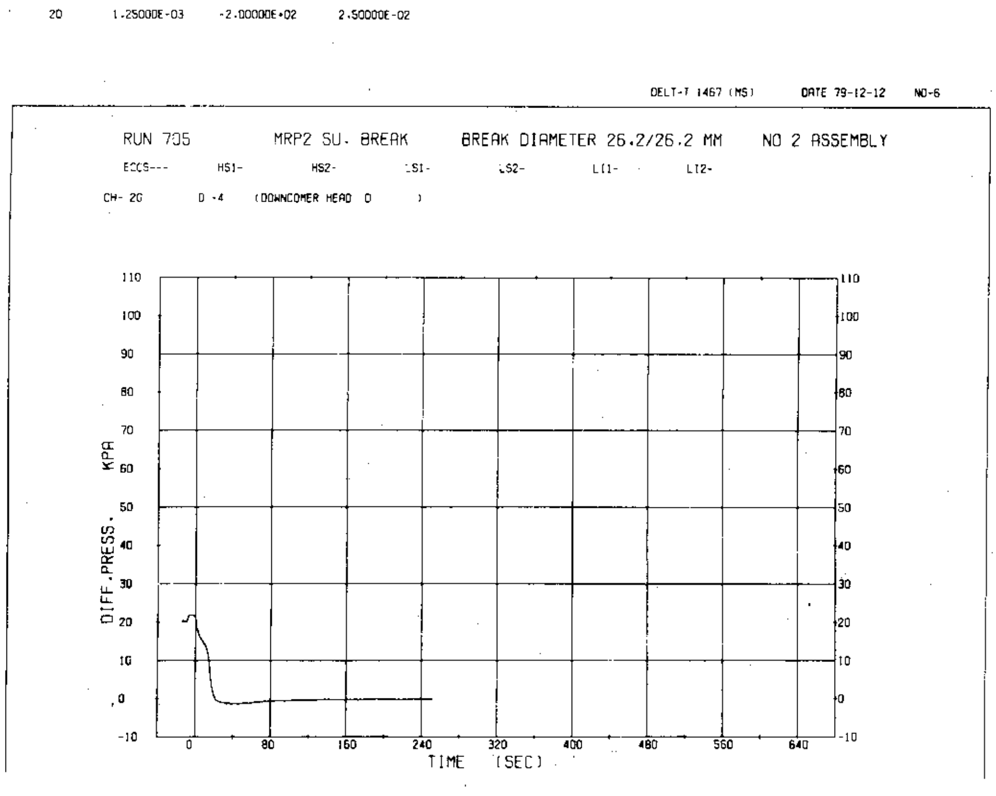

Fig. 5.6 Downcomer head

22 5.00000E-03 -4.00000E+02 4.50000E-02 23 3.12500E-02 -2.00000E+02 0.0
24 5.00000E-03 -4.00000E+02 8.00000E-02 25 3.12500E-02 -2.00000E+02 0.0

DELT-T 1467 (MS) DATE 79-12-12 NO-7

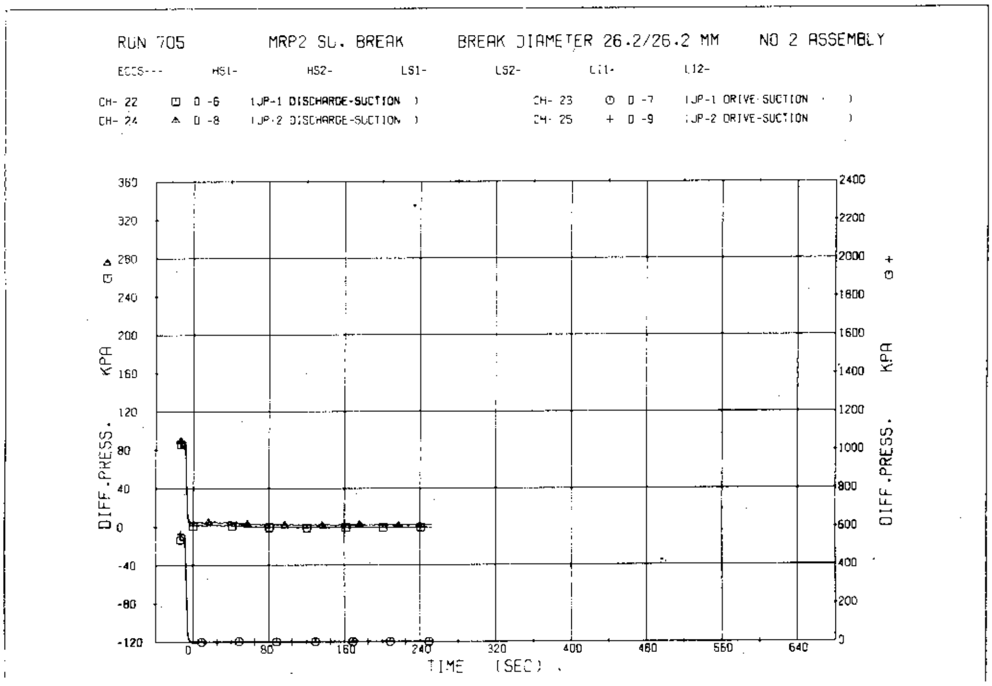

Fig. 5. 7 Differential pressures between discharge and suction, and between drive and suction of intact loop jet pumps

26 5.00000E-03 -4.00000E+02 3.50000E-02 27 3.75000E-02 -3.33000E+02 2.50000E-01
28 5.00000E-03 -4.00000E+02 0.0 29 3.75000E-02 -3.33000E+02 2.00000E-01

DELT-T 1467 (MS) DATE 79-12-12 NO-8

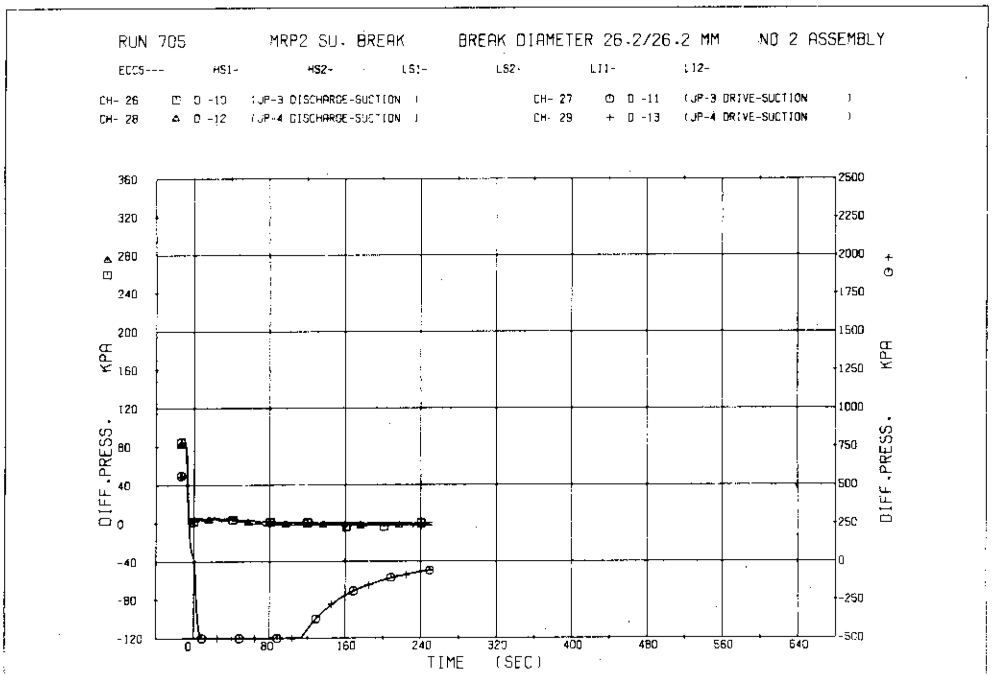

Fig. 5.8 Differential pressures between discharge and suction, and between drive and suction of broken loop jet pumps

30 3.25000E-02 -2.35000E+02 0.0 31 3.25000E-02 -2.30000E+02 0.0

DELT-T 1457 (MS) DATE 79-12-12 NO-9

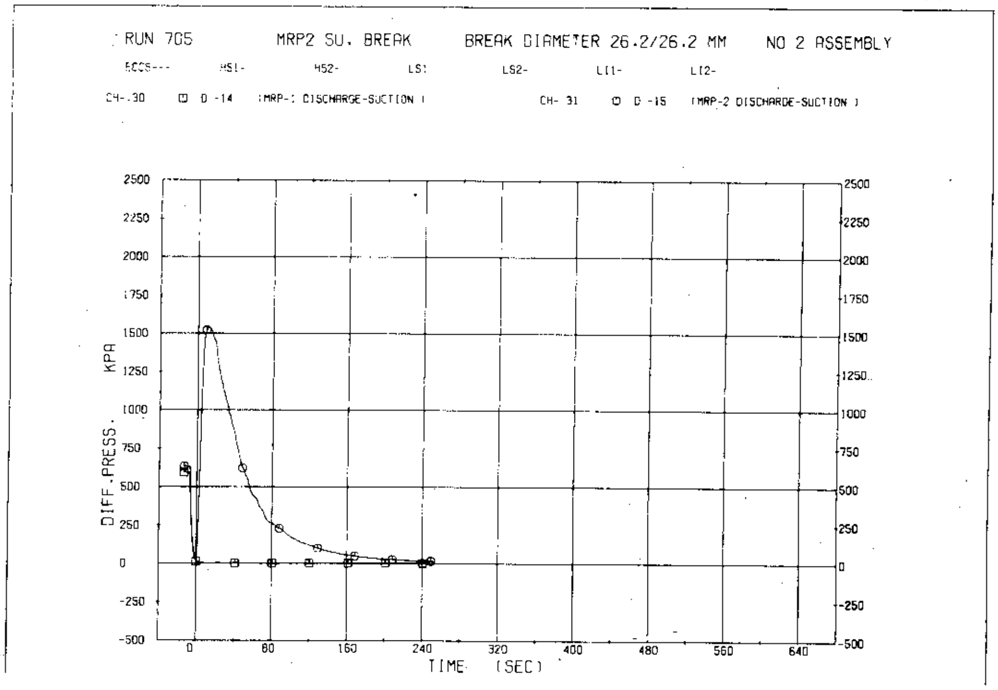

Fig. 5.9 Differential pressures between delivery and suction of recirculation pump

33 3.75000E-03 -2.00000E+02 0.0

DELT-T 733 (MS) DATE 79-12-12 NO-10

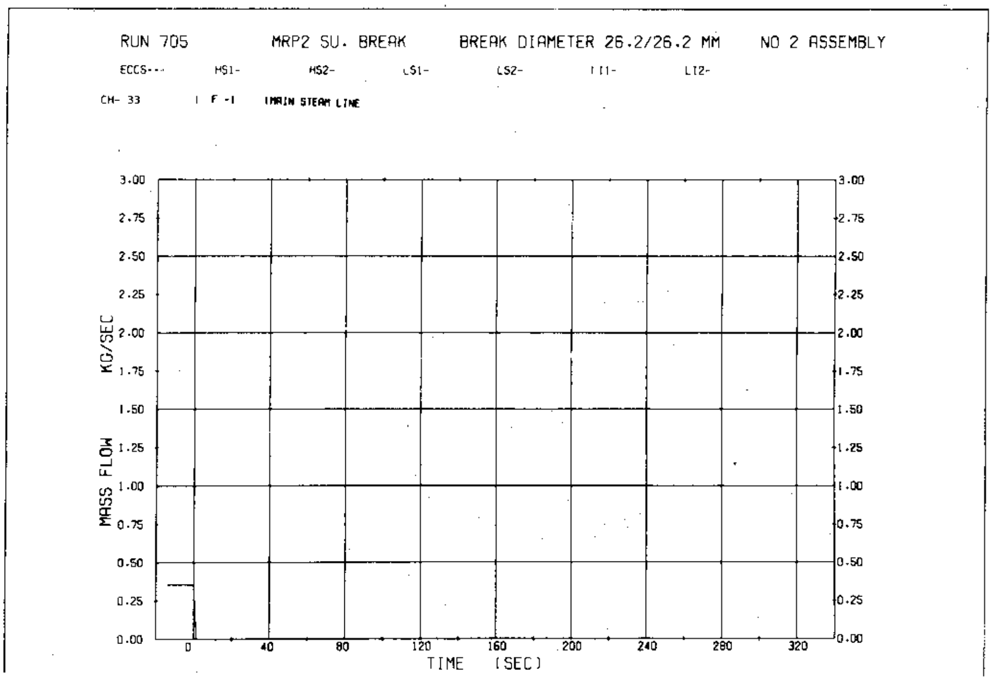

Fig. 5.10 Flow rates of naim steam line

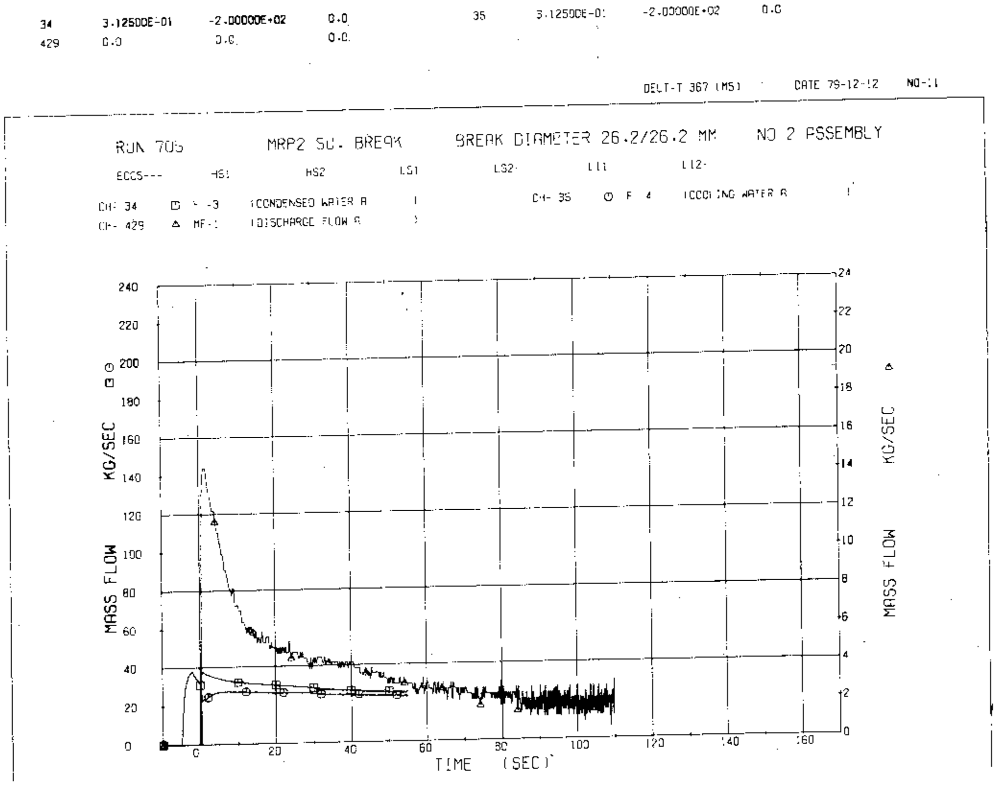

Fig. 5.11 Discharge flow rate at the vessel side break

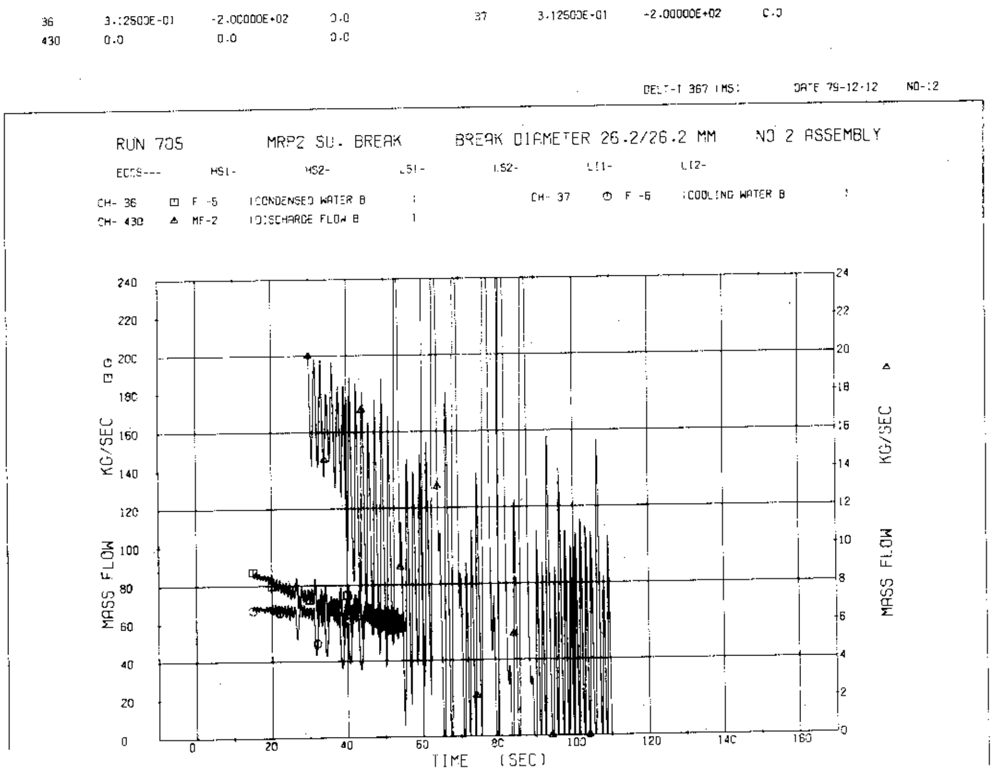

Fig. 5.12 Discharge flow rate at the pump side break

57 5.00000E+00 0.0 0.0 58 5.00000E+00 0.0 0.0

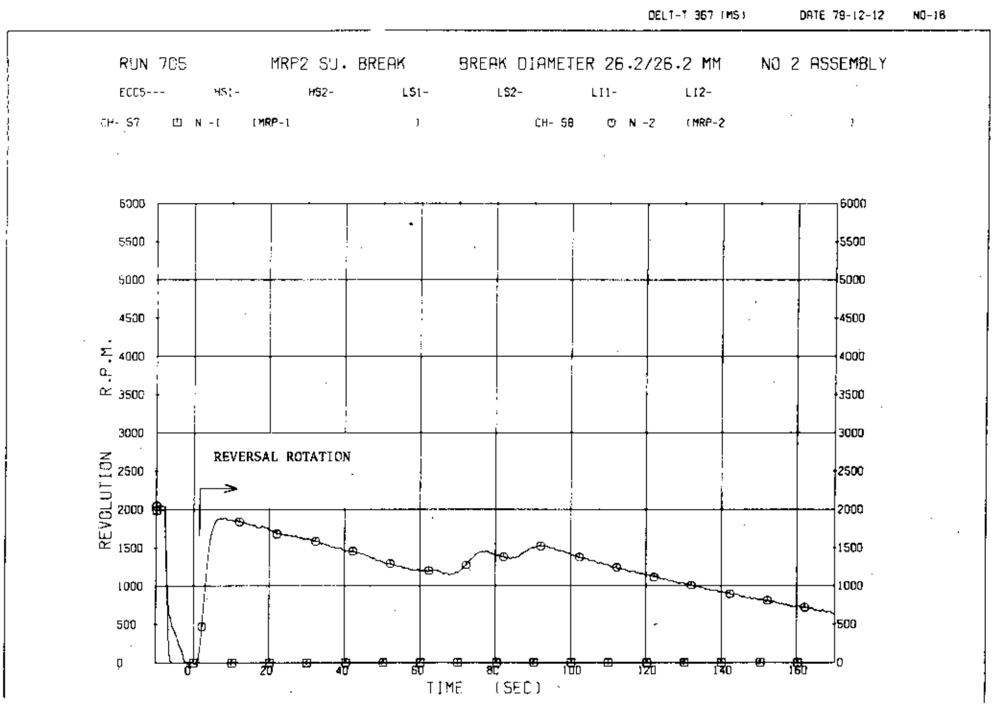

Fig. 5.13 Pump speeds of both recirculation line

59 1.00000E-02 0.0 0.0 60 1.00000E-02 0.0 0.0
61 1.00000E-02 0.0 0.0

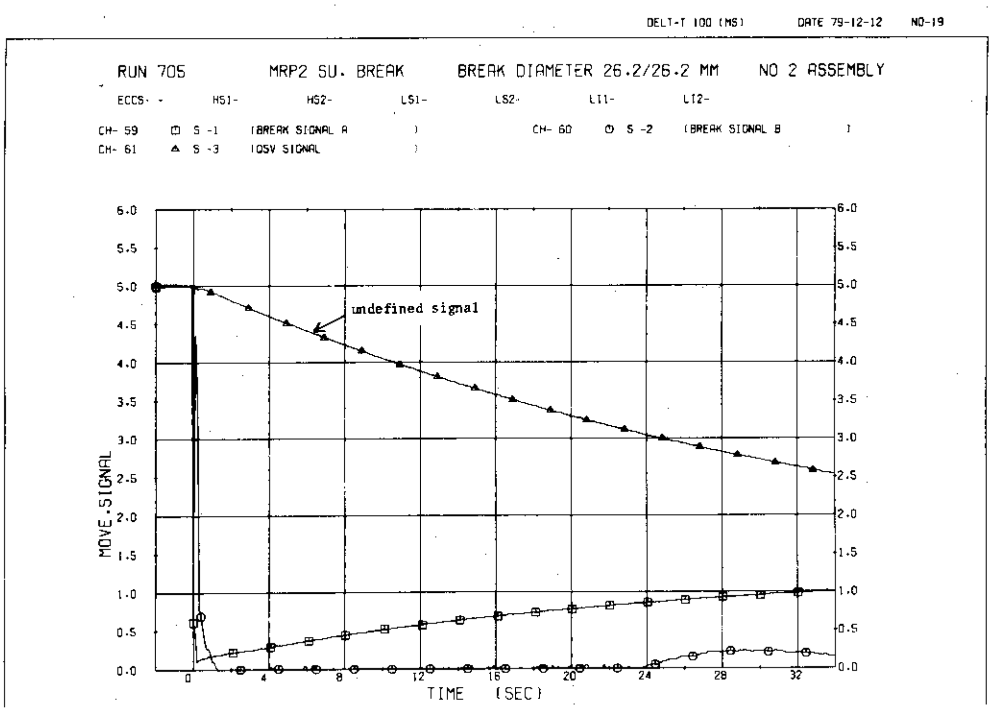

Fig. 5.14 Break signals

65	4.00000E-01	0.0	0.0	66	4.00000E-01	0.0	0.0
67	4.00000E-01	0.0	0.0	68	4.00000E-01	0.0	0.0
69	4.00000E-01	0.0	0.0				

DELT-T 1467 (MS) DATE 79-12-12 ND-21

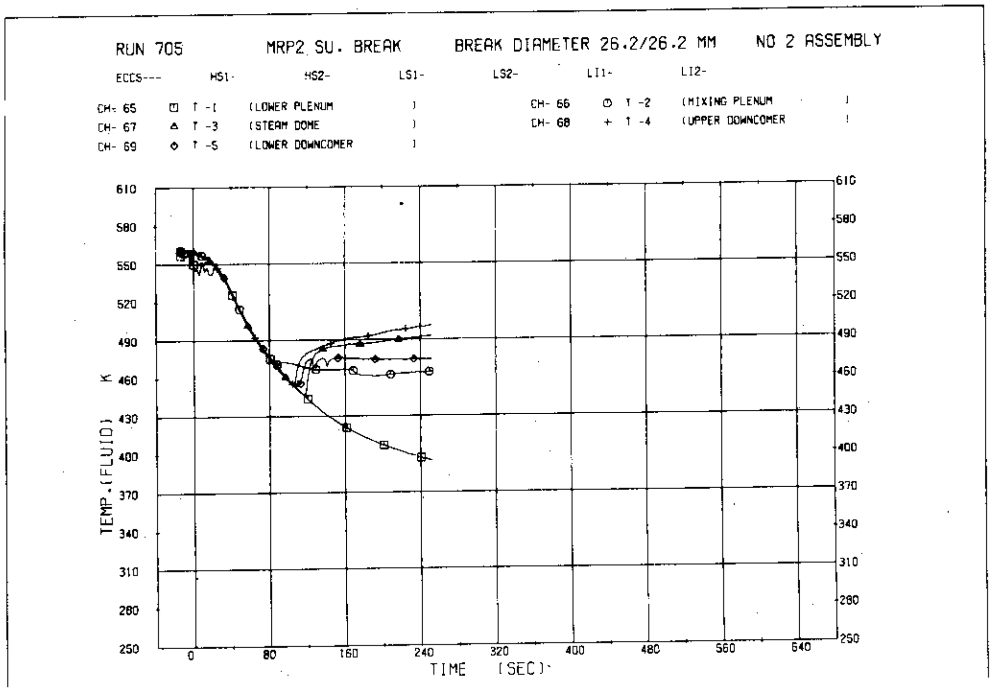

Fig. 5.15 Fluid temperatures in pressure vessel

70	4.00000E-01	0.0	0.0	71	4.00000E-01	0.0	0.0
74	4.00000E-01	0.0	0.0	75	4.00000E-01	0.0	0.0

DELT-T 1467 (MS) DATE 79-12-12 ND-22

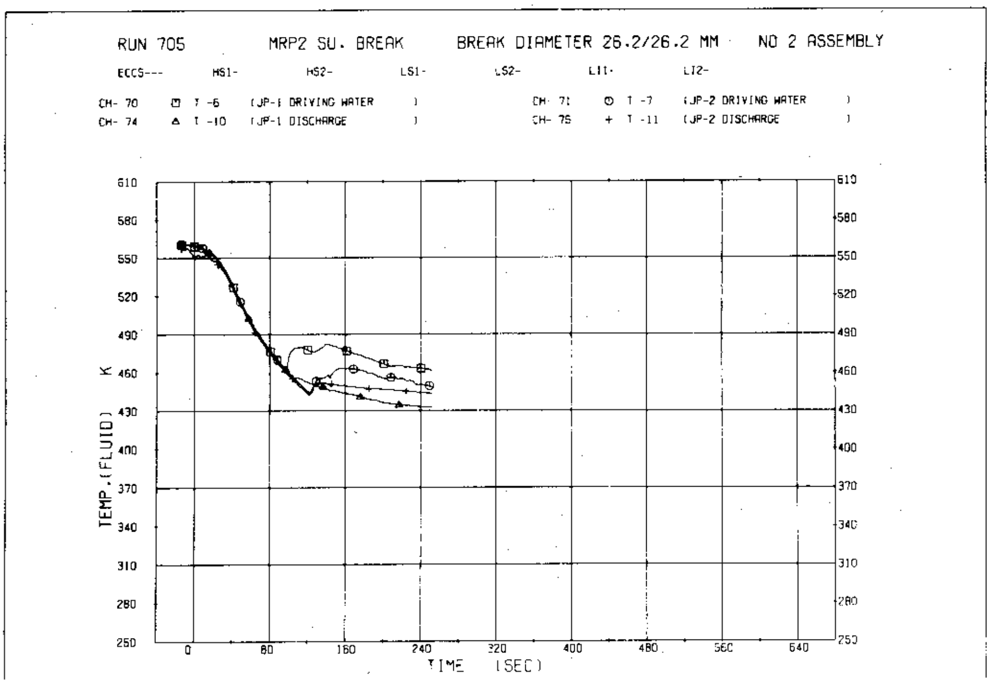

Fig. 5.16 Fluid temperatures in intact loop jet pumps

72 4.00000E-01 0.0 0.0 73 4.00000E-01 0.0 0.0
76 4.00000E-01 0.0 0.0 77 4.00000E-01 0.0 0.0

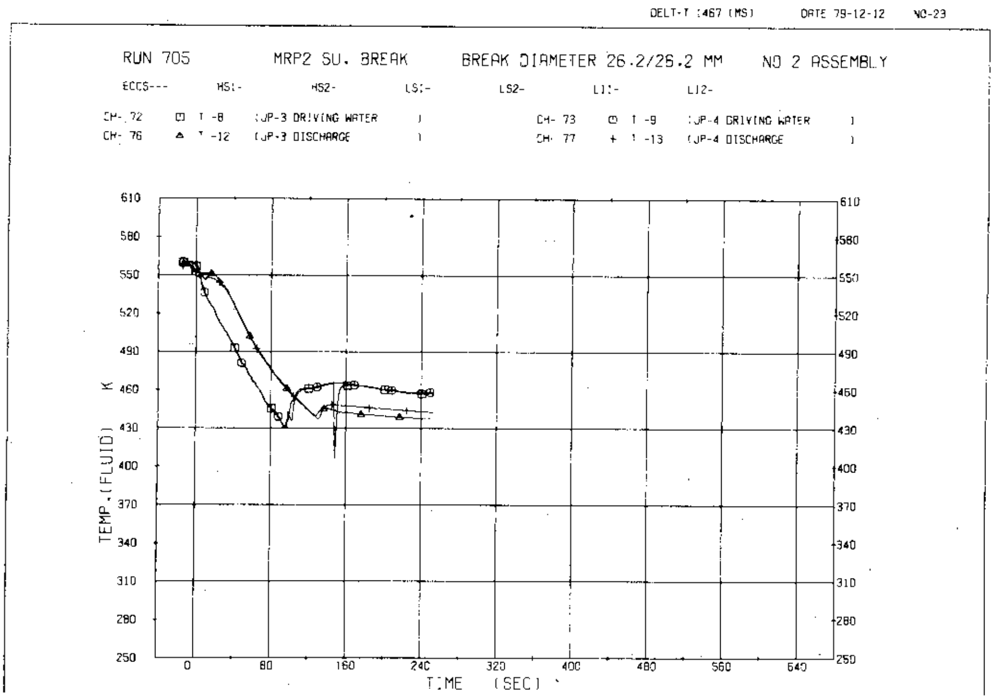

Fig. 5.17 Fluid temperatures in broken loop jet pumps

78 4.00000E-01 0.0 0.0 79 4.00000E-01 0.0 0.0

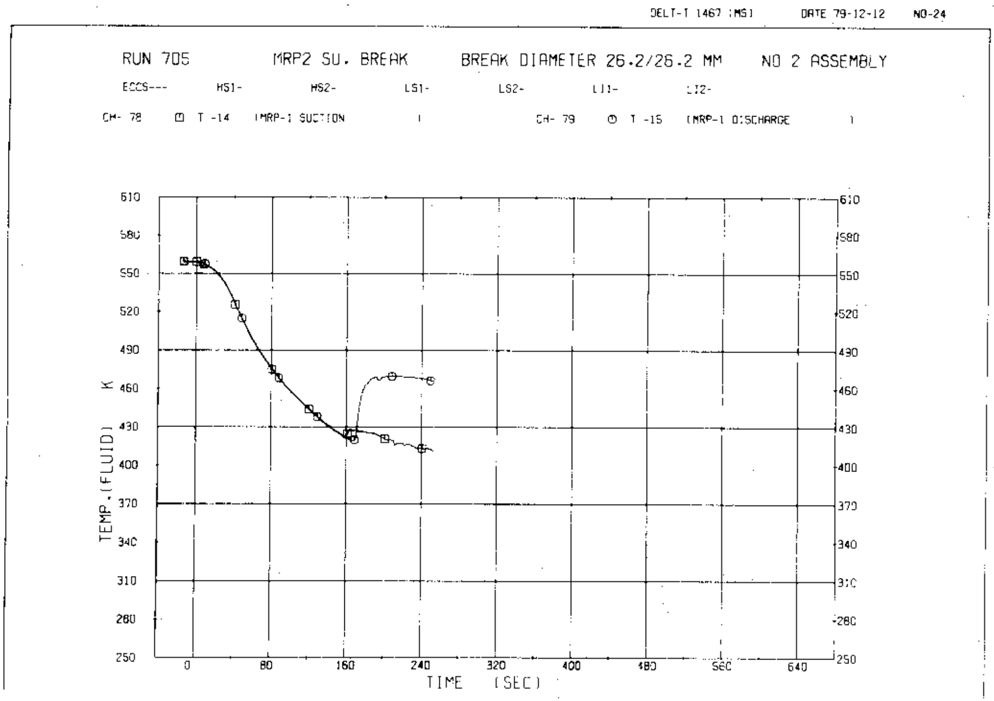

Fig. 5.18 Fluid temperatures at recirculation pump suction and delivery of intact loop

80 4.00000E-01 0.0 0.0 81 4.00000E-01 0.0 0.0
82 4.00000E-01 0.0 0.0 83 4.00000E-01 0.0 0.0

DELT-T 1467 (MS) DATE 79-12-12 NO-25

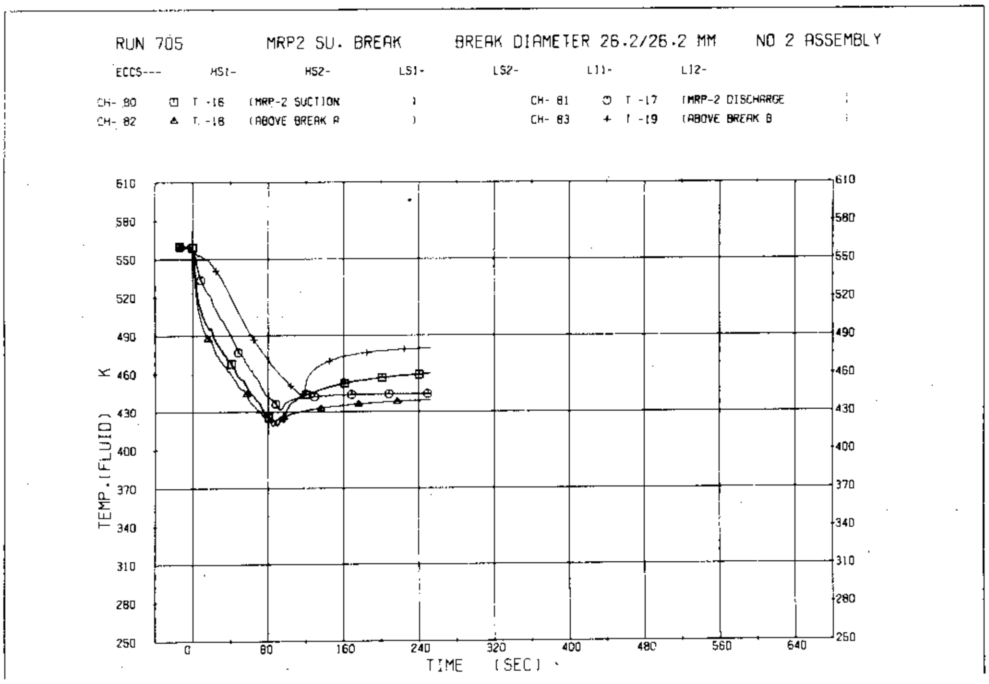

Fig. 5.19 Fluid temperatures at recirculation pump suction and delivery of broken loop, and at upstream of breaks

85 4.25000E-01 0.0 0.0 437 0.0 0.0 0.0

DELT-T 357 (MS) DATE 79-12-12 NO-26

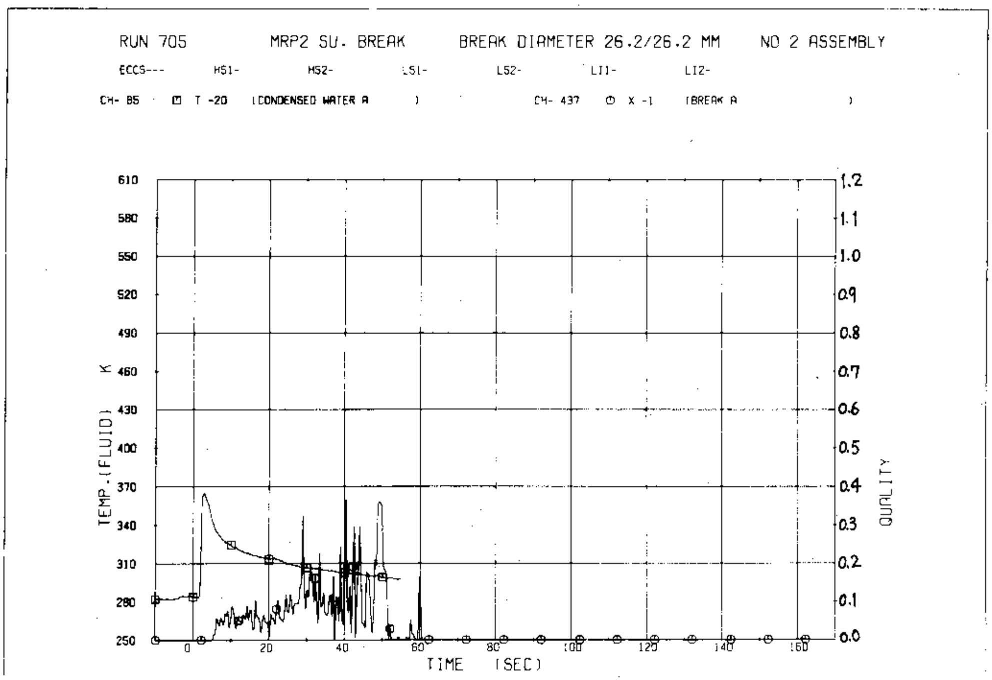

Fig. 5.20 Condensed water temperature of pump side break, and discharged fluid quality

84 4.25000E-01 0.0 0.0 438 0.0 0.0 0.0

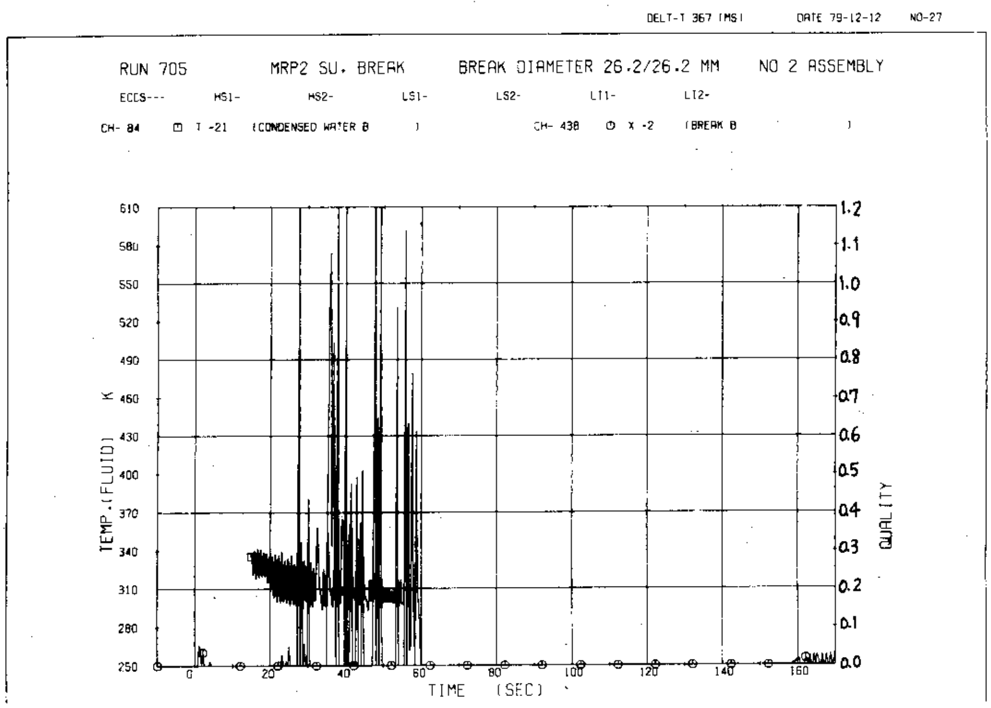

Fig. 5.21 Condensed water temperature of vessel side break

86 4.00000E-01 0.0 0.0

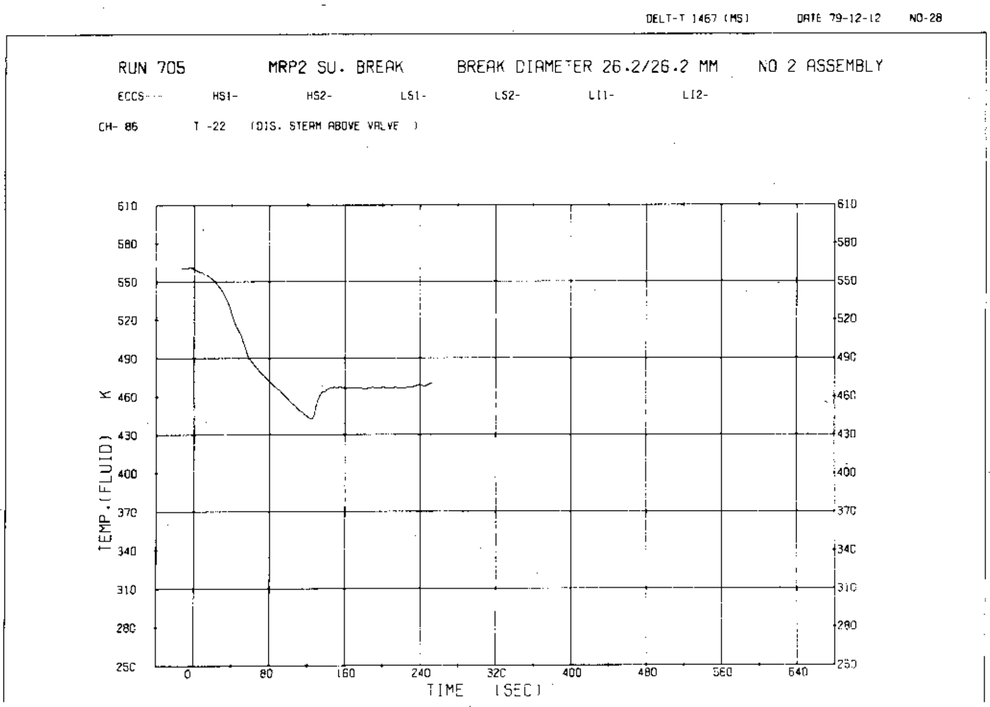

Fig. 5.22 Discharged steam temperatures at up-stream of control valve in the main steam line

88	4.00000E-01	0.0	0.0	89	4.00000E-01	0.0	0.0
90	4.00000E-01	0.0	0.0	91	4.00000E-01	0.0	0.0

DELT-T 1467 (MS) DATE 79-12-12 NO-29

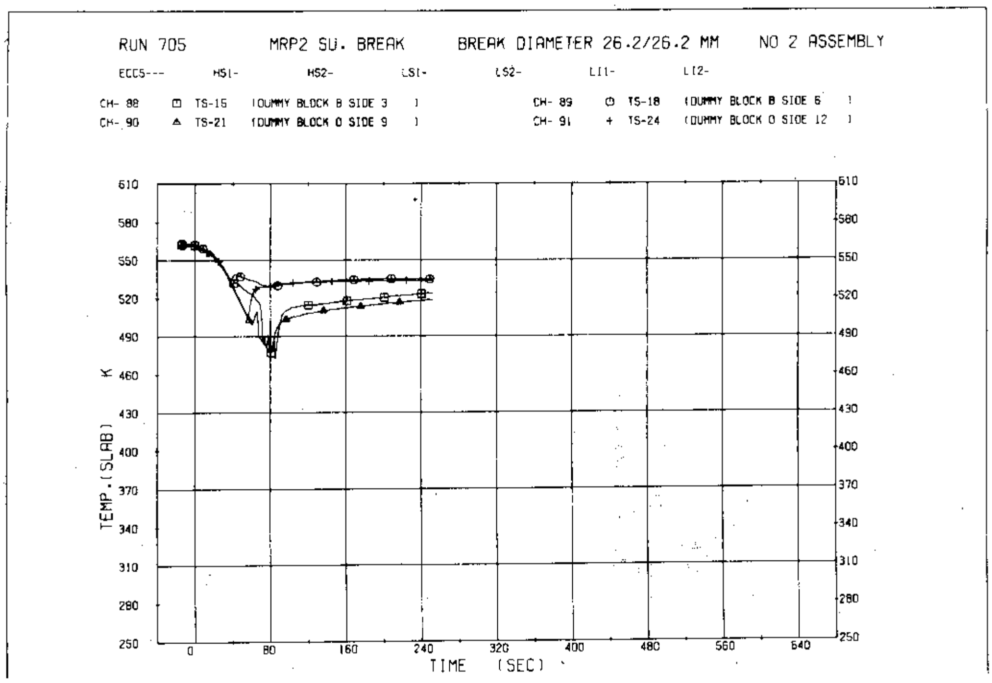

Fig. 5.23 Surface temperatures of filler blocks

92	4.00000E-01	0.0	0.0	93	4.00000E-01	0.0	0.0
94	4.00000E-01	0.0	0.0	95	4.00000E-01	0.0	0.0

DELT-T 1467 (MS) DATE 79-12-12 NO-30

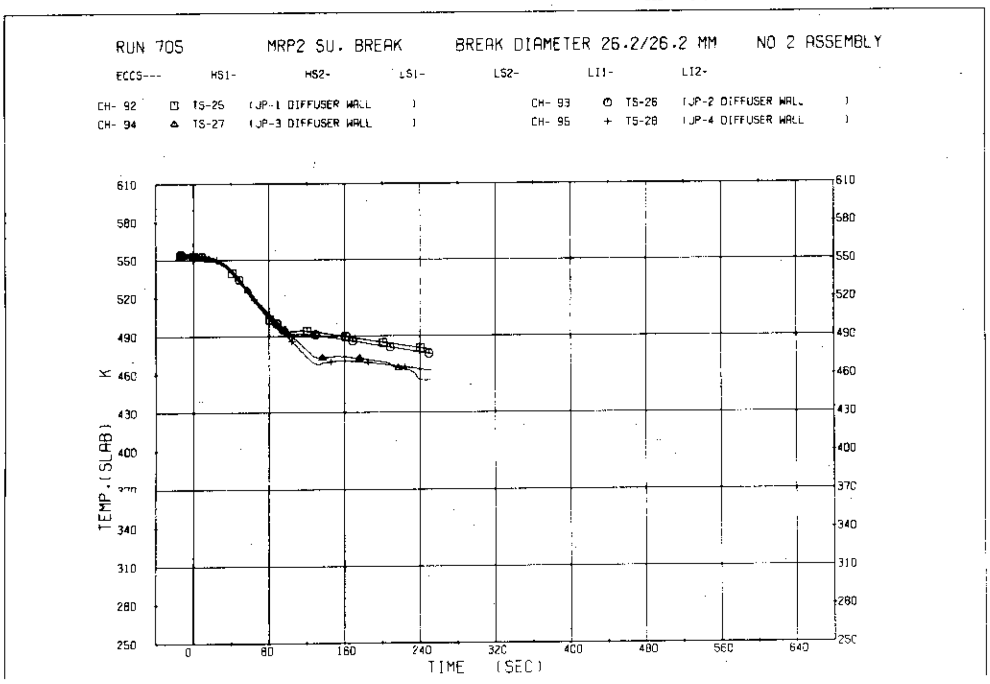

Fig. 5.24 Slab temperatures of jet pump diffuser

96 4.00000E-01 0.0 0.0 97 4.00000E-01 0.0 0.0
98 4.00000E-01 0.0 0.0 102 4.00000E-01 0.0 0.0
103 4.00000E-01 0.0 0.0

DELT-T 1467 (MS) DATE 79-12-12 NO-31

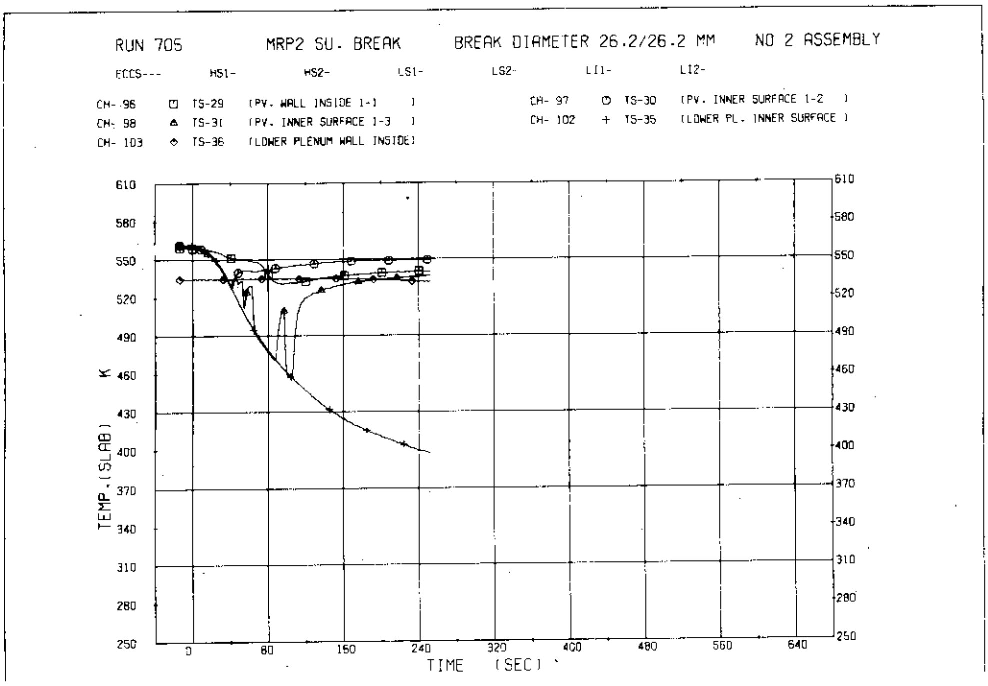

Fig. 5.25 Inner surface temperatures of pressure vessel

99 4.00000E-01 0.0 0.0 100 4.00000E-01 0.0 0.0
101 4.00000E-01 0.0 0.0

DELT-T 1467 (MS) DATE 79-12-12 NO-32

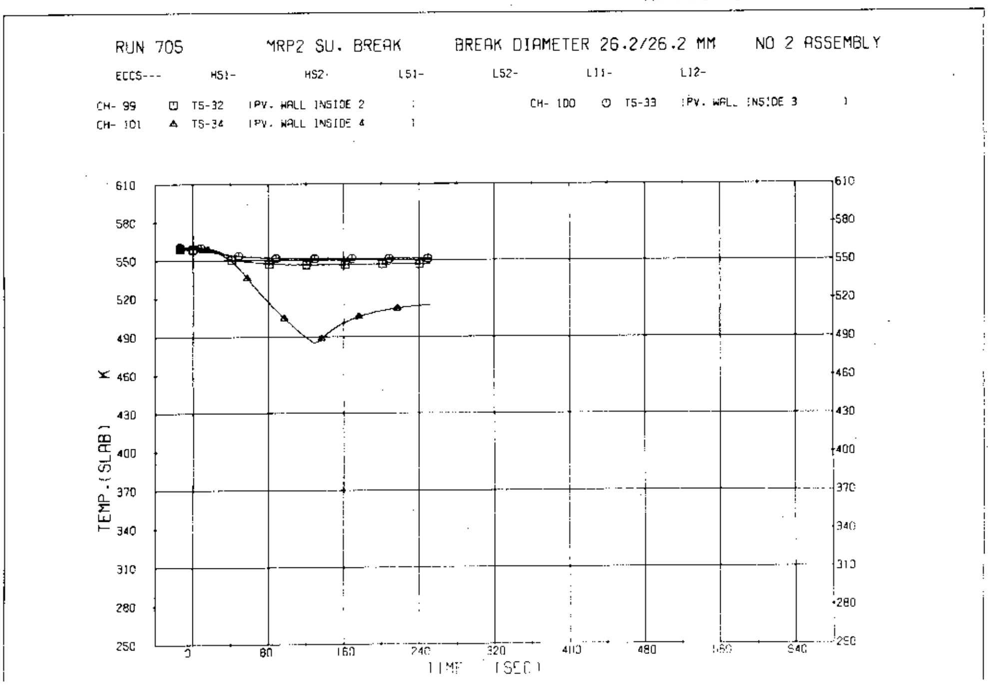

Fig. 5.26 Slab temperatures of pressure vessel

104 1.20000E+00 0.0 0.0 105 1.20000E+00 0.0 0.0
106 1.20000E+00 0.0 0.0

DELT-T 1467 (MS) DATE 79-12-12 NO-33

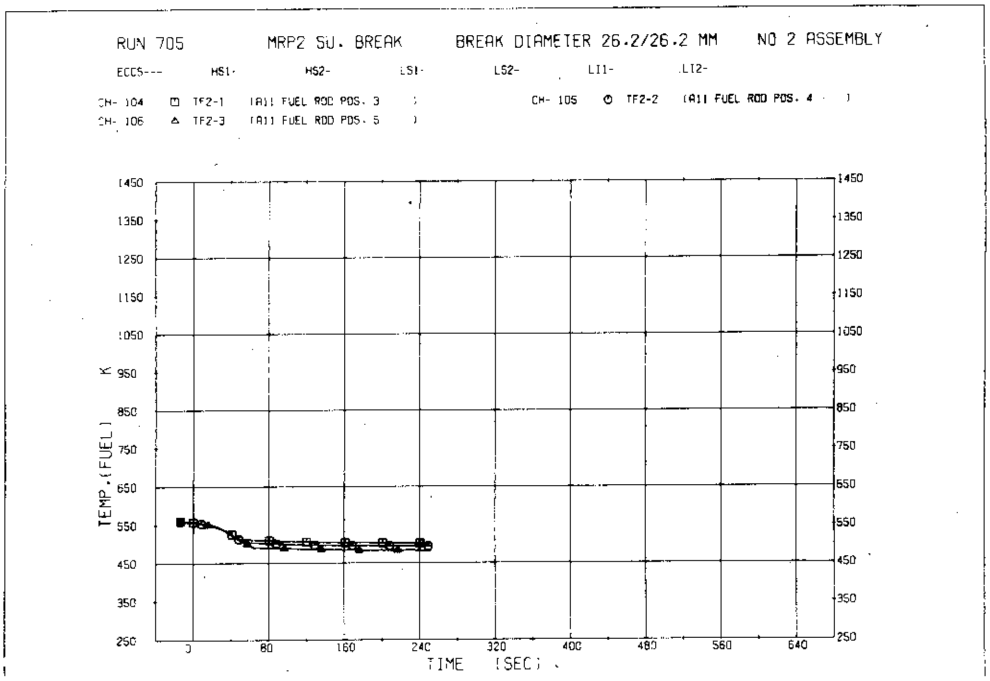

Fig. 5.27 Surface temperatures of fuel rod A11

107 1.20000E+00 0.0 0.0 108 1.20000E+00 0.0 0.0
109 1.20000E+00 0.0 0.0

DELT-T 1467 (MS) DATE 79-12-12 NO-34

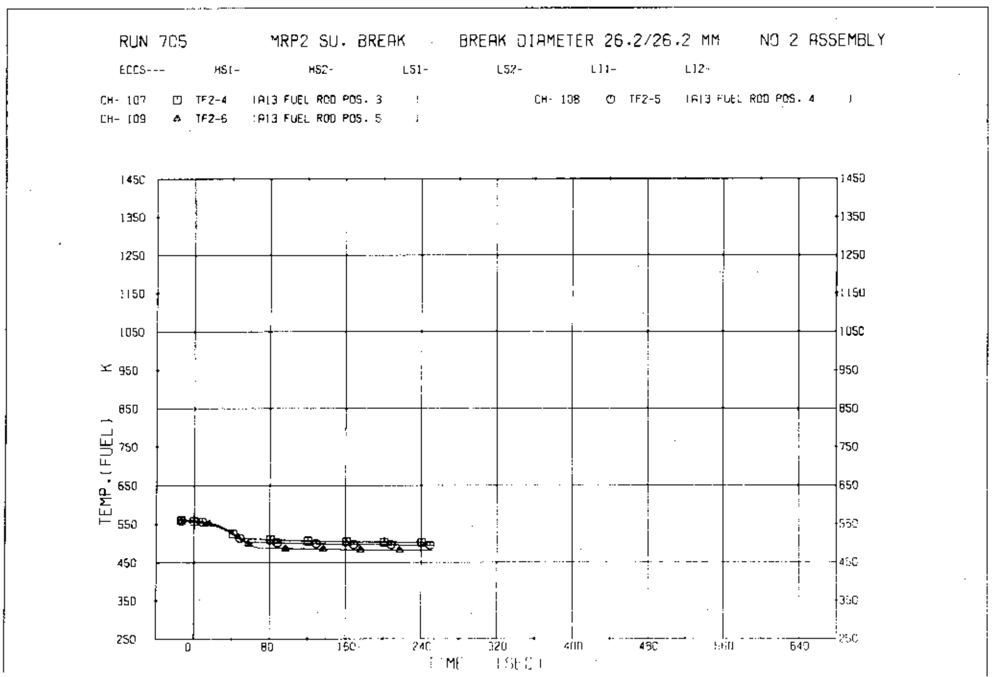

Fig. 5.28 Surface temperature of fuel rod A13

110	1.20000E+00	0.0	0.0	111	1.20000E+00	0.0	0.0
112	1.20000E+00	0.0	0.0				

DELT-T 1467 (MS) DATE 79-12-12 NO-35

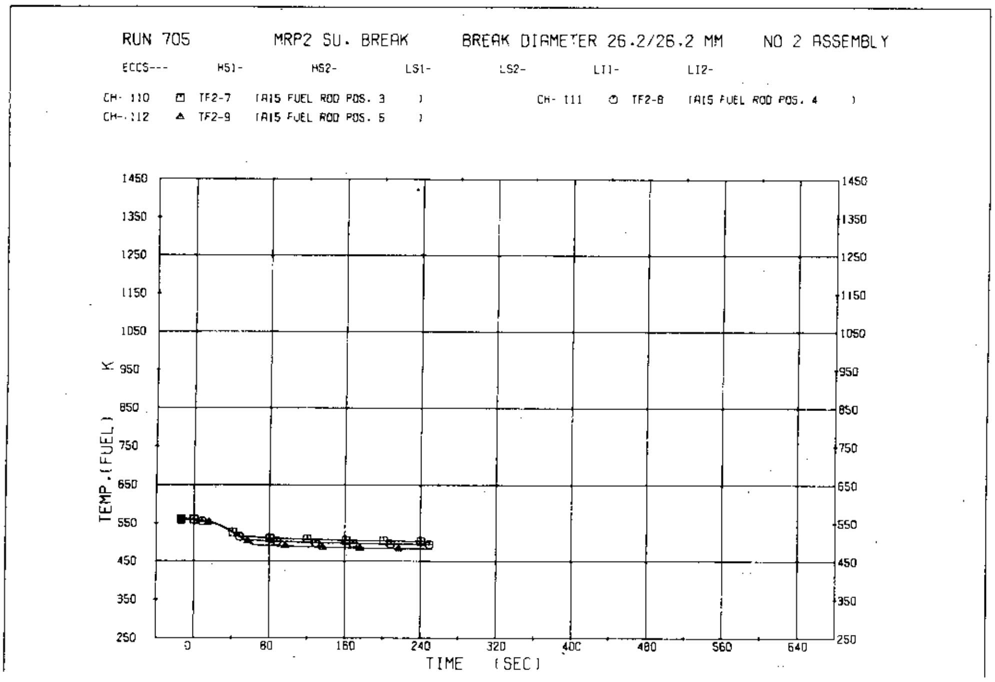

Fig. 5.29 Surface temperature of fuel rod A15

113	1.20000E+00	0.0	0.0	114	1.20000E+00	0.0	0.0
115	1.20000E+00	0.0	0.0				

DELT-T 1467 (MS) DATE 79-12-12 NO-36

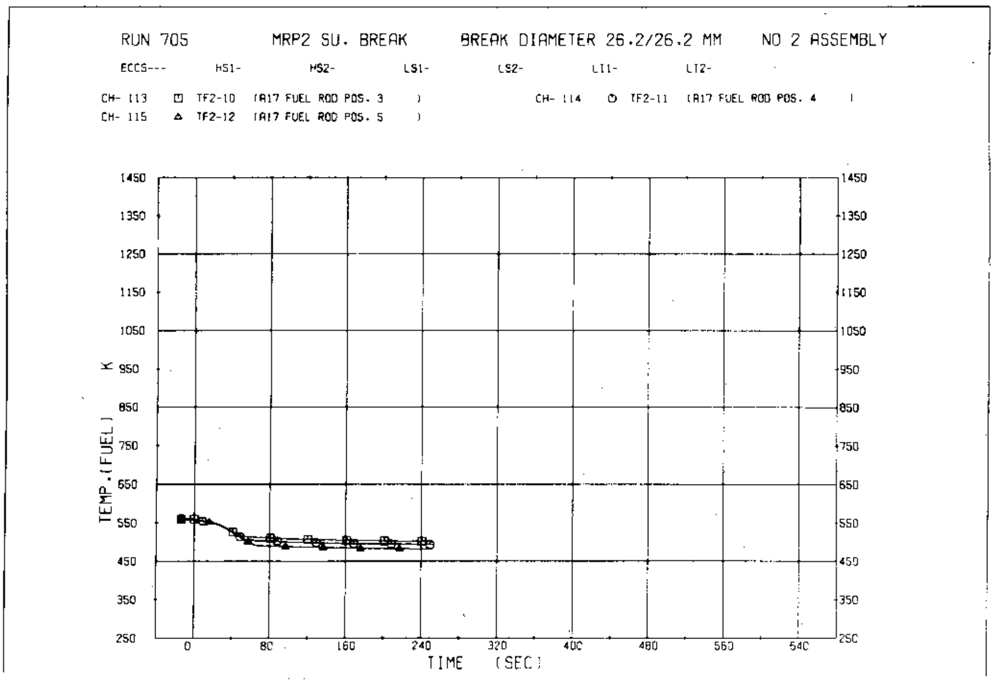

Fig. 5.30 Surface temperature of fuel rod A17

116	1.20000E+00	0.0	0.0	117	1.20000E+00	0.0	0.0
118	1.20000E+00	0.0	0.0				

DELT-T 1467 (MS) DATE 79-12-12 NO-37

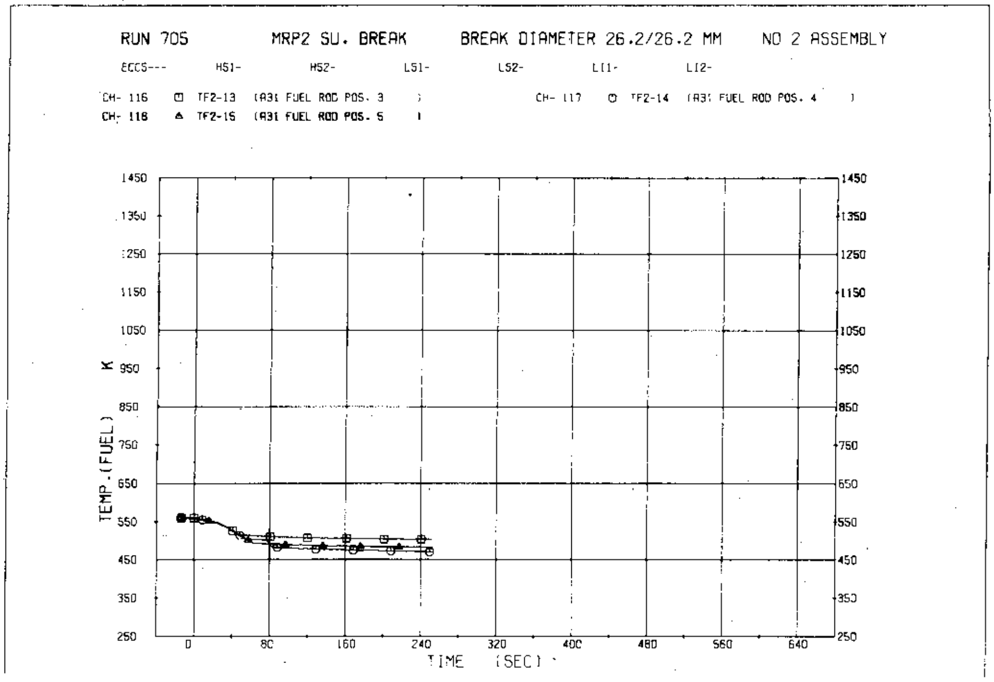

Fig. 5.31 Surface temperature of fuel rod A31

119	1.20000E+00	0.0	0.0	120	1.20000E+00	0.0	0.0
121	1.20000E+00	0.0	0.0	122	1.20000E+00	0.0	0.0
123	1.20000E+00	0.0	0.0	124	1.20000E+00	0.0	0.0
125	1.20000E+00	0.0	0.0				

DELT-T 1467 (MS) DATE 79-12-12 NO-38

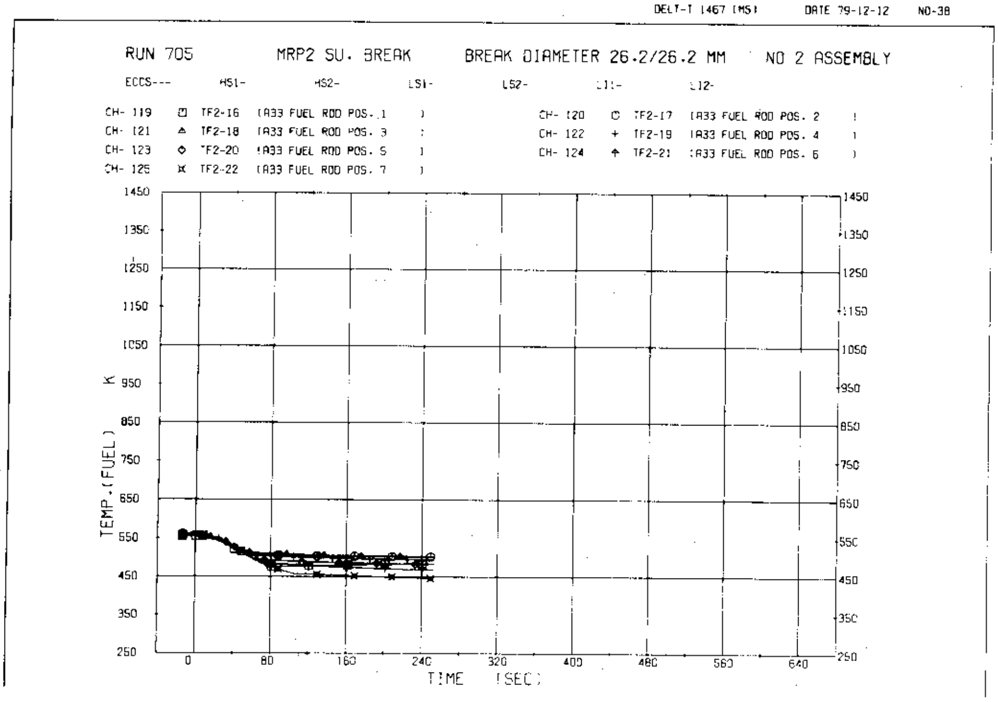

Fig. 5.32 Surface temperature of fuel rod A33

126	1.20000E+00	0.0	0.0	127	1.20000E+00	0.0	0.0
128	1.20000E+00	0.0	0.0				

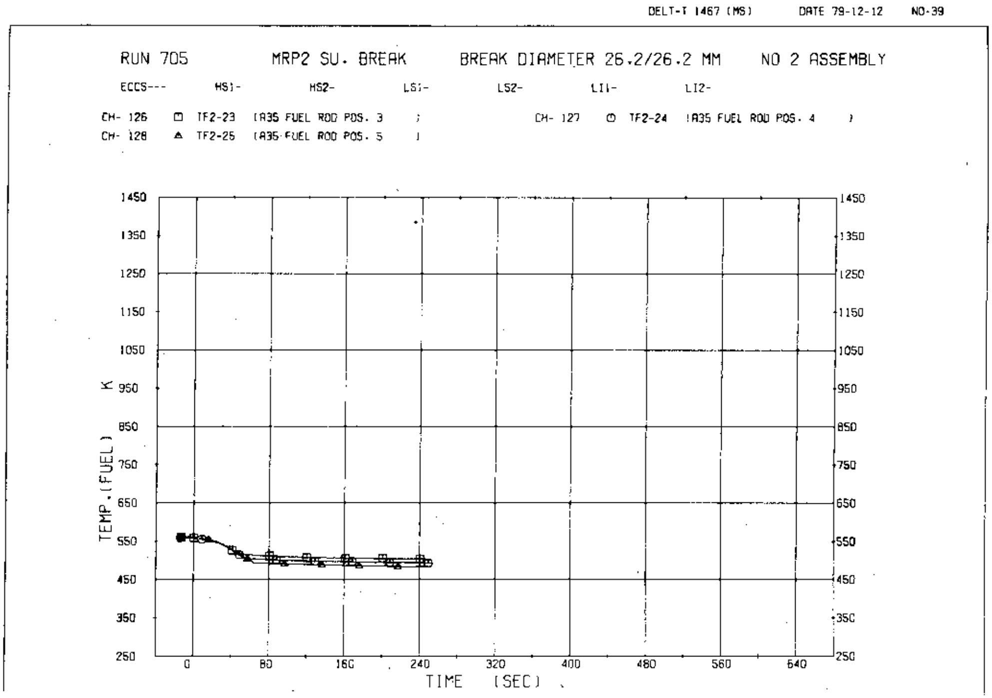

Fig. 5.33 Surface temperature of fuel rod A35

129	1.20000E+00	0.0	0.0	130	1.20000E+00	0.0	0.0
131	1.20000E+00	0.0	0.0				

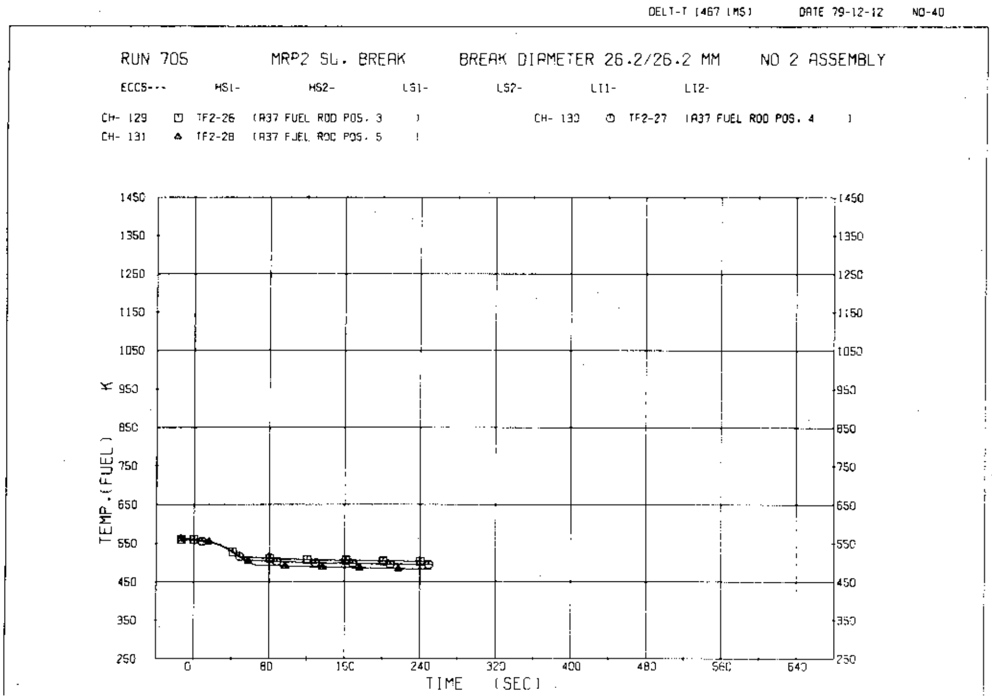

Fig. 5.34 Surface temperature of fuel rod A37

132 1.20000E+00 0.0 0.0 133 1.20000E+00 0.0 0.0
134 1.20000E+00 0.0 0.0

DELT-T 1467 (MS) DATE 79-12-12 NO-41

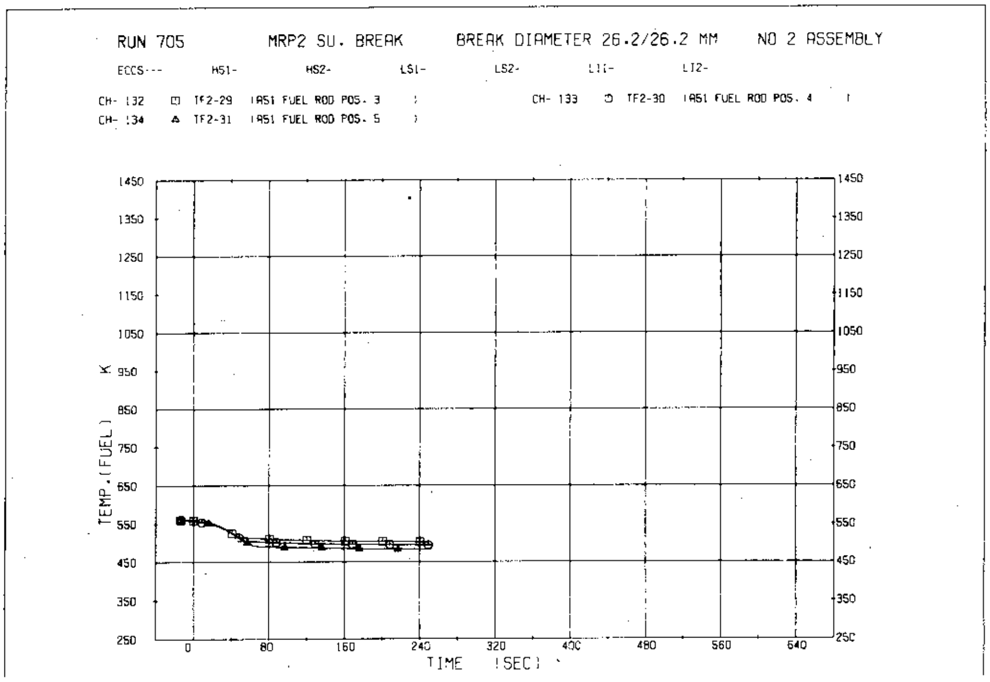

Fig. 5.35 Surface temperature of fuel rod A51

135 1.20000E+00 0.0 0.0 136 1.20000E+00 0.0 0.0
137 1.20000E+00 0.0 0.0

DELT-T 1467 (MS) DATE 79-12-12 NO-42

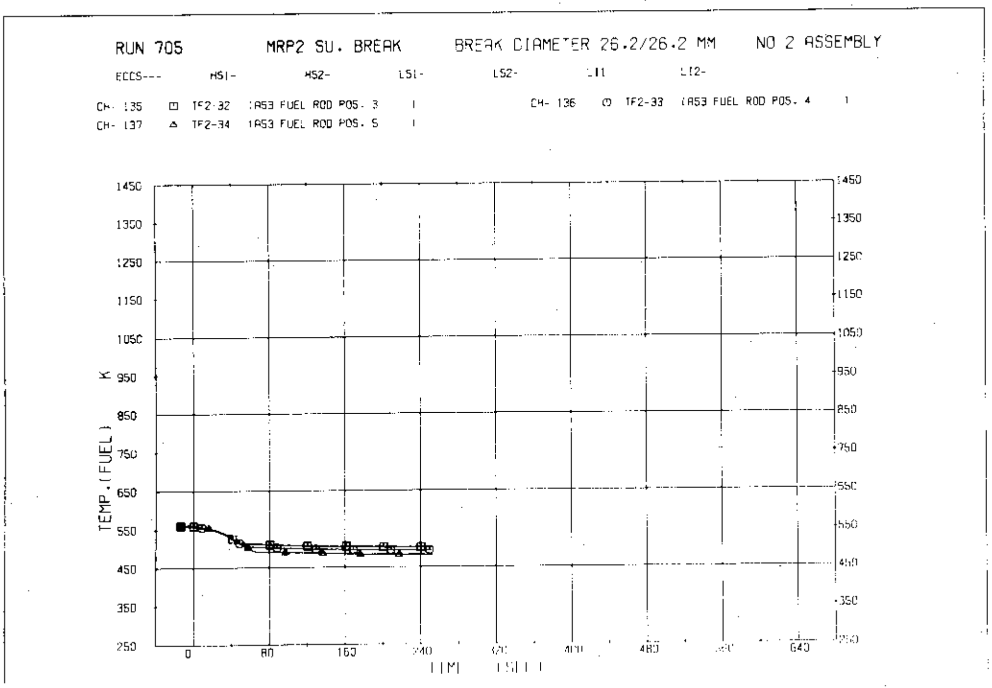

Fig. 5.36 Surfact temperature of fuel rod A53

138	1.20000E+00	0.0	0.0	139	1.22000E+00	0.0	0.0
140	1.22000E+00	0.0	0.0				

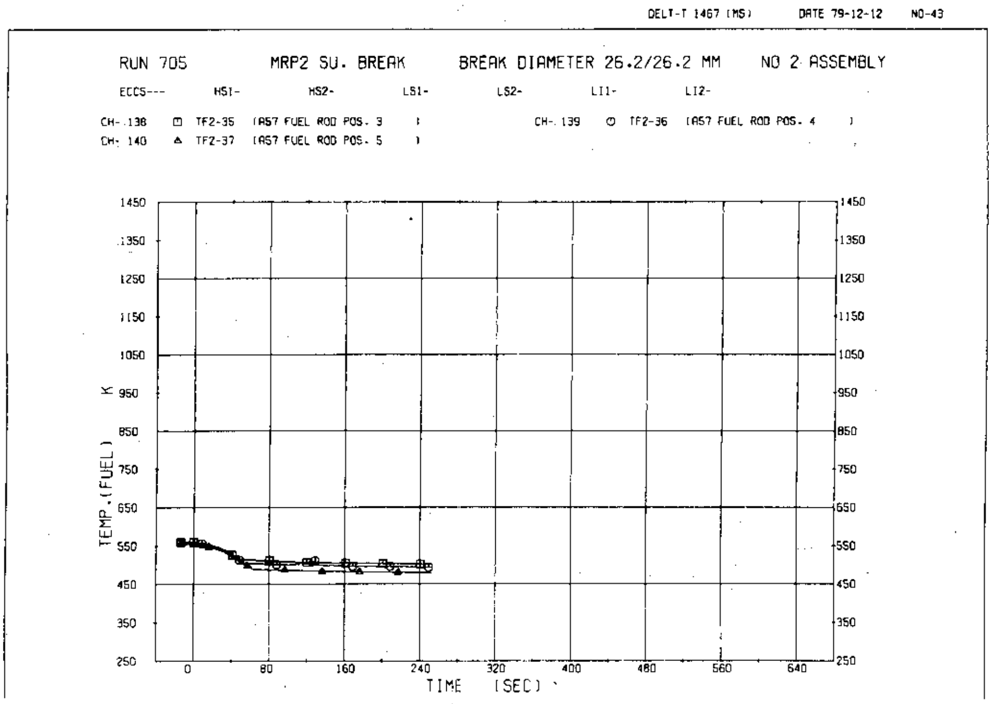

Fig. 5.37 Surface temperature of fuel rod A57

141	1.22000E+00	0.0	0.0	142	1.22000E+00	0.0	0.0
143	1.22000E+00	0.0	0.0				

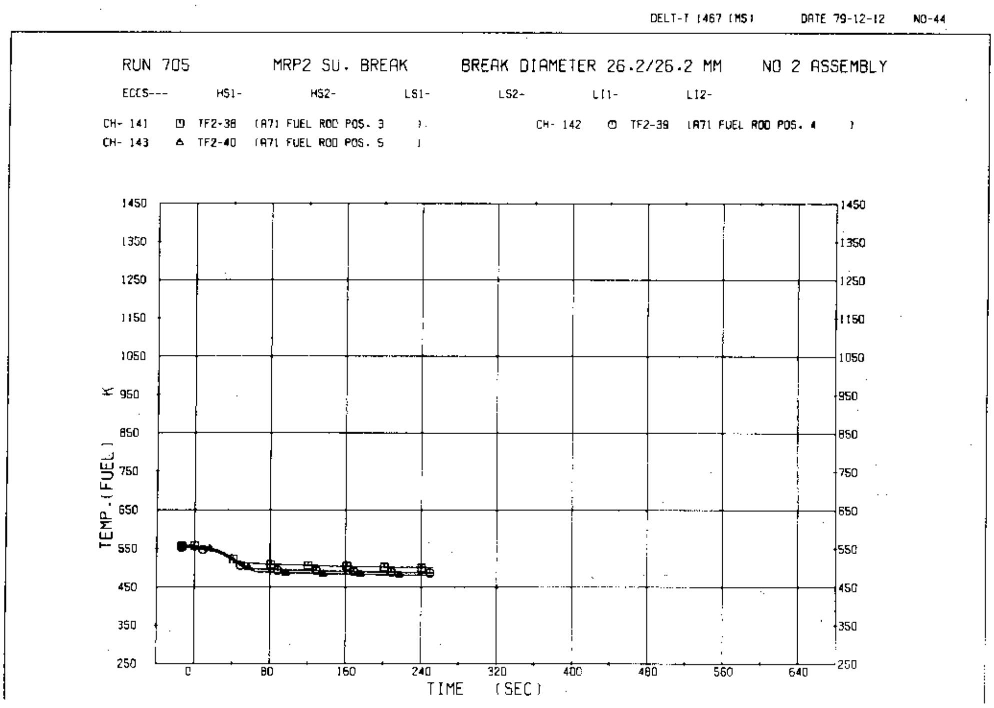

Fig. 5.38 Surface temperature of fuel rod A71

144 1.22000E+00 0.0 0.0 145 1.22000E+00 0.0 0.0
146 1.22000E+00 0.0 0.0

DELT-T 1467 (MS) DATE 79-12-12 NO-45

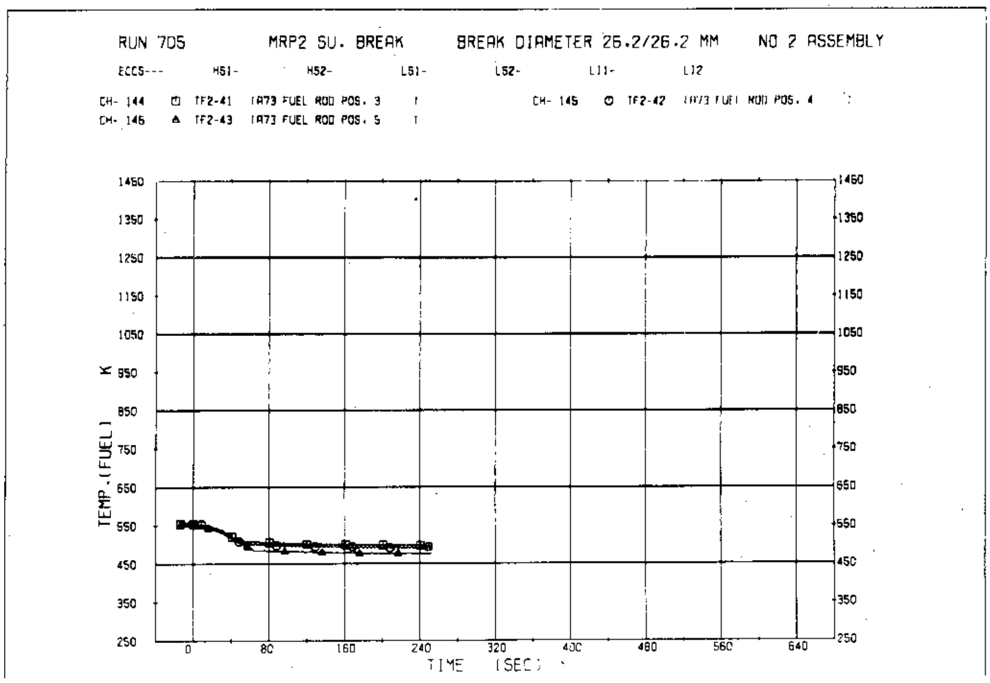

Fig. 5.39 Surface temperature of fuel rod A73

147 1.22000E+00 0.0 0.0 148 1.22000E+00 0.0 0.0
149 1.22000E+00 0.0 0.0

DELT-T 1467 (MS) DATE 79-12-12 NO-46

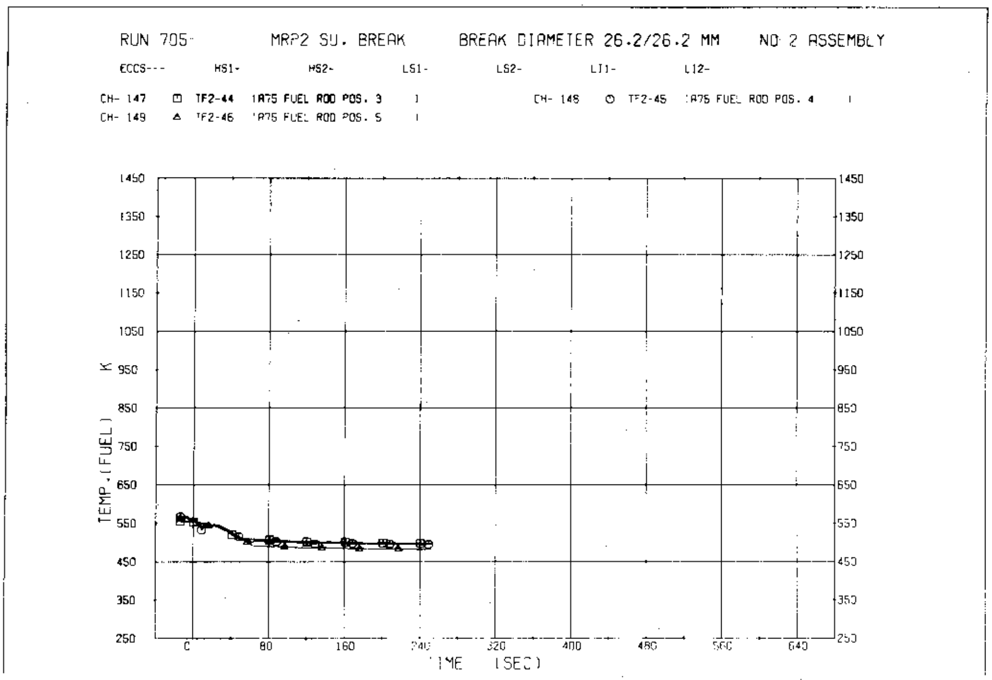

Fig. 5.40 Surface temperature of fuel rod A75

150	1.22000E+00	0.0	0.0	151	1.22000E+00	0.0	0.0
152	1.22000E+00	0.0	0.0	153	1.22000E+00	0.0	0.0
154	1.22000E+00	0.0	0.0	155	1.22000E+00	0.0	0.0
156	1.22000E+00	0.0	0.0				

DELT-T 1467 (MS) DATE 79-12-12 NO-47

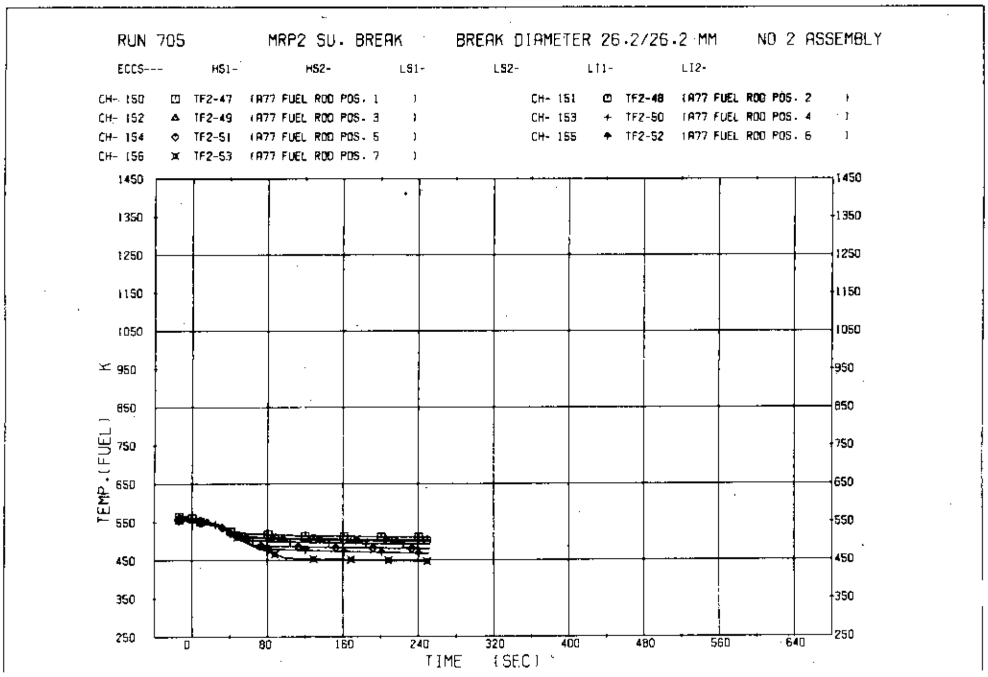

Fig. 5.41 Surface temperature of fuel rod A77

157	1.22000E+00	0.0	0.0	158	1.22000E+00	0.0	0.0
159	1.22000E+00	0.0	0.0	160	1.22000E+00	0.0	0.0
161	1.22000E+00	0.0	0.0	162	1.22000E+00	0.0	0.0
163	1.22000E+00	0.0	0.0				

DELT-T 1467 (MS) DATE 79-12-12 NO-48

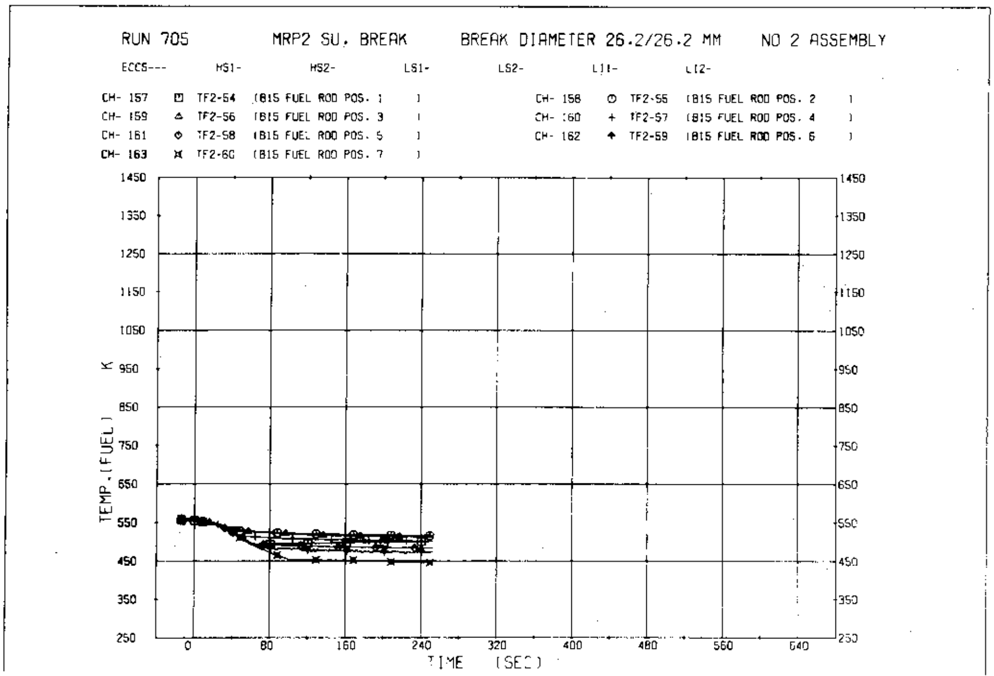

Fig. 5.42 Surface temperature of fuel rod B15

164	1.22000E+00	0.0	0.0	165	1.22000E+00	0.0	0.0
166	1.22000E+00	0.0	0.0	167	1.22000E+00	0.0	0.0
168	1.22000E+00	0.0	0.0	169	1.22000E+00	0.0	0.0
170	9.75900E-01	0.0	0.0				

DELT-T 1467 (MS) DATE 79-12-12 NO-49

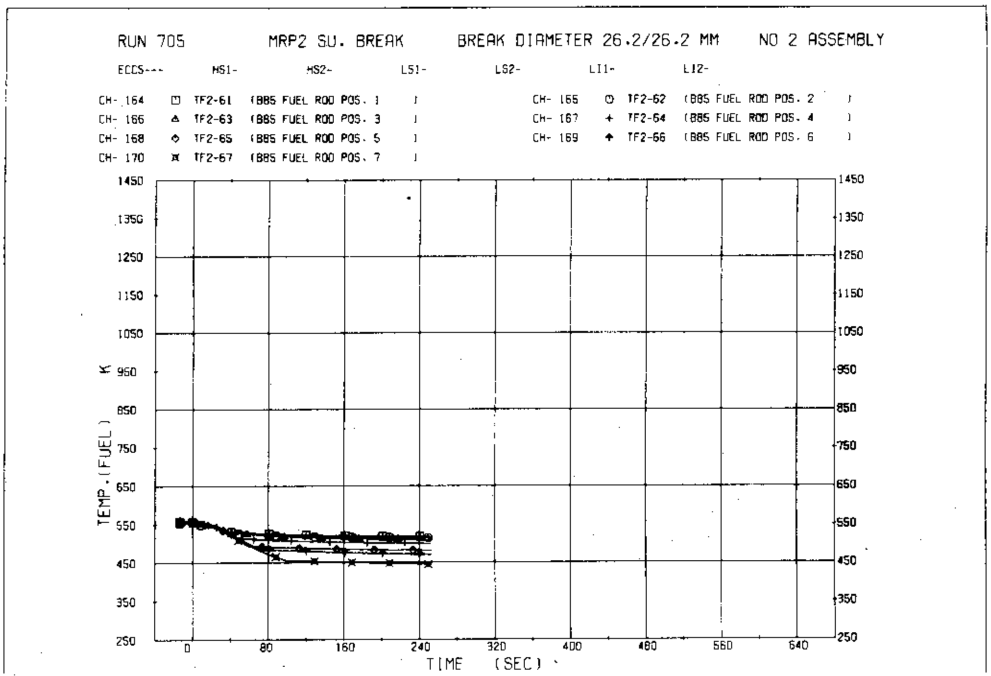

Fig. 5.43 Surface temperature of fuel rod B85

171	9.75900E-01	0.0	0.0	172	9.75900E-01	0.0	0.0
173	9.75900E-01	0.0	0.0				

DELT-T 1467 (MS) DATE 79-12-12 NO-50

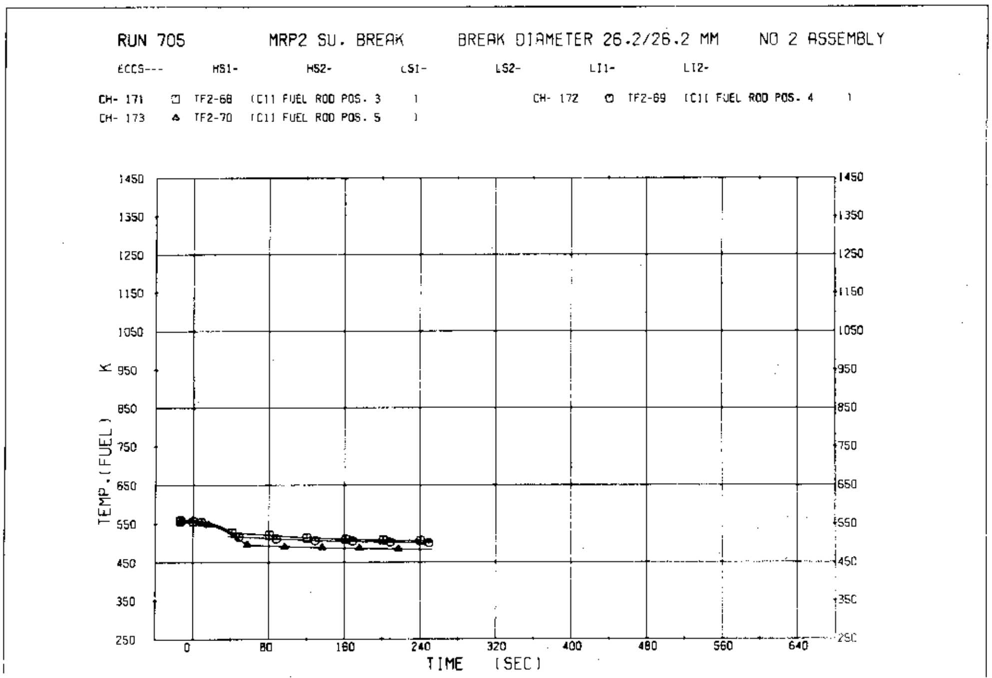

Fig. 5.44 Surface temperature of fuel rod C11

174 9.75900E-01 0.0 0.0 175 9.75900E-01 0.0 0.0
176 9.75900E-01 0.0 0.0

DELT-T 1467 (MS) DATE 79-12-12 NO-51

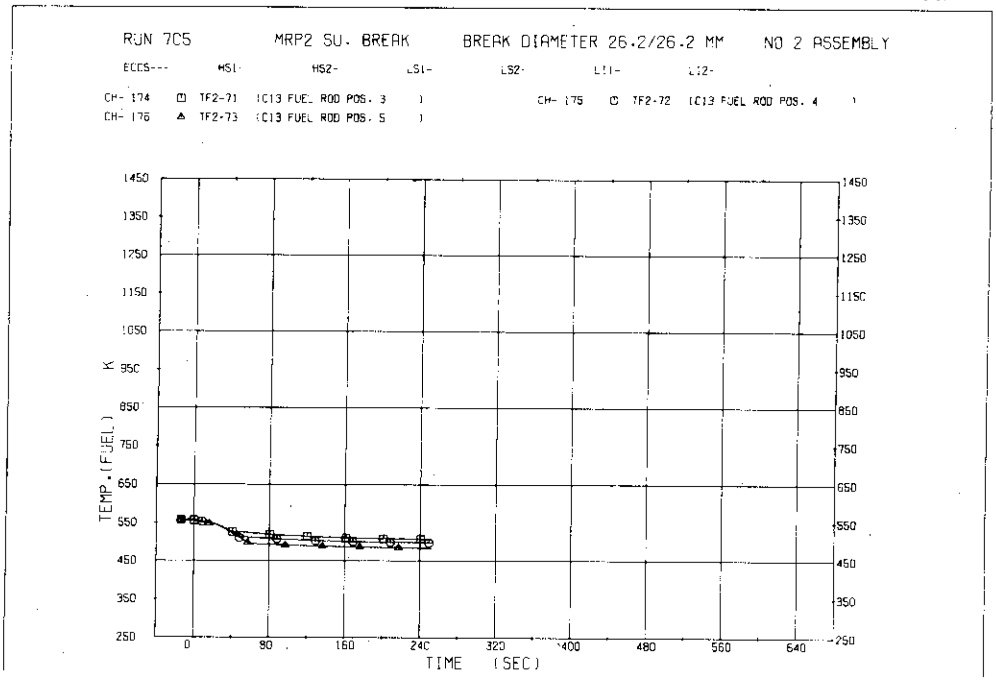

Fig. 5.45 Surface temperature of fuel rod C13

177 9.75900E-01 0.0 0.0 178 9.75900E-01 0.0 0.0
179 9.75900E-01 0.0 0.0

DELT-T 1467 (MS) DATE 79-12-12 NO-52

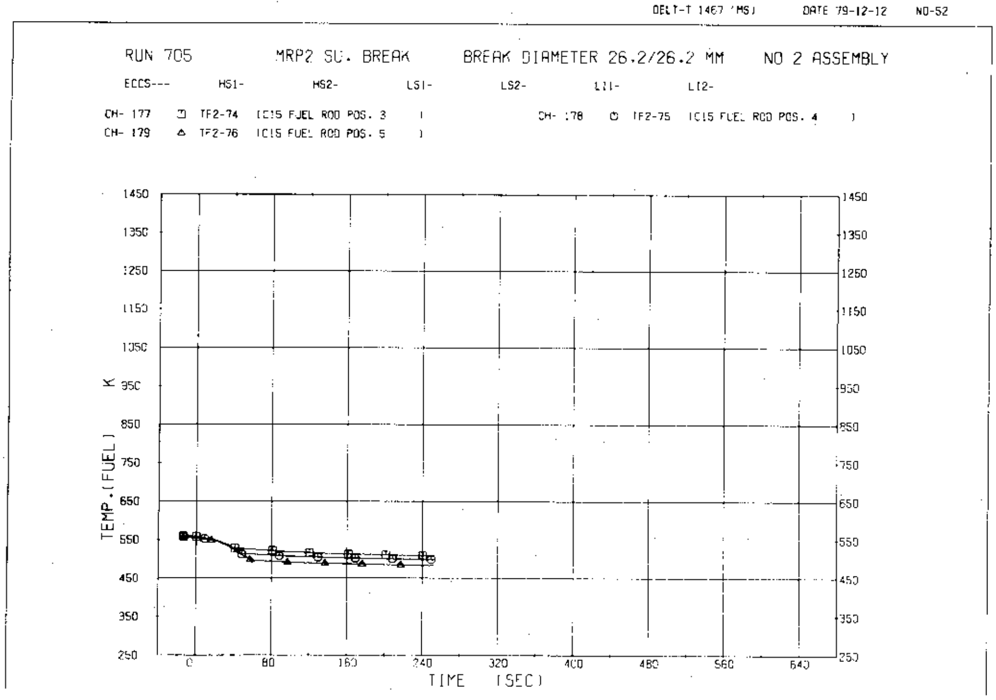

Fig. 5.46 Surface temperature of fuel rod C15

180	9.75900E-01	0.0	0.0	181	9.75900E-01	0.0	0.0
182	9.75900E-01	0.0	0.0				

DELT-T 1467 (MS) DATE 79-12-12 NO-53

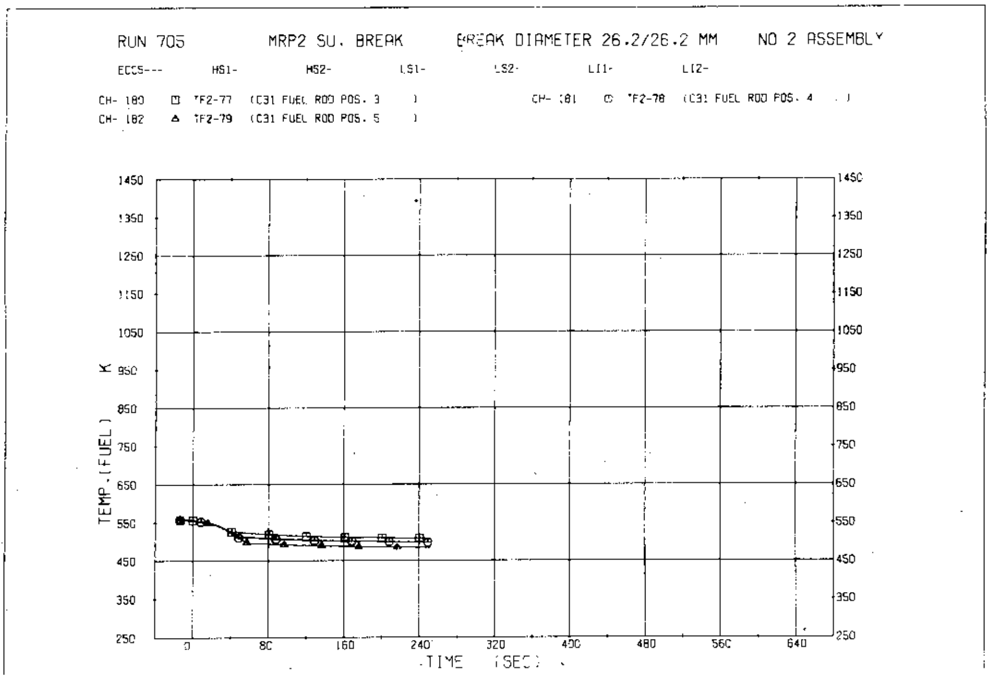

Fig. 5.47 Surface temperature of fuel rod C31

183	9.75900E-01	0.0	0.0	184	9.75900E-01	0.0	0.0
185	9.75900E-01	0.0	0.0	186	9.75900E-01	0.0	0.0
187	9.75900E-01	0.0	0.0	188	9.75900E-01	0.0	0.0
189	9.75900E-01	0.0	0.0				

DELT-T 1467 (MS) DATE 79-12-12 NO-54

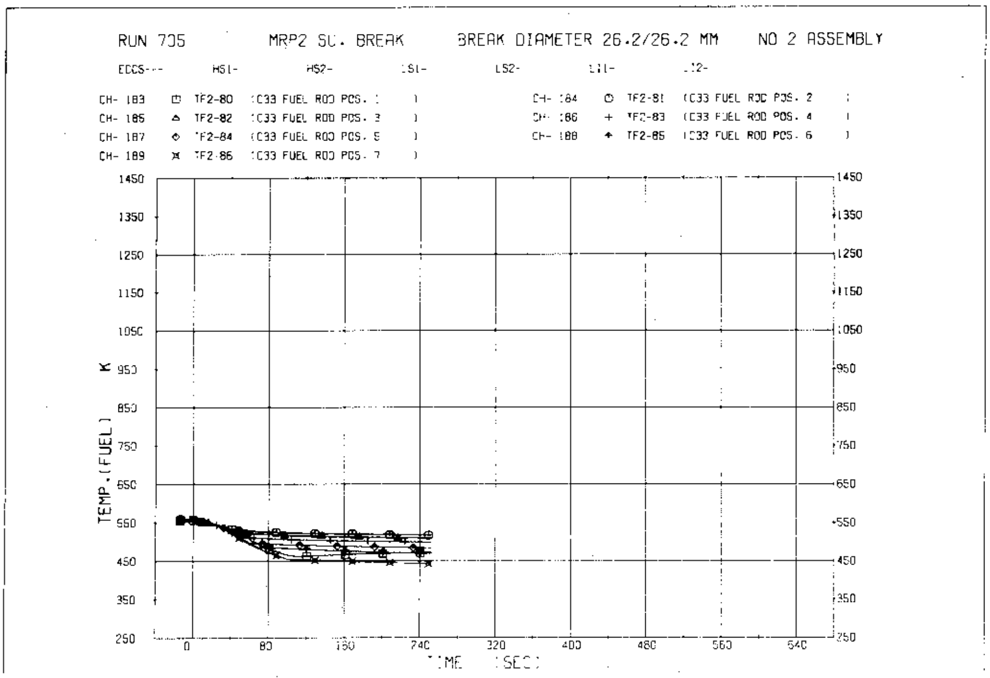

Fig. 5.48 Surface temperature of fuel rod C33

190 9.75900E-01 0.0 0.0 191 9.75900E-01 0.0 0.0
192 9.75900E-01 0.0 0.0

DELT-T 1467 (MS) DATE 79-12-12 NO-55

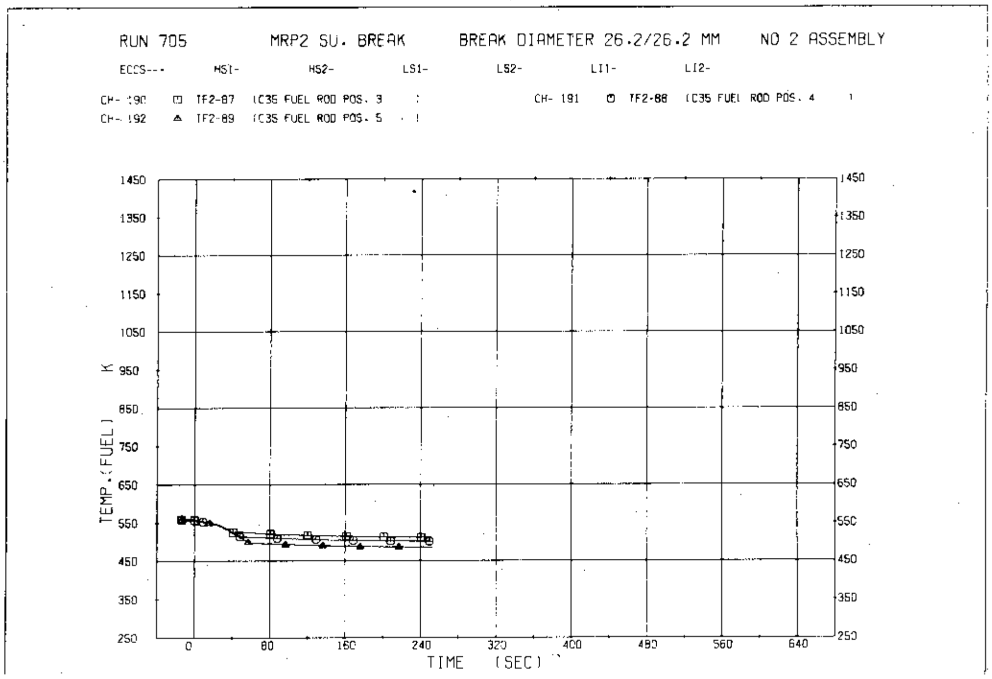

Fig. 5.49 Surface temperature of fuel rod C35

193 9.75900E-01 0.0 0.0 194 9.75900E-01 0.0 0.0
195 9.75900E-01 0.0 0.0

DELT-T 1467 (MS) DATE 79-12-12 NO-56

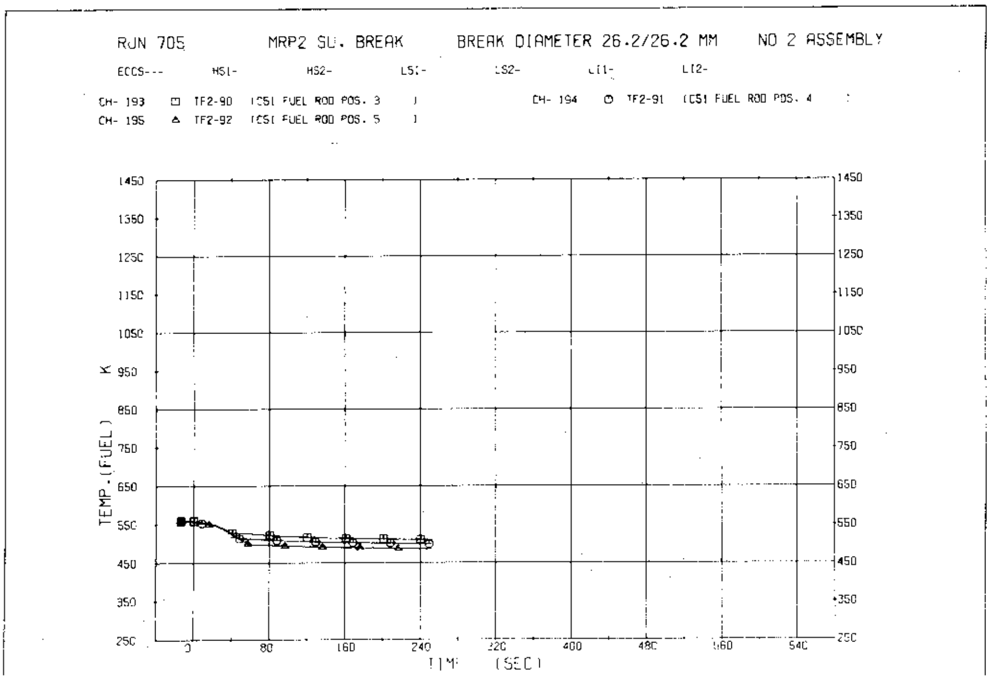

Fig. 5.50 Surface temperature of fuel rod C51

196	9.75900E-01	0.0	0.0	197	9.75900E-01	0.0	0.0
198	9.75900E-01	0.0	0.0				

DELT-T 1467 (MS) DATE 79-12-12 NO-57

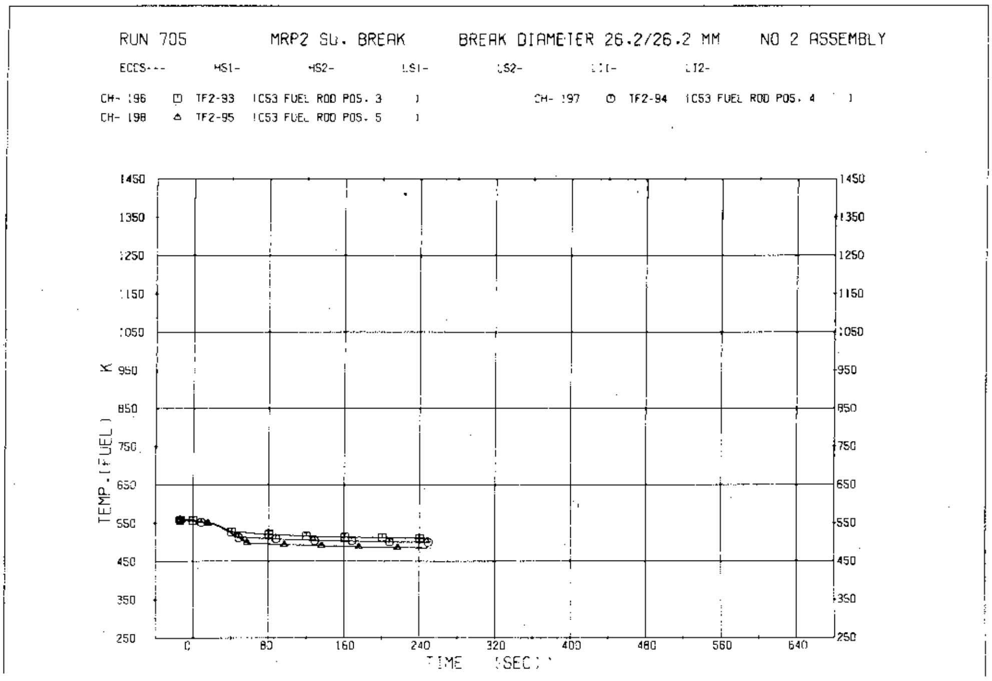

Fig. 5.51 Surface temperature of fuel rod C53

199	9.75900E-01	0.0	0.0	200	9.75900E-01	0.0	0.0
201	9.75900E-01	0.0	0.0	202	9.75900E-01	0.0	0.0
203	9.75900E-01	0.0	0.0	204	9.75900E-01	0.0	0.0
205	9.75900E-01	0.0	0.0				

DELT-T 1467 (MS) DATE 79-12-12 NO-58

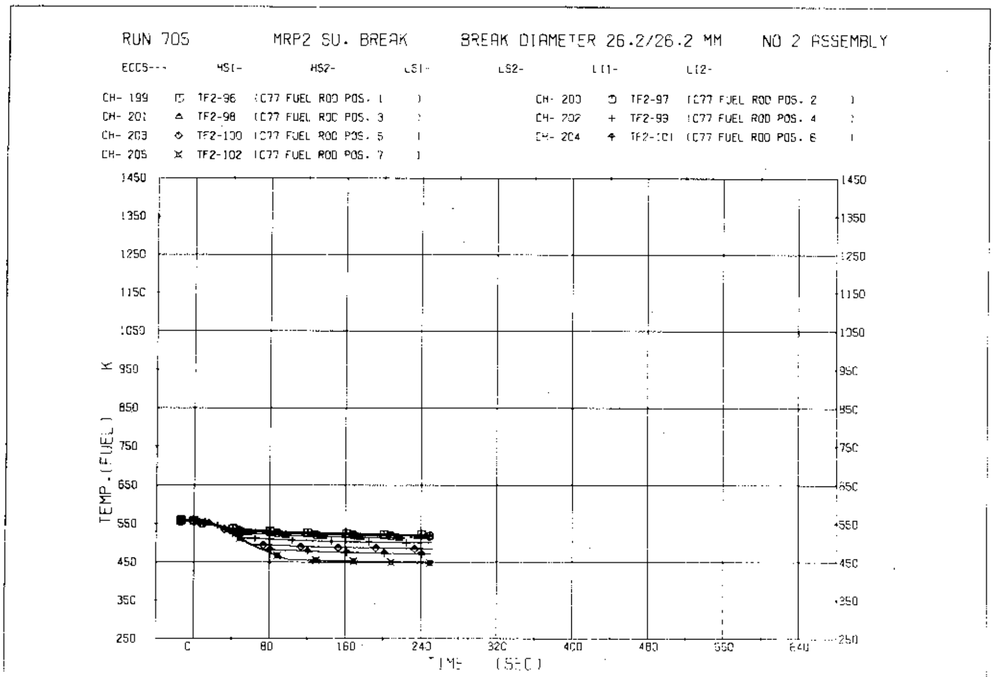

Fig. 5.52 Surface temperature of fuel rod C77

206	9.75900E-01	0.0	0.0	207	9.75900E-01	0.0	0.0
208	9.75900E-01	0.0	0.0	209	9.75900E-01	0.0	0.0
210	9.75900E-01	0.0	0.0	211	9.75900E-01	0.0	0.0
212	9.75900E-01	0.0	0.0				

DELT-T 1467 (MS) DATE 79-12-12 NO-59

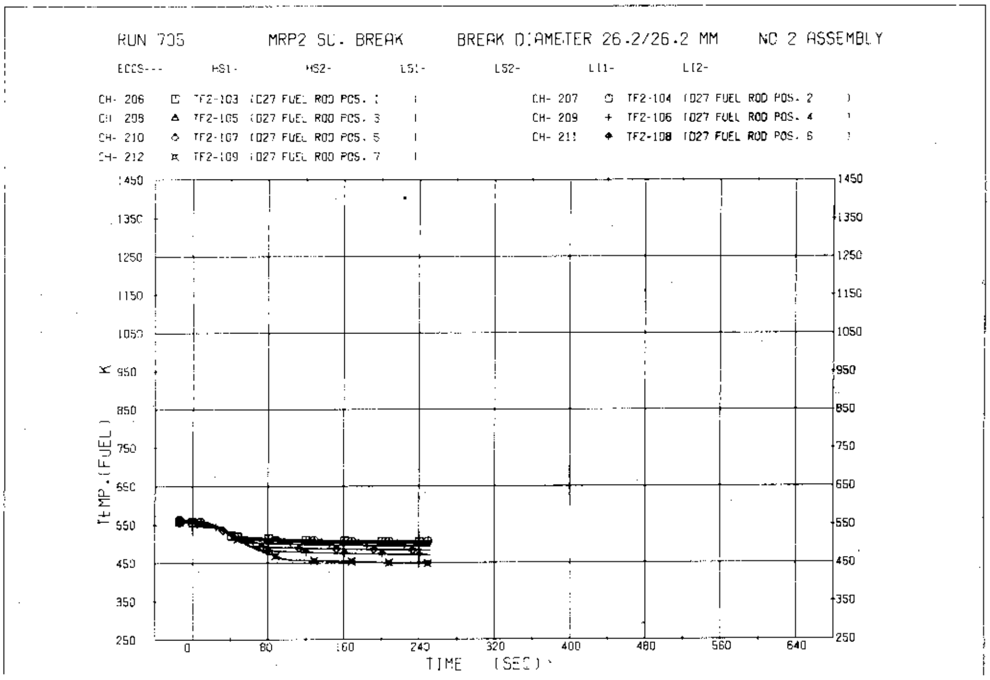

Fig. 5.53 Surface temperature of fuel rod D27

213	9.75900E-01	0.0	0.0	214	9.75900E-01	0.0	0.0
215	9.75900E-01	0.0	0.0	216	9.75900E-01	0.0	0.0
217	9.75900E-01	0.0	0.0	218	9.75900E-01	0.0	0.0
219	9.75900E-01	0.0	0.0				

DELT-T 1467 (MS) DATE 79-12-12 NO-60

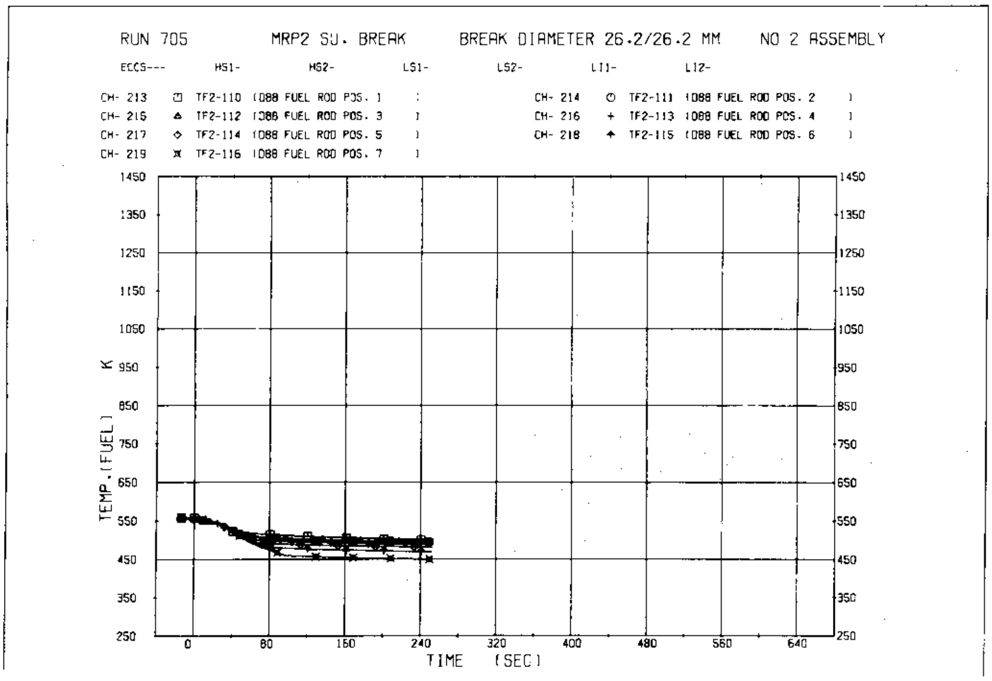

Fig. 5.54 Surface temperature of fuel rod D88

220	9.75900E-01	0.0	0.0	221	9.75900E-01	0.0	0.0
222	9.75900E-01	0.0	0.0	223	9.75900E-01	0.0	0.0
224	9.75900E-01	0.0	0.0	225	9.75900E-01	0.0	0.0
226	9.75900E-01	0.0	0.0				

DELT-T 1467 (MS) DATE 79-12-12 NO-61

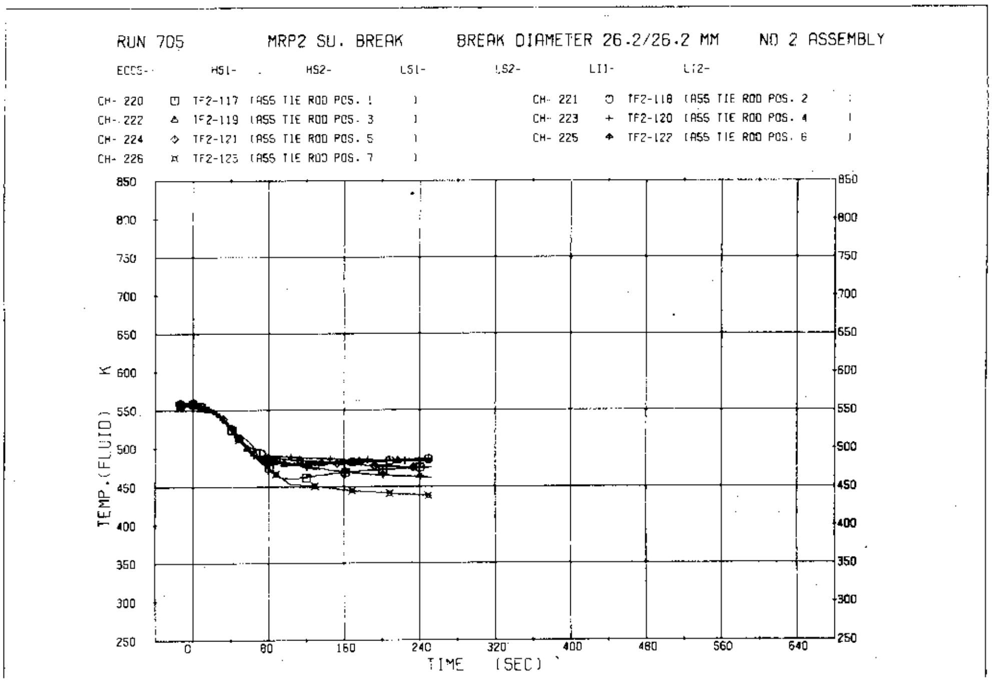

Fig. 5.55 Fluid temperatures around tie rod A55

227	9.75900E-01	0.0	0.0	228	9.75900E-01	0.0	0.0
229	9.75900E-01	0.0	0.0	230	9.75900E-01	0.0	0.0
231	9.75900E-01	0.0	0.0	232	9.75900E-01	0.0	0.0
233	9.75900E-01	0.0	0.0				

DELT-T 1467 (MS) DATE 79-12-12 NO-62

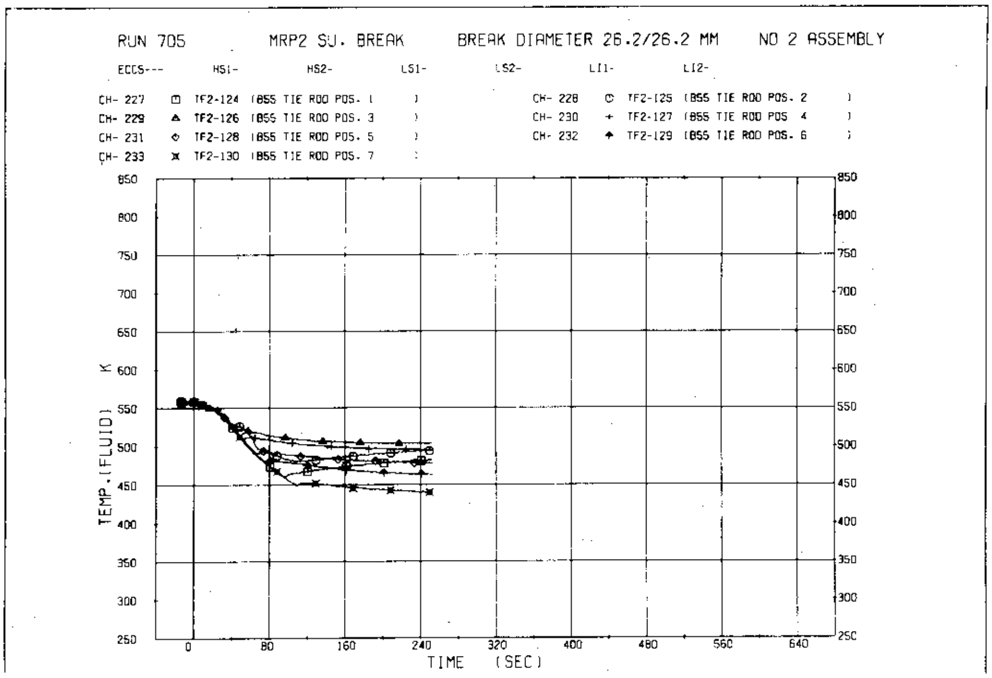

Fig. 5.56 Fluid temperatures around tie rod B55

220	9.75900E-01	0.0	0.0	221	9.75900E-01	0.0	0.0
222	9.75900E-01	0.0	0.0	223	9.75900E-01	0.0	0.0
224	9.75900E-01	0.0	0.0	225	9.75900E-01	0.0	0.0
226	9.75900E-01	0.0	0.0				

DELT-T 1467 (MS) DATE 79-12-12 NO-61

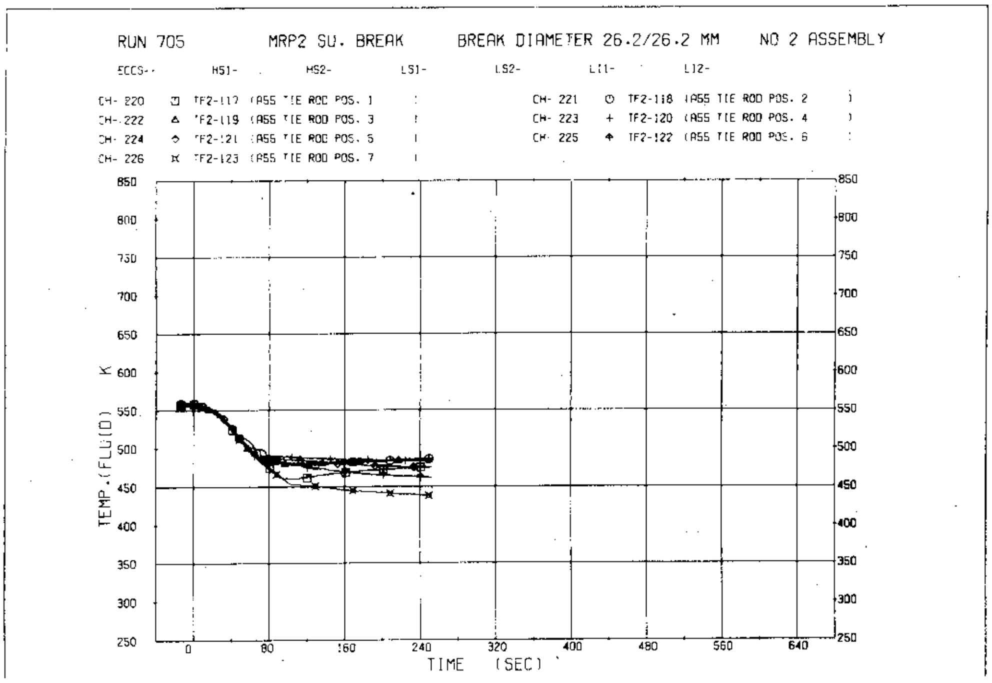

Fig. 5.55 Fluid temperatures around tie rod A55

227	9.75900E-01	0.0	0.0	228	9.75900E-01	0.0	0.0
229	9.75900E-01	0.0	0.0	230	9.75900E-01	0.0	0.0
231	9.75900E-01	0.0	0.0	232	9.75900E-01	0.0	0.0
233	9.75900E-01	0.0	0.0				

DELT-T 1467 (MS) DATE 79-12-12 NO-62

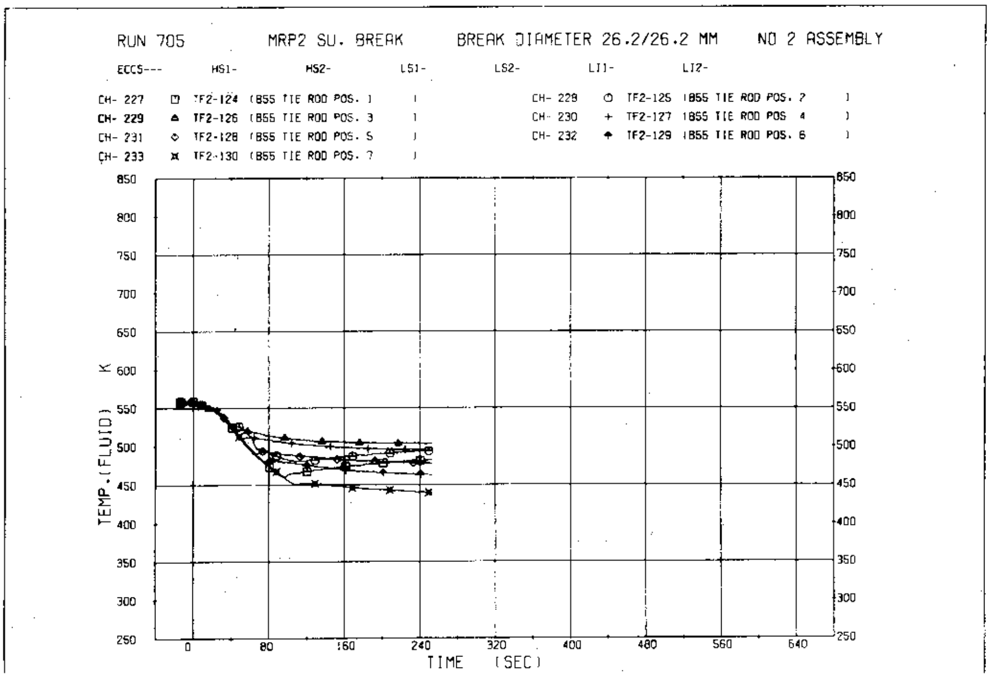

Fig. 5.56 Fluid temperatures around tie rod B55

234	9.75900E-01	0.0	0.0	235	9.75900E-01	0.0	0.0
236	9.75900E-01	0.0	0.0	237	9.75900E-01	0.0	0.0
238	9.75900E-01	0.0	0.0	239	9.75900E-01	0.0	0.0
240	9.75900E-01	0.0	0.0				

DELT-T 1467 (MS) DATE 79-12-12 NO-63

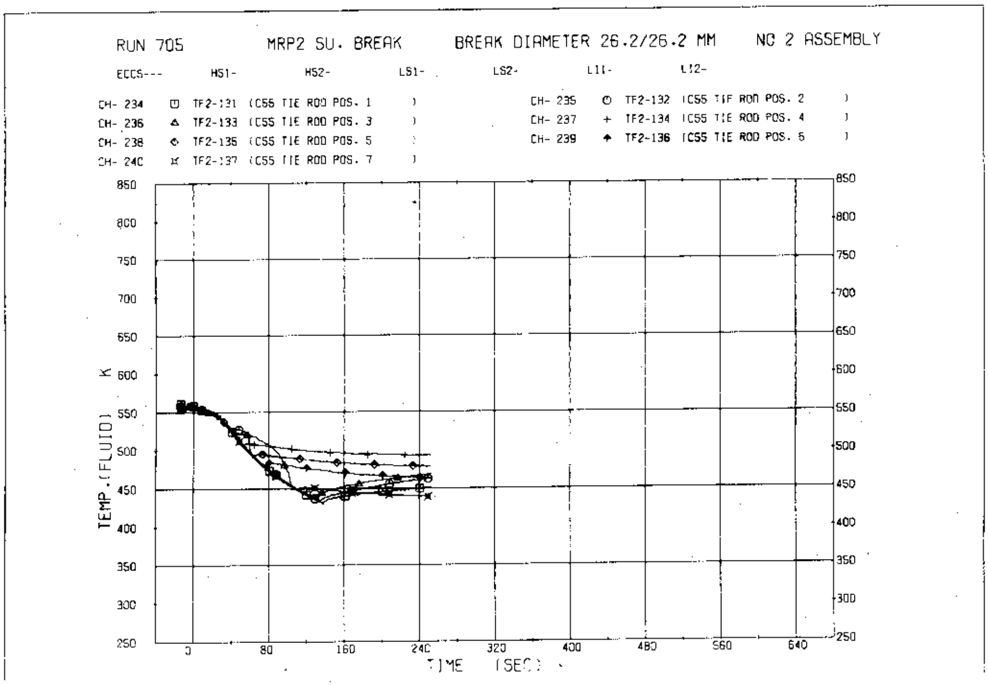

Fig. 5.57 Fluid temperatures around tie rod C55

241	9.75900E-01	0.0	0.0	242	9.75900E-01	0.0	0.0
243	9.75900E-01	0.0	0.0	244	9.75900E-01	0.0	0.0
245	9.75900E-01	0.0	0.0	246	9.75900E-01	0.0	0.0
247	9.75900E-01	0.0	0.0				

DELT-T 1467 (MS) DATE 79-12-12 NO-64

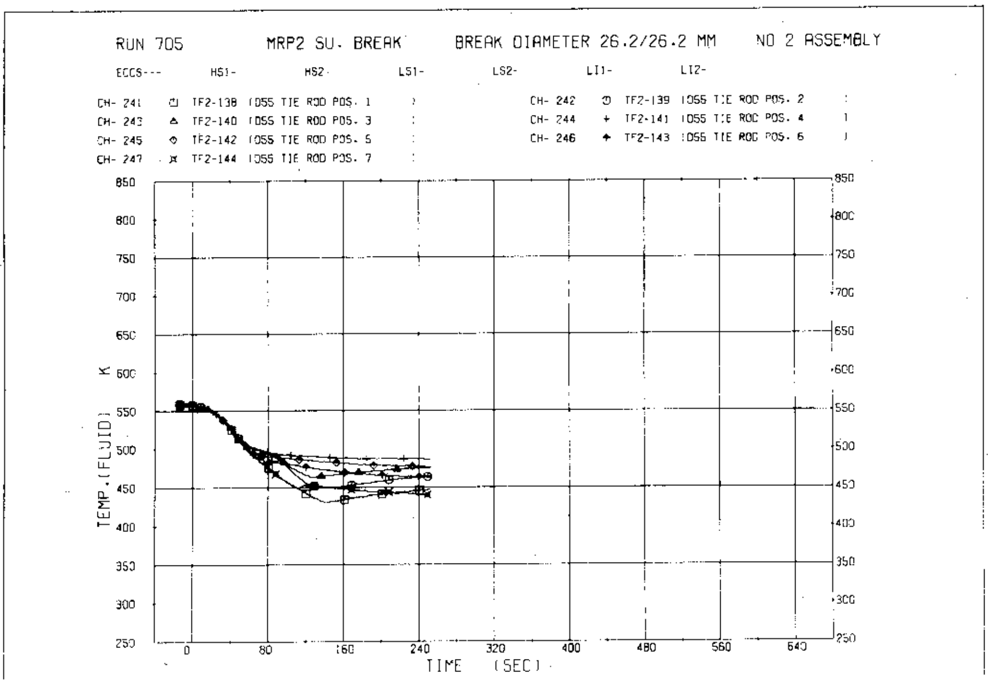

Fig. 5.58 Fluid temperatures around tie rod D55

248	9.75900E-01	0.0	0.0	250	9.75900E-01	0.0	0.0
252	9.75900E-01	0.0	0.0	254	9.75900E-01	0.0	0.0

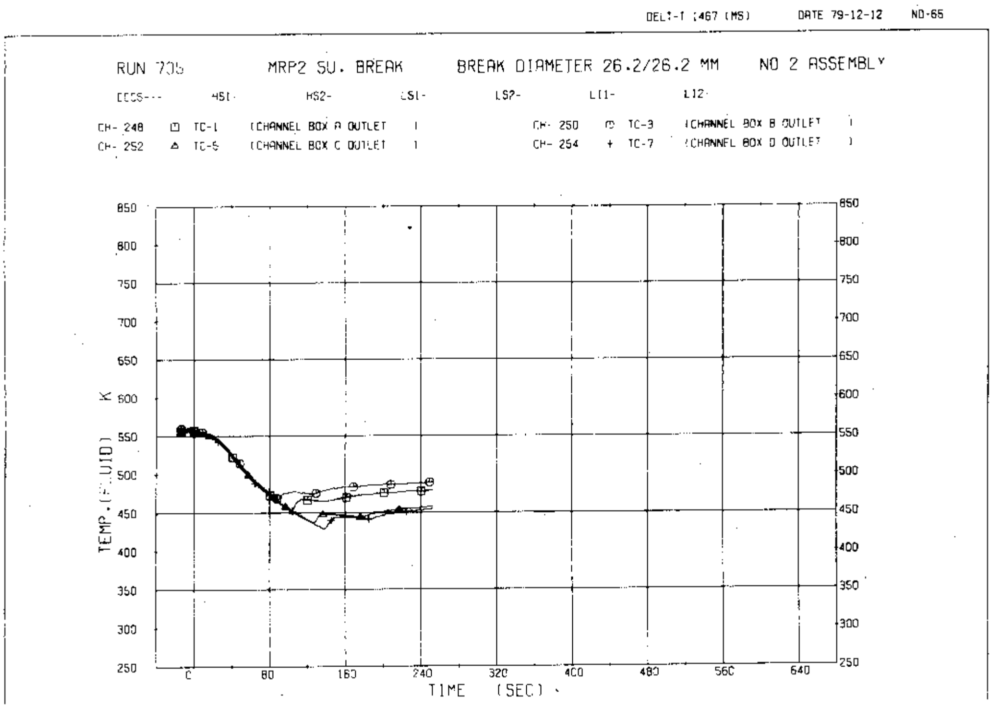

Fig. 5.59 Fluid temperatures at channel box outlet

249	9.75900E-01	0.0	0.0	251	9.75900E-01	0.0	0.0
253	9.75900E-01	0.0	0.0	255	9.75900E-01	0.0	0.0

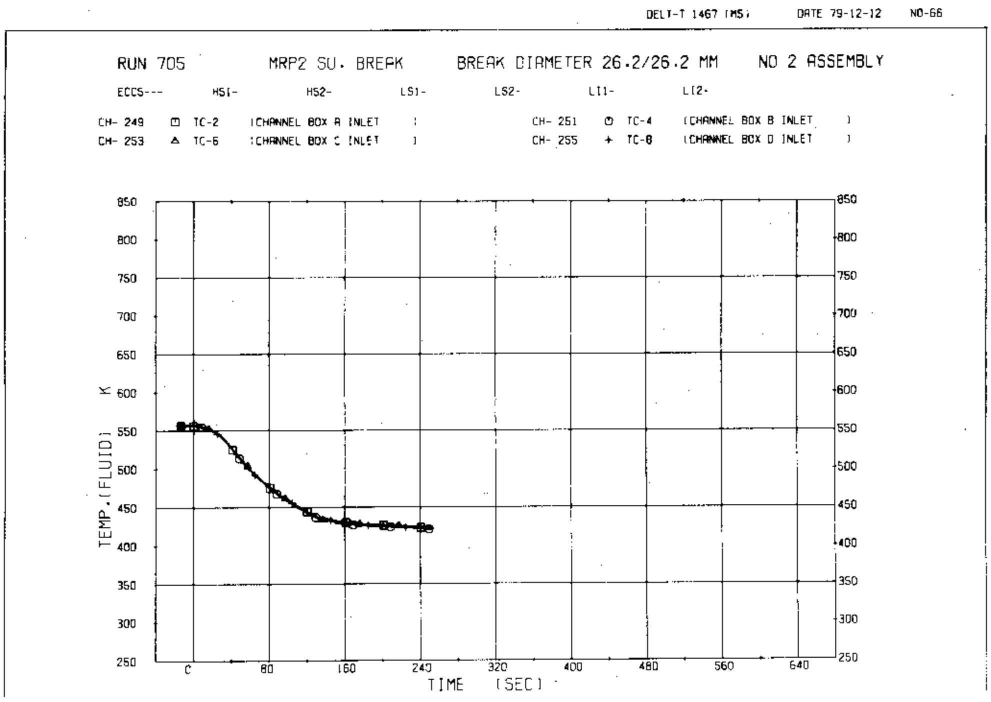

Fig. 5.60 Fluid temperatures at channel box inlit

256	9.75900E-01	0.0	0.0	257	9.75900E-01	0.0	0.0
258	9.75900E-01	0.0	0.0	259	9.75900E-01	0.0	0.0
260	9.75900E-01	0.0	0.0	261	9.75900E-01	0.0	0.0
262	9.75900E-01	0.0	0.0				

DELT-T 1467 (MS) DATE 79-12-12 NO 67

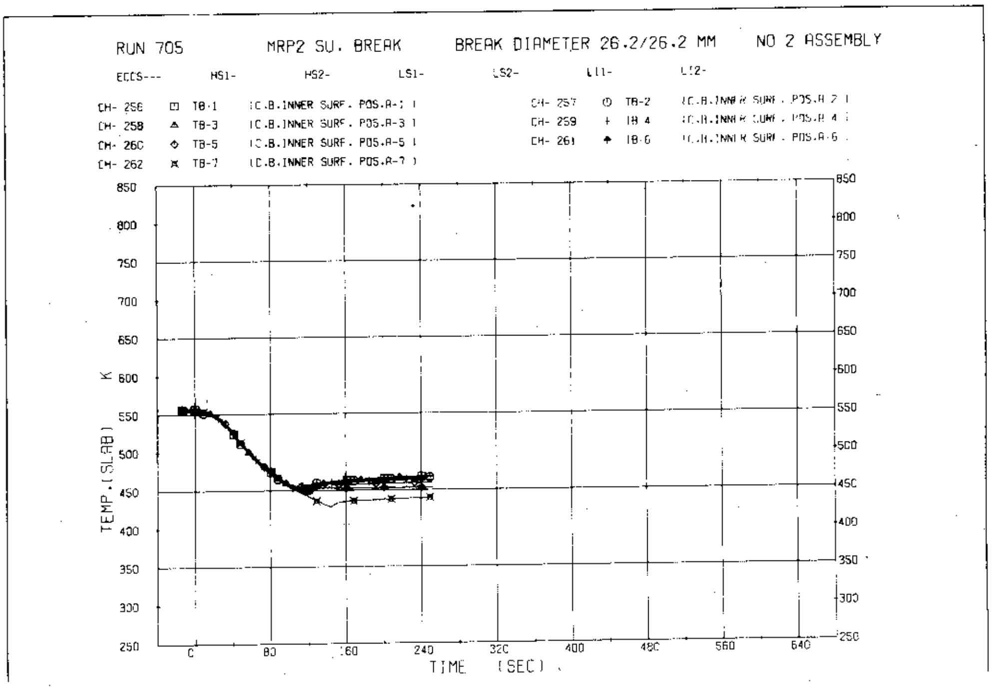

Fig. 5.61 Inner surface temperatures of channel box A

263	9.75900E-01	0.0	0.0	264	9.75900E-01	0.0	0.0
265	9.75900E-01	0.0	0.0	266	9.75900E-01	0.0	0.0
267	9.75900E-01	0.0	0.0	268	9.75900E-01	0.0	0.0
269	9.75900E-01	0.0	0.0				

DELT-T 1467 (MS) DATE 79-12-12 NO-68

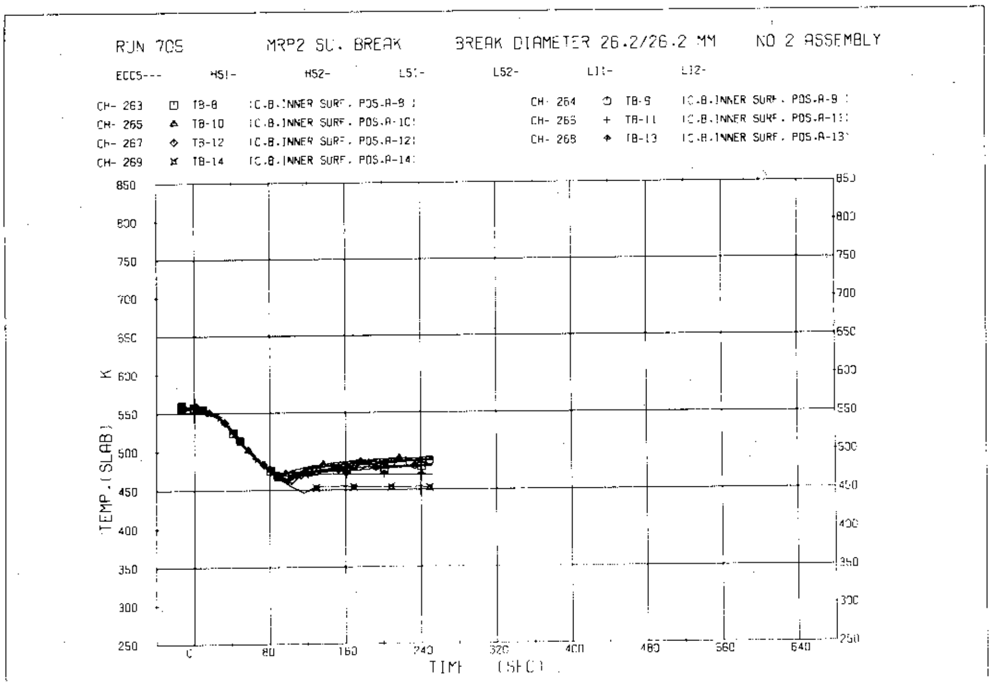

Fig. 5.62 Inner surface temperatures of channel box A

270	9.75900E-01	0.0	0.0	271	9.75900E-01	0.0	0.0
272	9.75900E-01	0.0	0.0	273	9.75900E-01	0.0	0.0
274	9.75900E-01	0.0	0.0	275	9.75900E-01	0.0	0.0

DELT-T 1467 (MS) DATE 79-12-12 NO-69

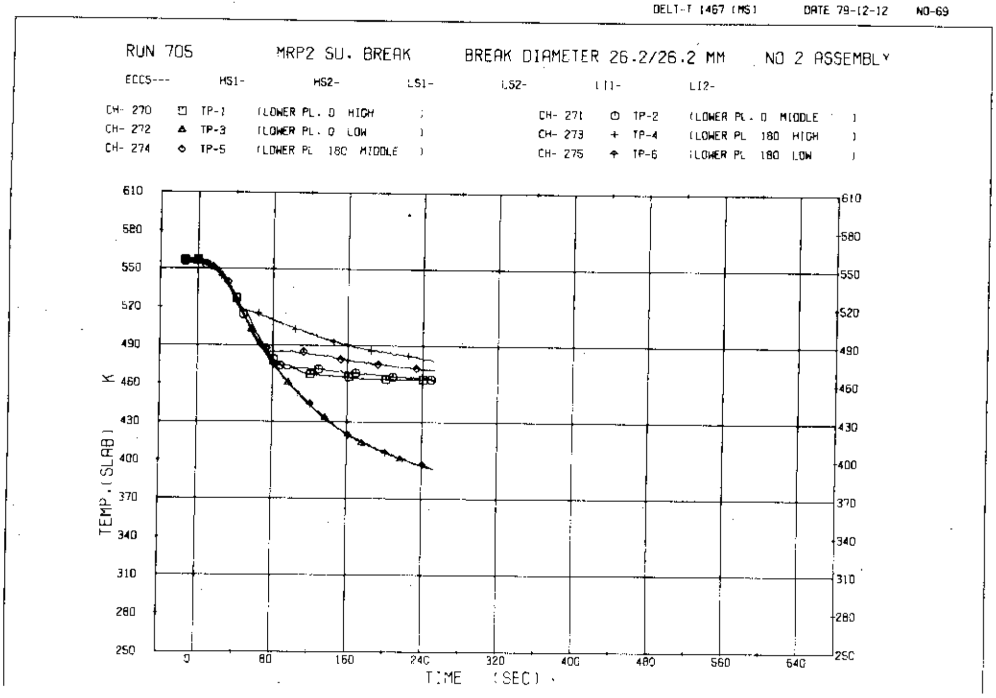

Fig. 5.63 Surface temperatures of core support in the lower plenum

276	9.75900E-01	0.0	0.0	277	9.75900E-01	0.0	0.0
278	9.75900E-01	0.0	0.0	279	[illegible]	0.0	0.0

DELT-T 1467 (MS) DATE 80-01-29 NO-1

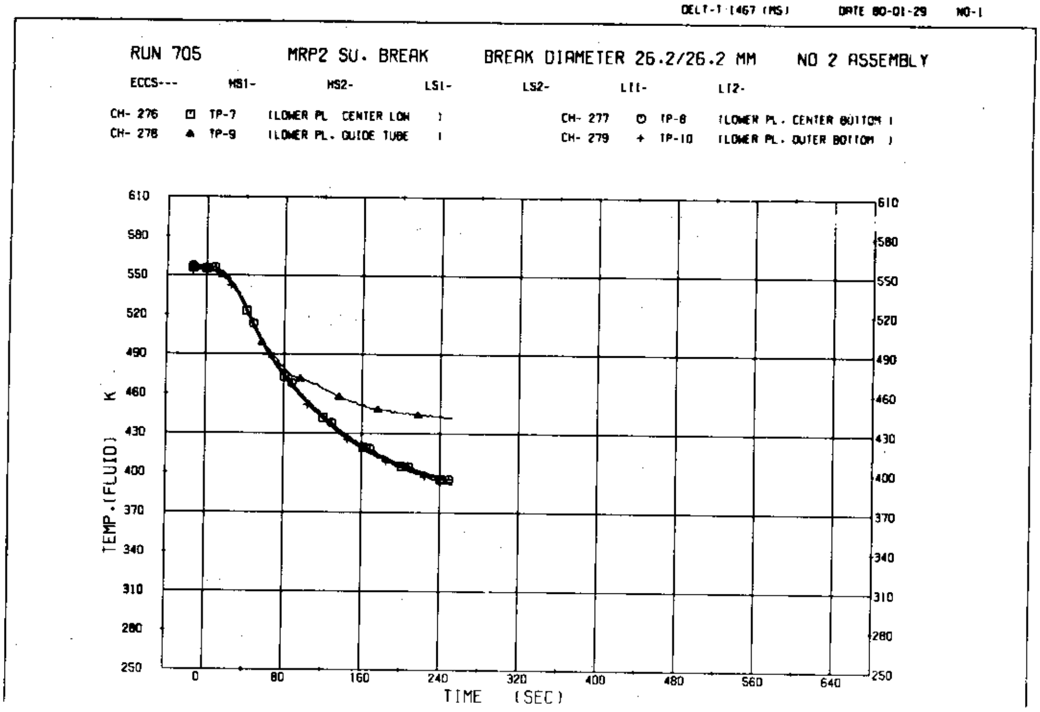

Fig. 5.64 Fluid temperatures in lower plenum

280	9.75900E-01	0.0	0.0	281	9.75900E-01	0.0	0.0
282	9.75900E-01	0.0	0.0	283	9.75900E-01	0.0	0.0
284	9.75900E-01	0.0	0.0				

DELT-T 1467 (MS) DATE 79-12-12 NO-71

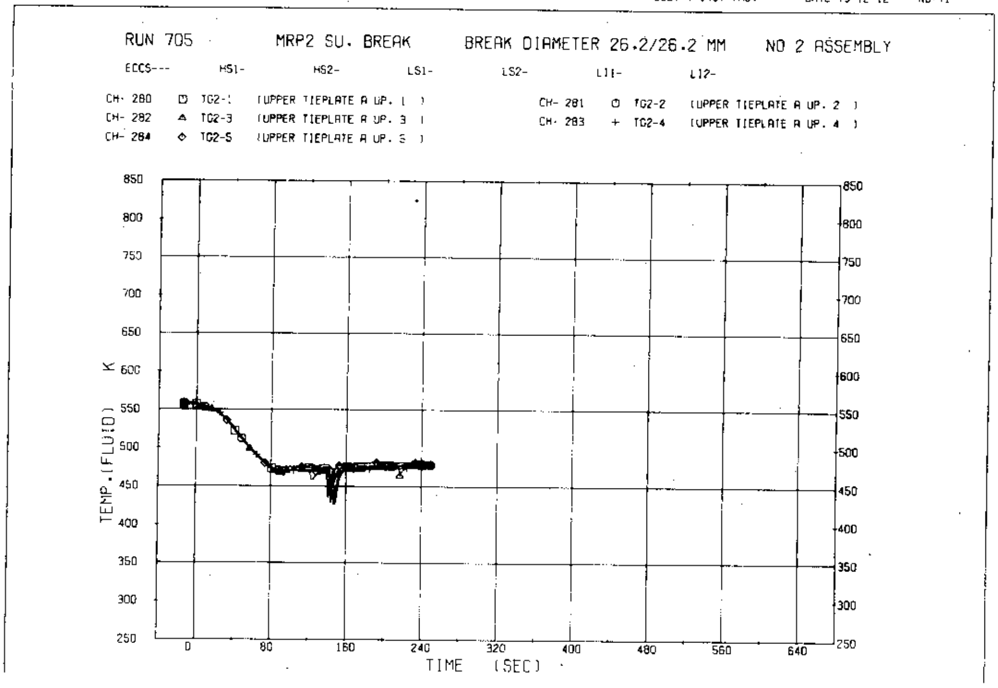

Fig. 5.65 Fluid temperatures just above upper tie plate A

285	9.75900E-01	0.0	0.0	286	9.75900E-01	0.0	0.0
287	9.75900E-01	0.0	0.0	288	9.75900E-01	0.0	0.0
289	9.75900E-01	0.0	0.0				

DELT-T 1467 (MS) DATE 79-12-12 NO-72

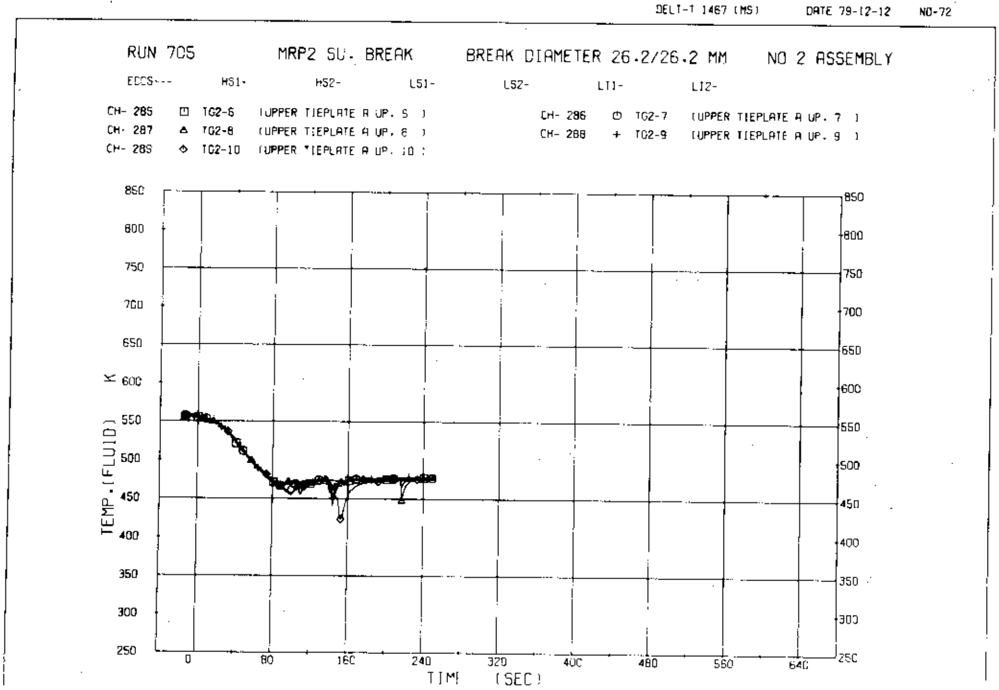

Fig. 5.66 Fluid temperatures just above upper tie plate A

290	9.75900E-01	0.0	0.0	291	9.75900E-01	0.0	0.0
292	9.75900E-01	0.0	0.0	293	9.75900E-01	0.0	0.0
294	9.75900E-01	0.0	0.0				

DELT-T 1467 (MS) DATE 79-12-12 NO-73

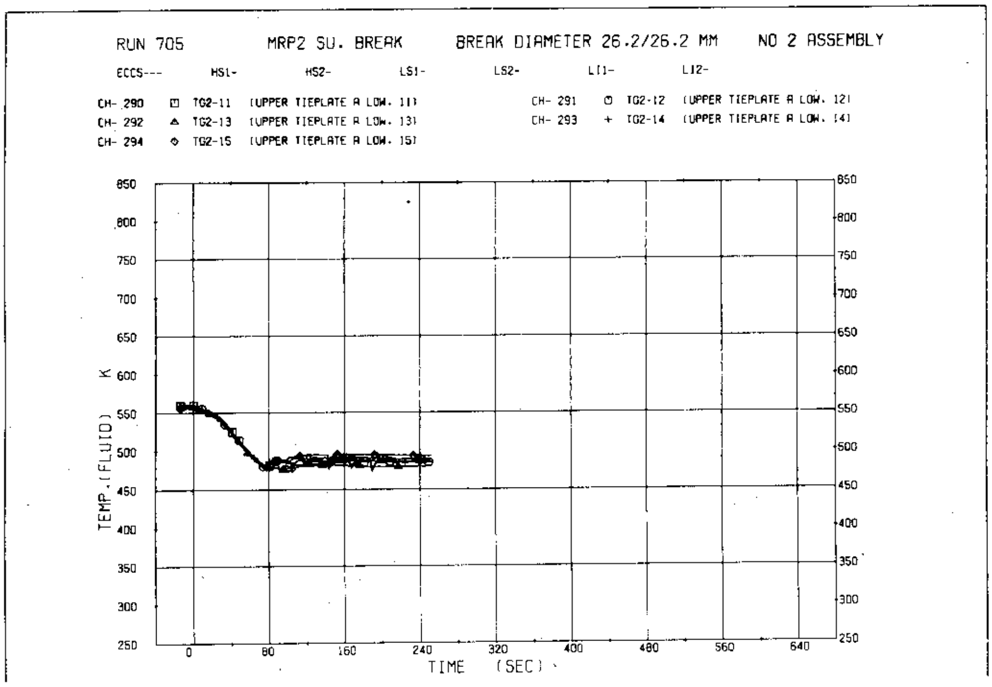

Fig. 5.67 Fluid temperatures just below upper tie plate A

295	9.75900E-01	0.0	0.0	296	9.75900E-01	0.0	0.0
297	9.75900E-01	0.0	0.0	298	9.75900E-01	0.0	0.0
299	9.75900E-01	0.0	0.0				

DELT-T 1467 (MS) DATE 79-12-12 NO-74

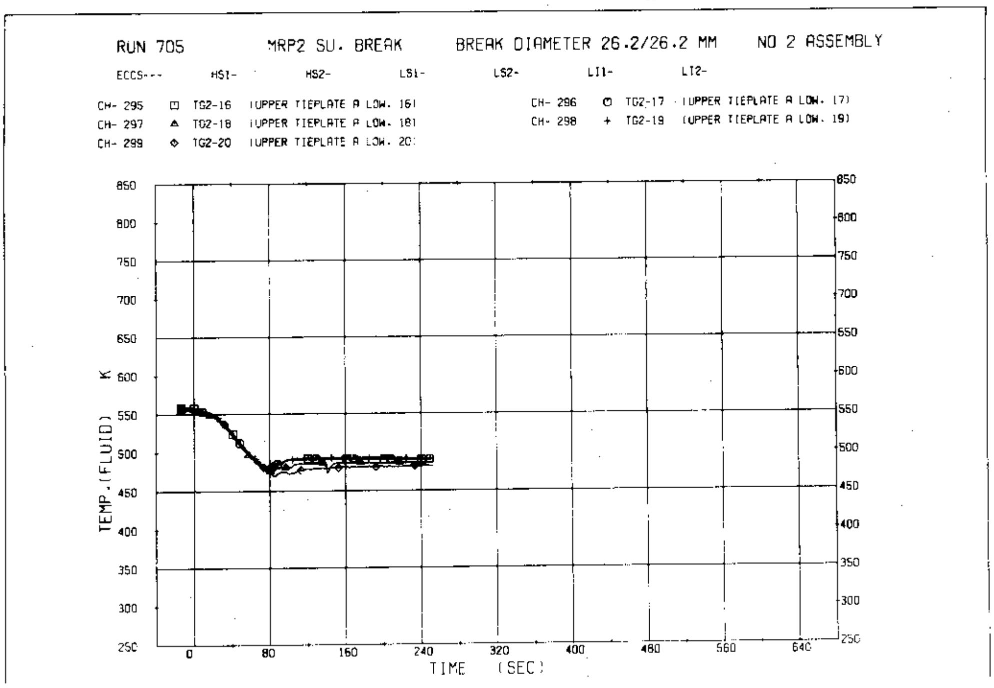

Fig. 5.68 Fluid temperatures just below upper tie plate A

300	1.00000E-03	0.0	0.0	301	1.00000E-03	0.0	0.0
302	1.00000E-03	0.0	0.0	303	1.00000E-03	0.0	0.0

DELT-T 1467 (MS) DATE 79-12-12 NO-75

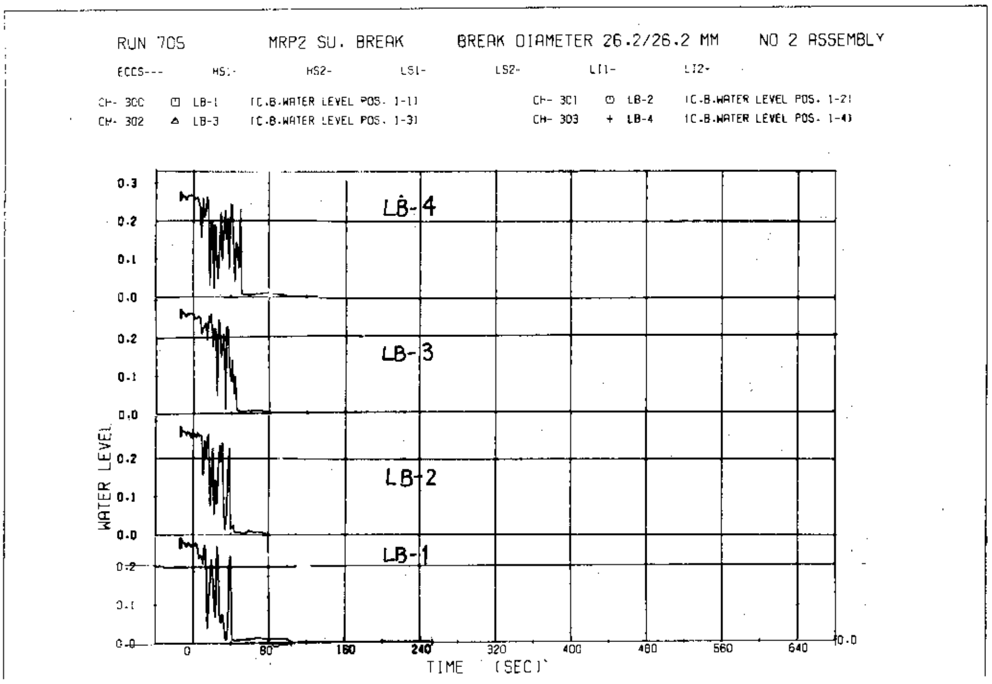

Fig. 5.69 Water level in channel box A (Pos. 1)

304	1.00000E-03	0.0	0.0	305	1.00000E-03	0.0	0.0
306	1.00000E-03	0.0	0.0				

DELT-T 1467 (MS) DATE 79-12-12 NO-76

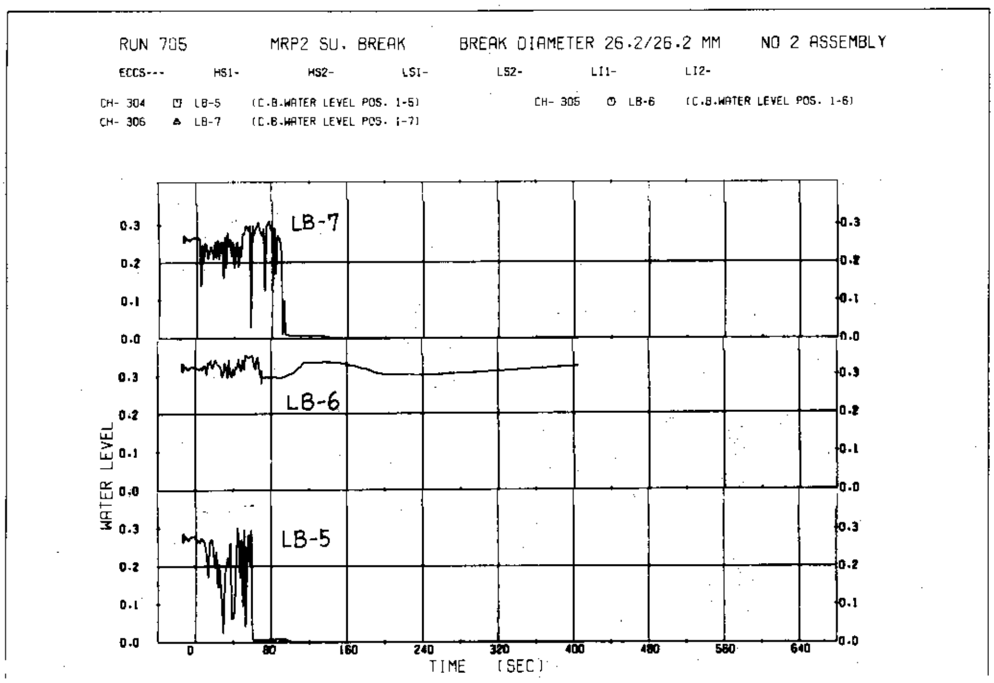

Fig. 5.70 Water level in channel box A (Pos. 1)

307 1.00000E-03 0.0 0.0 308 1.00000E-03 0.0 0.0
309 1.00000E-03 0.0 0.0 310 1.00000E-03 0.0 0.0

DELT-T 1467 (MS) DATE 79-12-12 NO-77

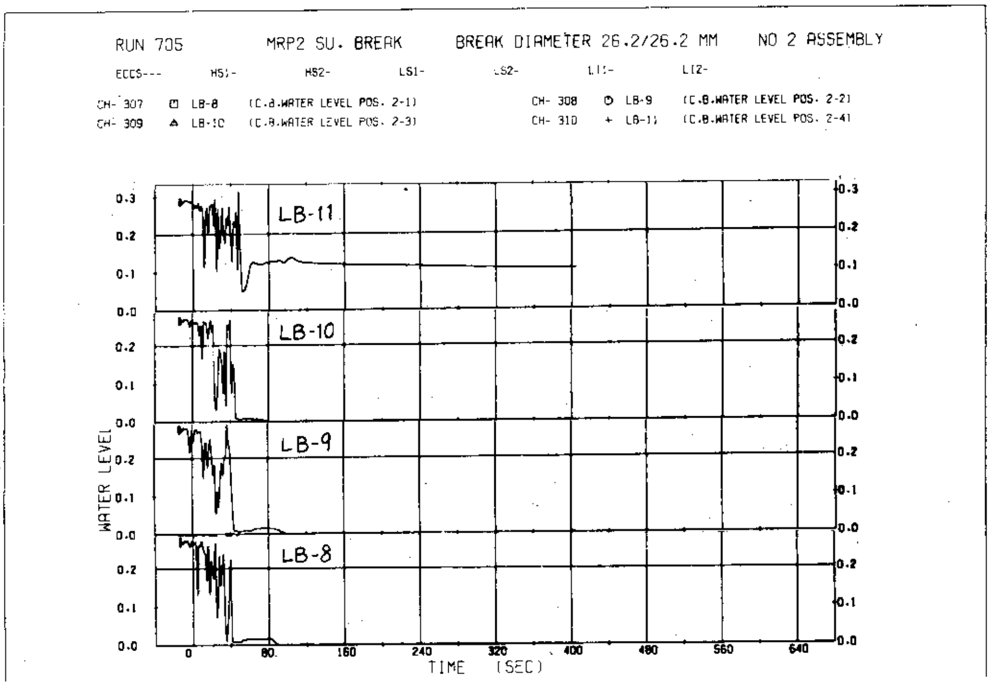

Fig. 5.71 Water level in channel box A (Pos. 2, center of core)

311 1.00000E-03 0.0 0.0 312 1.00000E-03 0.0 0.0
313 1.00000E-03 0.0 0.0

DELT-T 1467 (MS) DATE 79-12-12 NO-78

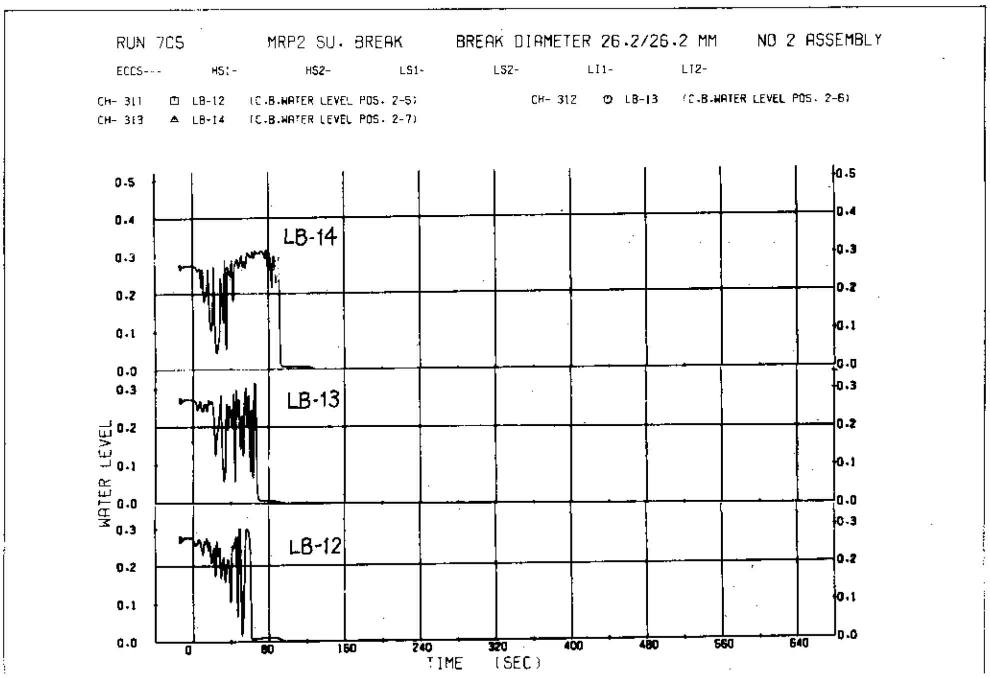

Fig. 5.72 Water level in channel box A (Pos. 2, center of core)

314	1.00000E-03	0.0	0.0	315	1.00000E-03	0.0	0.0
316	1.00000E-03	0.0	0.0	317	1.00000E-03	0.0	0.0

DELT-T 1467 (MS) DATE 79-12-12 NO-79

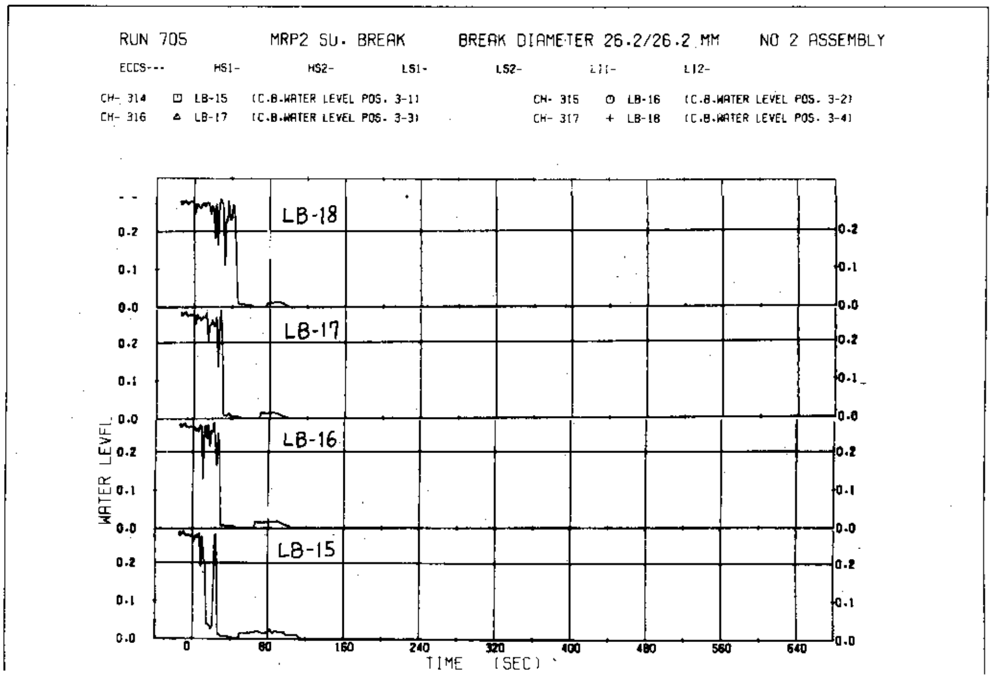

Fig. 5.73 Water level in channel box C

318	1.00000E-03	0.0	0.0	319	1.00000E-03	0.0	0.0
320	1.00000E-03	0.0	0.0				

DELT-T 1467 (MS) DATE 79-12-12 NO-80

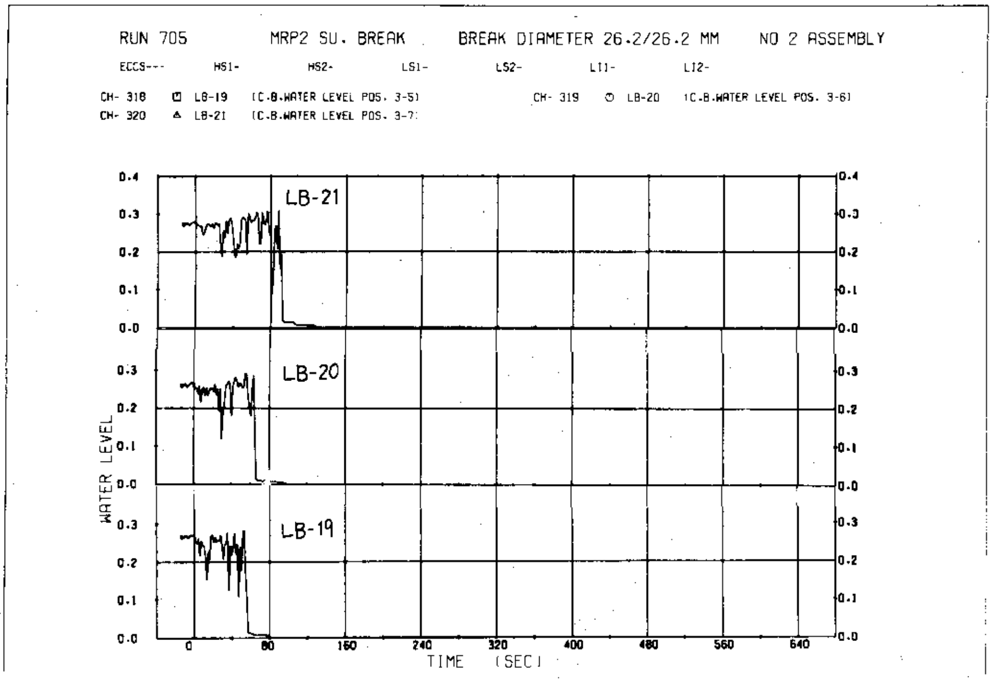

Fig. 5.74 Water level in channel box C

321 1.00000E-03 0.0 0.0 322 1.00000E-03 0.0 0.0
323 1.00000E-03 0.0 0.0 324 1.00000E-03 0.0 0.0

DELT-T 1467 (MS) DATE 79-12-12 NO-81

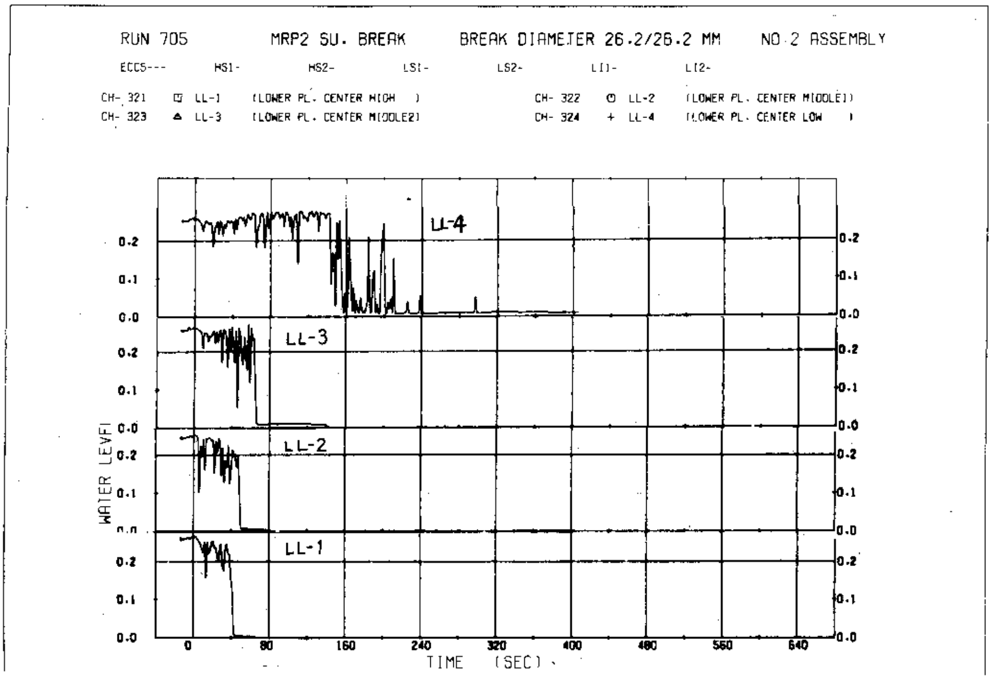

Fig. 5.75 Water level in lower plenum

325 1.00000E-03 0.0 0.0 327 1.00000E-03 0.0 0.0

DELT-T 1467 (MS) DATE 79-12-12 NO-82

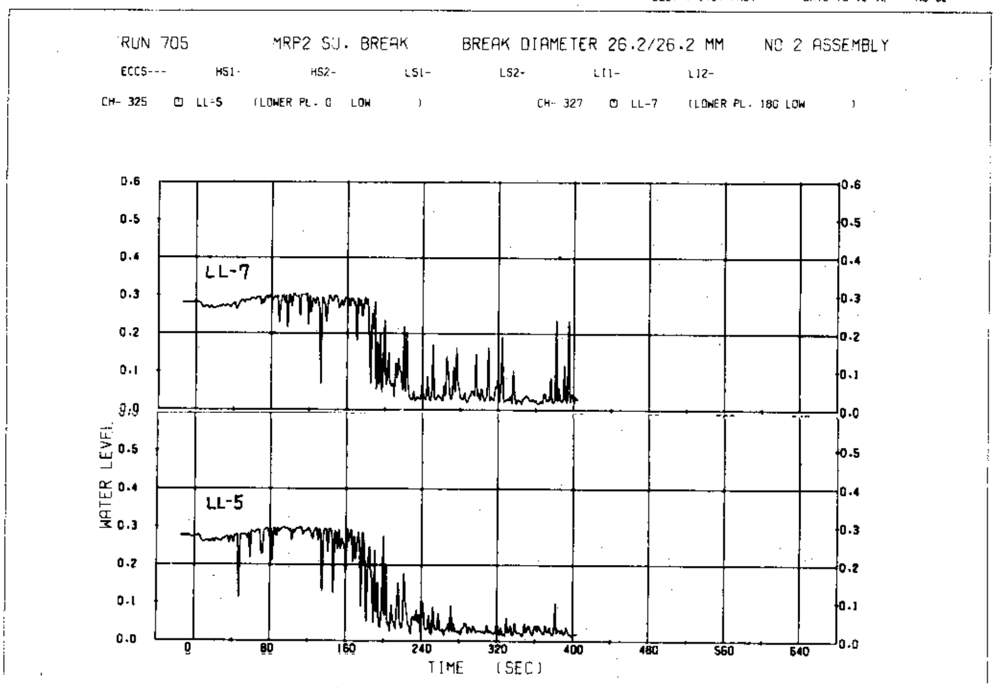

Fig. 5.76 Water level in lower plenum

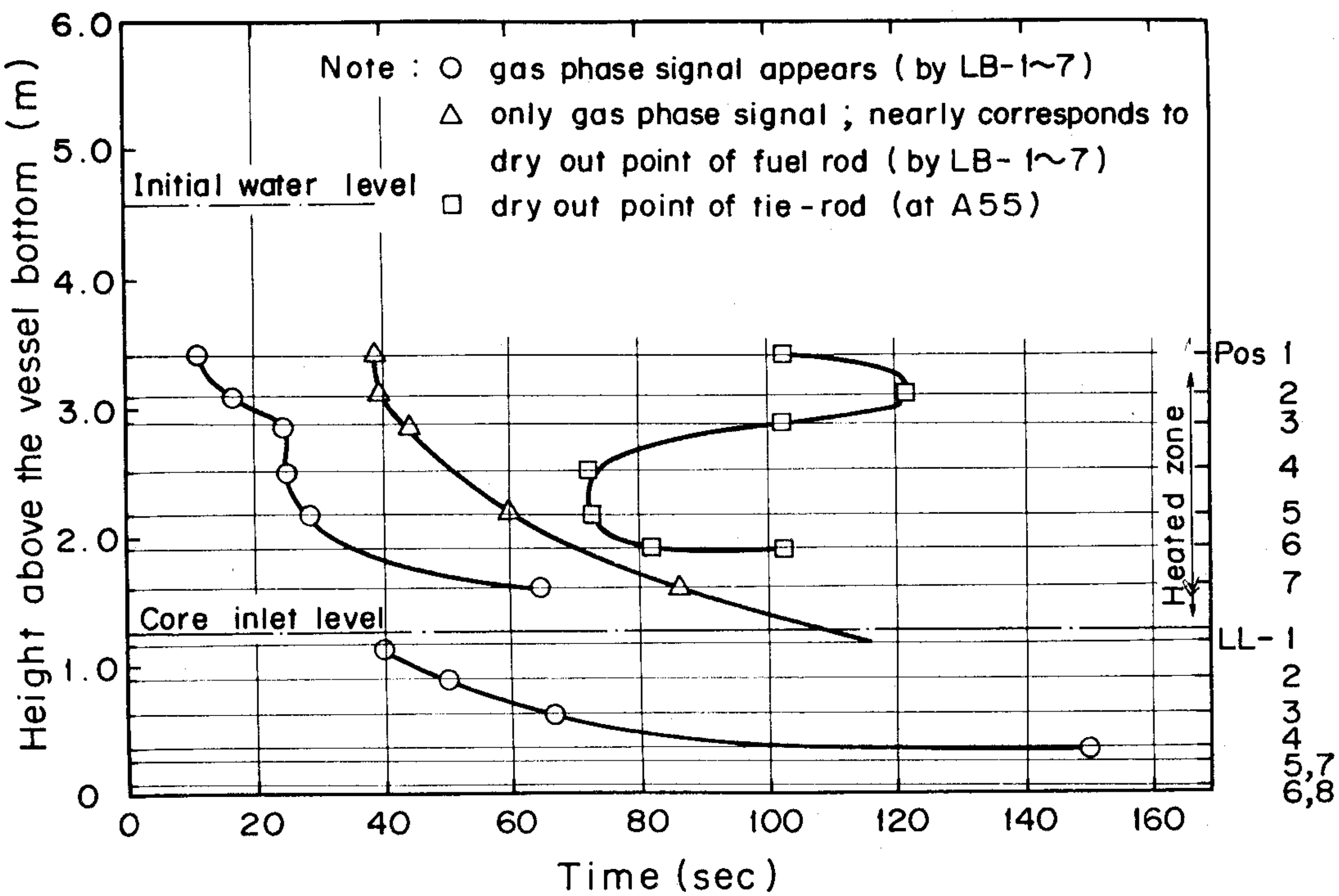

Fig. 5.77 Change of water level in core and in lower plenum